

**Universität
Rostock**



Traditio et Innovatio

**Protective Role of Gut Commensal Bacteria on
Epithelial Barrier Disruption and Ulcerative Colitis
in vitro and *in vivo***

Dissertation

in partial fulfilment of the requirements for the academic degree of

Doctor rerum naturalium (Dr. rer. nat.)

From the Faculty of Mathematics and Natural Science

University of Rostock

Germany

by

Nooshin Mohebali

Born on 08.08.1986, Tehran, Iran

Rostock, 2023



Dieses Werk ist lizenziert unter einer
Creative Commons Namensnennung - Nicht kommerziell -
Keine Bearbeitungen 4.0 International Lizenz.

Gutachter:

Prof. Dr. Bernd Kreikemeyer

Universitätsmedizin Rostock

Institut für Medizinische Mikrobiologie, Virologie und Hygiene

Schillingallee 70

18057 Rostock

Prof. Dr. Mirko Basen

Universität Rostock

Institut für Biowissenschaften

Abteilung Mikrobiologie

Albert-Einstein-Str. 3

18051 Rostock

Jahr der Einreichung: 2023

Jahr der Verteidigung: 2024

Table of Content

Table of Content

Table of Content.....	I
List of Tables	V
List of Figures.....	VI
Abbreviation.....	VIII
Summary.....	XI
Zusammenfassung	XIII
1 Introduction	1
1.1 The human gastro-intestinal tract	1
1.2 The physiological structure of the intestinal barrier	1
1.2.1 Tight junction.....	4
1.2.2 Immune function of the intestine	5
1.2.3 Intestinal microbiota	6
1.2.4 The role of commensal bacteria in human health	7
1.3 Inflammatory bowel disease	9
1.3.1 Current therapy	11
1.3.2 Animal models of IBD.....	12
1.3.3 Dextran sodium sulfate -induced colitis	13
2 Objective	15
3 Material and Methods.....	16
3.1 Materials	16
3.1.1 Chemicals and Reagent.....	16
3.1.2 Consumables.....	17
3.1.3 Kits.....	18
3.1.4 Stimulus	18

Table of Content

3.1.5	Bacterial strains.....	19
3.1.6	Device	19
3.1.7	Buffer	20
3.2	<i>In vitro</i> Methods.....	22
3.2.1	Bacterial culture medium.....	22
3.2.2	Long term storage of bacterial cultures	22
3.2.3	Growth behaviour	23
3.2.4	Colony forming units	23
3.2.5	Preparation of <i>Faecalibacterium prausnitzii</i>	24
3.2.6	Preparation of <i>Bacteroides faecis</i>	24
3.2.7	Preparation of <i>Roseburia intestinalis</i>	24
3.2.8	Preparation of bacterial cultures	24
3.2.9	Intestinal epithelial cells	25
3.2.10	Maintenance of Caco-2 and HT29-MTX.....	25
3.2.11	Long term storage of Caco-2 and HT29-MTX.....	25
3.2.12	Thawing of frozen cells	25
3.2.13	Preparation of eukaryotic cell	26
3.2.14	Growing intestinal epithelial cell lines on Transwell inserts.....	26
3.2.15	Transepithelial electrical resistance	27
3.2.16	Trypan Blue staining.....	28
3.2.17	Live/Dead staining.....	29
3.2.18	Adhesion assay	29
3.2.19	Effect of bacterial density on cell barrier permeability	30
3.2.20	Induction of barrier dysfunction	30
3.2.21	Bacterial treatment.....	30
3.2.22	Determination of paracellular permeability	31

Table of Content

3.2.23	Immunofluorescence staining	31
3.2.24	Western Blot analysis	32
3.2.25	Determination of cytokine secretion by ELISA	32
3.3	<i>In vivo</i> methods	34
3.3.1	Study design and bacteria treatment	34
3.3.2	Organ removal and tissue preservation.....	35
3.3.3	Clinical scoring of colitis	35
3.3.4	Histological analysis	36
3.3.5	Intestinal permeability assay.....	37
3.3.6	Homogenization of the tissue	38
3.3.7	Myeloperoxidase activity assay	38
3.3.8	Measurement of cytokines	38
3.3.9	Immunohistochemistry analysis	39
3.3.10	Western Blot assay.....	40
3.3.11	Analysis of Treg cells in spleen	41
3.3.12	Microbial DNA extraction	41
3.3.13	16S rRNA gene sequencing.....	42
3.4	Statistical analysis.....	42
4	Results	43
4.1	Monitoring bacterial growth	43
4.2	Viability of the commensal bacteria in cell culture medium	44
4.3	Cultivation of eukaryotic cells under anaerobic conditions.....	47
4.4	Bacterial adherence to intestinal epithelial cells.....	50
4.5	Effects of commensal bacteria on healthy polarized epithelial monolayers	51
4.6	Effects of commensal bacteria on inflamed intestinal epithelial cell function	54

Table of Content

4.7	The paracellular permeability of epithelial cell monolayers	56
4.8	Bacterial effects on host cell cytokine secretion.....	58
4.9	Immunofluorescence microscopic localization of tight junction proteins..	60
4.10	Effects of bacteria on tight junction protein expression in epithelial cell monolayers	63
4.11	The effects of the commensal bacteria on acute colonic inflammation in mice	66
4.12	Myeloperoxidase activity assay	69
4.13	Histological analysis	70
4.14	Intestinal barrier function in DSS-induced colitis mice.....	73
4.15	Tight junction protein expression in acute DSS-induced colitis.....	75
4.16	Cytokine levels in colonic tissue in acute DSS-induced colitis.....	78
4.17	Treg percentages in mice with DSS-induced colitis.....	80
4.18	Influence of bacteria treatments on the gut microbiome composition.....	82
5	Discussion	84
5.1	The influence of commensal bacteria on intestinal inflammation <i>in vitro</i> .	84
5.2	The influence of commensal bacteria on intestinal inflammation <i>in vivo</i> ..	90
6	Conclusions	99
7	Limitations	101
8	References	102
9	Acknowledgment	123
	Declaration of Independence	124
	Curriculum Vitae	126

List of Tables

List of Tables

Table 1. Components used for the preparation of anaerobic brain-heart infusion broth.	22
Table 2. Disease activity index (DAI) score parameters	36
Table 3. Histological score to quantify the degree of colitis.	37
Table 4. Primary and secondary antibodies used for immunohistochemical staining....	39
Table 5. Primary and secondary antibodies used for Western Blot.....	40
Table 6. Adhesion of <i>F. prausnitzii</i> , <i>B. faecis</i> , and <i>R. intestinalis</i> to differentiated intestinal epithelial cell monolayers.	51

List of Figures

List of Figures

Figure 1. Schematic representation of the intestinal mucosal barrier.....	4
Figure 2. The health-promoting effects of probiotic bacteria.....	9
Figure 3. Interactions between the gut microbiota, host and environmental factors in the pathogenesis of IBD.....	11
Figure 4. Illustration of a Transwell cell culture insert.....	27
Figure 5. Transepithelial/endothelial electrical resistance (TEER) measurement using EVOM instrument.....	28
Figure 6. The growth curve of <i>F. prausnitzii</i> , <i>B. faecis</i> , and <i>R. intestinalis</i>	44
Figure 7. Growth curve for <i>F. prausnitzii</i> , <i>B. faecis</i> , and <i>R. intestinalis</i> in anaerobic cell culture medium and bacteria culture medium.....	46
Figure 8. Survival of differentiated Caco-2 under aerobic and anaerobic conditions. ...	48
Figure 9. Survival of differentiated HT29-MTX under aerobic and anaerobic conditions.. ..	49
Figure 10. Effect of the commensal bacteria on the transepithelial electrical resistance (TEER) of differentiated Caco-2 and HT29-MTX cell monolayers.....	53
Figure 11. Effect of <i>F. prausnitzii</i> , <i>B. faecis</i> , and <i>R. intestinalis</i> individually and in combination on TEER in inflamed epithelial barrier.....	55
Figure 12. Effect of <i>F. prausnitzii</i> , <i>B. faecis</i> , and <i>R. intestinalis</i> on paracellular permeability.. ..	57
Figure 13. IL-8 and MCP-1 secretion by differentiated Caco-2 and HT29-MTX cells expose to inflammatory cytokine and LPS.	59
Figure 14. Immunofluorescence localization of the tight junction protein occludin in Caco-2 and HT-29-MTX epithelial cells.	61
Figure 15. Immunofluorescence localization of the tight junction proteins claudin-2 in Caco-2 and HT-29-MTX epithelial cells.	62
Figure 16. Western blot analysis of claudin-2 and occludin expression after treatment with <i>F. prausnitzii</i> , <i>B. faecis</i> , and <i>R. intestinalis</i> , alone and in combination.....	65
Figure 17. Impact of <i>F. prausnitzii</i> , <i>B. faecis</i> , and <i>R. intestinalis</i> on DSS-induced colitis.....	68
Figure 18. Effect of <i>F. prausnitzii</i> , <i>B. faecis</i> , and <i>R. intestinalis</i> on MPO activity.	70

List of Figures

Figure 19. Impact of <i>F. prausnitzii</i> , <i>B. faecis</i> , and <i>R. intestinalis</i> on histopathological features and goblet cells of DSS-induced colitis mice.	72
Figure 20. Levels of FITC dextran in the serum of mice with DSS induced colitis.....	74
Figure 21. Effect of <i>F. prausnitzii</i> , <i>B. faecis</i> , and <i>R. intestinalis</i> alone and in combination on epithelial tight junction protein expression.....	76
Figure 22. Immunohistochemically staining of tight junction proteins.....	77
Figure 23. Regulation of the innate immune response in the colon by <i>F. prausnitzii</i> , <i>B. faecis</i> , and <i>R. intestinalis</i>	79
Figure 24. <i>F. prausnitzii</i> , <i>B. faecis</i> , and <i>R. intestinalis</i> alone and in combination expand the Treg population in mice with experimental colitis.	81
Figure 25. Alterations of the fecal microbiome due to DSS and bacterial treatments. ..	83

Abbreviation

Abbreviation

5-FU	5-Fluoracil
ANOVA	Analysis of variance
APC	Antigen presenting cell
BHI	Brain –heart infusion
CD	Crohn’s disease
CFU	Colony forming units
DAMP	Damage associated molecular pattern
DC	Dendritic cell
dH ₂ O	Distilled H ₂ O
DSS	Dextran sulfate sodium
EEC	Enteroendocrine cells
GJ	Gap junctions
GI	Gastrointestinal
GIT	Gastrointestinal tract
GALT	Gastrointestinal associated-lymphoid tissue
IBD	Inflammatory Bowel Diseases
IEC	Intestinal epithelial cells
IEL	Intraepithelial lymphocytes
IFN- γ	Interferon gamma
IL	Interleukin
Ig	Immunoglobulin
IgA	Immunoglobulin A
JAM	Junctional adhesion molecules

Abbreviation

LP	Lamina Propria
LPS	Lipopolysaccharide
MAMP	Microbe-associated molecular patterns
MCP	Monocyte chemoattractant-protein
MHC	Major histocompatibility complex
MLN	Mesenteric Lymph nodes
MPO	Myeloperoxidase
NF-kB	Nuclear factor kappa B
MOI	Multiplicity of infection
NOD	NOD-like receptor
OD	Optical density
PAMPs	pathogen-associated molecular patterns
PBS	Phosphate buffered saline
PRRs	Pathogen recognition receptors
PP	Peyer's patches
ROS	Reactive oxygen species
SCFA	Short chain fatty acids
STAT3	Signal transducer and activator of transcription 3
SDS	Sodium dodecyl sulfate
SEM	Standard error of the mean
TJs	Tight junctions
TEER	Transepithelial resistance
Treg	Regulatory T cells
TGF- β	Transforming growth factor β

Abbreviation

Th	T helper
TLR	Toll-like receptor
TNBS	Trinitrobenzenesulfonic acid
TNF- α	Tumor necrosis factor α
UC	Ulcerative colitis
Usp45	Unknown secreted protein of 45 KDa
ZO-1	Zonula occludin-1

Summary

Summary

The human intestinal tract is formed by a single layer of epithelial cells, responsible for regulating the permeability of the intestinal barrier. Within this tract a diverse microbiota composed of variable bacterial populations is found. These bacteria can be categorized into permanent inhabitants of the gut (commensal bacteria) or transient residents originating from external sources. There is evidence that gut microbiota regulates intestinal barrier function and may contribute to the protective mechanism of the intestinal mucosa against the development of chronic inflammation. The mechanism by which this protective effect is mediated may include the inhibition of pro-inflammatory cytokines, and stimulation of anti-inflammatory cytokines, which may affect barrier integrity.

In the first part of this study, the effects of *Faecalibacterium prausnitzii* (*F. prausnitzii*), *Bacteroides faecis* (*B. faecis*), and *Roseburia intestinalis* (*R. intestinalis*), both individually and in combination, on intestinal barrier function were investigated using an in vitro model of intestinal inflammation. To achieve this, the differentiated human intestinal epithelial cells (Caco-2 and HT29-MTX) were stimulated with a pro-inflammatory cocktail consisting of interleukin-1 β (IL-1 β), tumor necrosis factor- α (TNF- α), interferon- γ (IFN- γ), and lipopolysaccharide (LPS) to mimic intestinal inflammation.

The results obtained in this work demonstrated that all three bacterial species are able to recover the impairment of the epithelial barrier function induced by the inflammatory stimulus, as determined by an ameliorating of the transepithelial electrical resistance (TEER) and the paracellular permeability of the cell monolayer. Moreover, inflammatory stimulus-induced increases in claudin-2 expression and decreases in occludin expression, were improved in cells treated with commensal bacteria. Furthermore, the commensals are able to counteract the increased release of interleukin-8 (IL-8) and monocyte chemoattractant protein-1 (MCP-1) induced by the inflammatory stimulus. These findings indicated that *F. prausnitzii*, *B. faecis* and *R. intestinalis* improve the epithelial barrier integrity and limit inflammatory responses. The potential of enhancing the intestinal barrier and attenuation of inflammation in epithelial cells supports our hypothesis that the application of specific bacteria, which are underrepresented in inflammatory bowel disease (IBD) patients, could support common IBD therapy and thereby manage intestinal inflammatory disorders.

Summary

In the second part of this study, the *in vitro* results were translated into an *in vivo* mouse model. An experimental acute colitis mouse model induced by Dextran sulfate sodium (DSS) was employed to examine the beneficial effects of these three commensal gut bacterial species on colitis. *F. prausnitzii*, *B. faecis*, and *R. intestinalis* are found to be reduced in the guts of ulcerative colitis patients.

The administration of these commensal bacteria, either individually or in combination, to DSS-induced colitis mice led to a reduction in disease activity index (DAI) scores, inhibition of colon shortening, reinforcement of the colonic epithelial barrier, and positive modulation of tight junction protein expression. The treatment also resulted in the mitigation of crypt disruption, goblet cell loss, submucosal edema, and the modulation of cytokine secretion and epithelial damage induced by DSS administration. Immune modulation was achieved through the inhibition of the loss of CD4⁺CD25⁺ regulatory T (Treg) cells in the spleen. Notably, no adverse effects of commensal bacterial treatment on the general composition of the gut microbial community were observed. Furthermore, commensal bacterial therapy demonstrated comparable efficacy to contemporary mesalazine treatment.

In summary, all treatments involving commensal bacterial species in this study contributed to the maintenance of intestinal barrier integrity, suppression of pro-inflammatory responses, and equilibrium in microbiota composition, factors that typically promote and maintain intestinal homeostasis.

Zusammenfassung

Der menschliche Darmtrakt wird durch eine einzige Schicht von Epithelzellen gebildet, die für die Regulation der Durchlässigkeit der Darmbarriere verantwortlich sind. Innerhalb dieses Trakts lebt eine vielfältige Mikrobiota, die aus verschiedenen bakteriellen Populationen besteht. Diese Bakterien können in ständige Bewohner des Darms (kommensale Bakterien) oder vorübergehende Bewohner aus externen Quellen eingeteilt werden. Es gibt Hinweise darauf, dass die Darmmikrobiota die Funktion der Darmbarriere regulieren und zum Schutzmechanismus der Darmmukosa gegen die Entwicklung einer chronischen Entzündung beitragen können. Der Mechanismus, durch den dieser Schutzeffekt vermittelt werden kann, könnte die Hemmung pro-inflammatorischer Zytokine und die Stimulation anti-inflammatorischer Zytokine umfassen, welche wiederum Einfluss auf die Integrität der Darmbarriere haben.

Im Rahmen der Arbeit wurden die Kommensale *Faecalibacterium prausnitzii* (*F. prausnitzii*), *Bacteroides faecis* (*B. faecis*), und *Roseburia intestinalis* (*R. intestinalis*) verwendet, da diese im Darm von Colitis Ulcerosa-Patienten vermindert vorliegen. Im ersten Teil dieser Studie wurde mit Hilfe eines In-vitro-Modells für Darmentzündung, die Auswirkungen von *F. prausnitzii*, *B. faecis*, und *R. intestinalis* sowohl einzeln als auch in Kombination auf die Funktion der Darmbarriere untersucht. Zu diesem Zweck wurden differenzierte humane Darmepithelzellen (Caco-2- und HT29-MTX) mit einem pro-inflammatorischen Cocktail aus Interleukin-1 β (IL-1 β), Tumornekrosefaktor- α (TNF- α), Interferon- γ (IFN- γ) und Lipopolysaccharid (LPS) stimuliert, um eine intestinale Entzündung nachzustellen. Die in dieser Arbeit gewonnenen Ergebnisse zeigten, dass alle drei Bakterienarten in der Lage sind, die Beeinträchtigung der Funktion der epithelialen Barriere, die durch den entzündlichen Reiz verursacht wurde, zu korrigieren, wie durch eine Verbesserung des transepithelialen elektrischen Widerstands (TEER) und der parazellulären Durchlässigkeit der Zellmonolage bestimmt wurde. Darüber hinaus wurden durch den entzündlichen Reiz erhöhte Claudin-2-Expression und verringerte Occludin-Expression in den Zellen verbessert, die mit den kommunalen Bakterien behandelt wurden. Des Weiteren sind die Kommensalen in der Lage, die verstärkte Freisetzung von Interleukin-8 (IL-8) und monozytenchemoattraktantem Protein-1 (MCP-1), die durch den entzündlichen Reiz verursacht wurde, entgegenzuwirken. Diese Ergebnisse deuten darauf hin, dass *F. prausnitzii*, *B. faecis*, und *R. intestinalis* die

Zusammenfassung

Integrität der epithelialen Barriere verbessern und pro-inflammatorische Prozesse begrenzen.

Im zweiten Teil dieser Studie wurden die In-vitro-Ergebnisse in ein In-vivo-Mausmodell übertragen. Hierfür wurde mittels Dextran sulfate sodium (DSS)-Gabe eine akute Kolitis im Kolon der Mäuse induziert, um die Effekte der drei Kommensale auf die Kolitis zu untersuchen.

Die orale Applikation dieser Bakterien, entweder einzeln oder in Kombination, resultierte in klinisch weniger stark ausgeprägten Krankheitssymptomen, zusammengefasst im Krankheitsaktivitätsindex (DAI), eine geringere Kolonverkürzung und der positiven Beeinflussung von epithelialer Barriere-Integrität und der Expression von Tight Junction Proteinen. Weiterhin führte die Behandlung zu einer Verbesserung des histologischen Scores, einer verminderten Sekretion von pro-inflammatorischen- und erhöhten Sekretion von anti-inflammatorischen Mediatoren. Eine weitere Immunmodulation konnte durch die Hemmung des DSS-assoziierten Verlusts von CD4+CD25+ regulatorischen T (Treg)-Zellen in der Milz nachgewiesen werden. Die Untersuchung der mikrobiellen Zusammensetzung der Darmmikrobiota wies keine nachteiligen Auswirkungen der bakteriellen Behandlung nach. Darüber hinaus zeigte die Behandlung mit den drei Bakterienarteneine vergleichbare Wirksamkeit wie die konventionelle Mesalazin-Therapie.

Zusammenfassend förderten alle drei Kommensale die Aufrechterhaltung der Darmbarriere-Integrität, wirkten modulierend auf das pro-inflammatorische Milieu und trugen zum Gleichgewicht der Mikrobiota-Zusammensetzung bei.

Das therapeutische Potential der drei Bakterienarten, was *in vitro* und *in vivo* nachgewiesen wurde, unterstützt unsere Hypothese, dass die Anwendung spezifischer Bakterien, welche bei chronisch-entzündlichen Darmerkrankungen (CED)-Patienten unterrepräsentiert sind, eine vielversprechende Therapieoption darstellt. Diese neue Art der Therapie kann unterstützend zur konventionellen CED-Therapie eingesetzt werden.

Introduction

1 Introduction

1.1 The human gastro-intestinal tract

The human digestive tract is divided into several compartments, including the mouth, esophagus, stomach, small intestine, large intestine, rectum, and anus. Its primary functions are the absorption of nutrients, salts, and water from food, as well as the exudation of non-absorbable food components and metabolic waste products. In the mouth the food is masticated and mixed with saliva, which contains digestive enzymes such as amylase, starting the digestion of polysaccharides. The food is then swallowed and via the esophagus, moved to the stomach. In the stomach, the masticated food is then mixed with hydrochloric acid and proteases secreted by various glands in the folded epithelium. The partially digested food (chyme) is finally passed through the pyloric sphincter to the duodenum (1, 2). The small intestine consists of the duodenum, jejunum, and ileum is the site, where most of the nutrients from the chyme are absorbed. In the duodenum, the chyme is mixed by peristaltic movements with bile, pancreatic and intestinal juice (1). For an effective absorption of nutrients, the surface of the small intestine is highly increased to about 200- 300 m² due to macroscopic and microscopic folding of the mucosa (villi and microvilli) (3). The large intestine is made up of the caecum, colon, rectum, and anus. Epithelial cells of the colon are forming crypts, which are lined with goblet cells, responsible for secreting mucus, and Paneth cells, which contribute to the regulation of the intestinal microenvironment. Under normal physiological conditions, the epithelium is covered by a mucus layer. This mucus layer plays diverse roles, including providing a physical barrier, preventing direct contact between the epithelial cells and luminal contents, and facilitating the maintenance of a balanced microbial community within the gut. The primary function of the colon is the absorption of water and electrolytes from the chyme and storing fecal material until defecation (4, 5) .

1.2 The physiological structure of the intestinal barrier

The intestinal mucosa is a critical barrier that separates the inner and outer areas of the intestinal lumen and is essential for the maintenance of mucosal homeostasis. It also serves to absorb nutrients from the lumen. The mucosa layer is considered the first line

Introduction

of defense against the hostile luminal environment and consists of a single epithelial cell layer and an intraepithelial tight junction (TJ) complex (6). In addition, this barrier acts as a selective filter, allowing the translocation of nutrients, electrolytes, and water from the intestinal lumen into the blood circulation (7–9). In general, the passage of molecules can occur either through transcellular or paracellular transport pathways (9). The former is associated with solute transport through the epithelial cells and is predominantly regulated by selective transporters for amino acids, electrolytes, short-chain fatty acids, and sugars (6). The cell-cell and cell-extracellular matrix (ECM) junctions within the epithelial tissues are crucial anchoring structures that provide architectural stability, mechanical resistance, and permeability control (10). Apically localized TJ proteins play an important role in epithelial barrier maintenance and paracellular permeability. TJ proteins, mediate epithelial cell polarity and maintain directional mass transfer (11). The structure and regulation of TJs, which represent the physical barrier, and the regulation of intestinal barrier integrity, with a specific focus on the regulation of TJ integrity by commensal and probiotic bacteria, are described in more detail in section 1.2.1. The mucosa is typically composed of a thin layer of epithelium that covers connective tissues and is composed of a variety of cells specialized in mucus secretion, nutrient adsorption, or antigen uptake. This underlying tissue contains some lymphoid organs but mostly isolated immune cells, such as macrophages, dendritic cells (DC), plasma cells, and B and T cells. Mucus layers protect the tight epithelium, immunoglobulin A (IgA) antibodies are secreted on the apical side of the epithelial cells, and both invariant and adaptive immune cells are scattered beneath the epithelium (12–14)

The mucus layer is a dynamic layer that covers the epithelial barrier and functions as an extra mechanical barrier, preventing direct contact with luminal antigens. In addition to water, filamentous glycoproteins known as mucins are the major components of this layer. In the small intestine, the mucus consists of a single layer, whereas in the large intestine, the mucus has an inner and an outer layer. The outer layer is looser and more permeable to bacteria and serves as a habitat for the microbiome. The inner layer is a thin, dense, and sterile layer that, along with glycocalyx, prevents microorganisms from adhering to the epithelium. The intestinal epithelium consists of the enterocyte, enteroendocrine cells (EEC), Paneth cells, and goblet cell lineages (15). Goblet cells are specialized secretory cells that are found throughout the intestine and are equipped with a specific biological machinery for mucus secretion. The glycosylated mucins that goblet

Introduction

cells produce and secrete are an adherent fluid that lubricates and protects the epithelial intestinal surface. Furthermore, goblet cells may function as antigen-presenting cells (APCs), delivering luminal antigens to CD103⁺ dendritic cells and promoting the development of regulatory T cells (Tregs) (16). In addition, specialized intestinal epithelial cells, such as paneth cells, secrete several antimicrobial lysozymes, defensins, and phospholipases into the lumen in order to eliminate microbes that eventually penetrate the mucus (17). In addition to the highly developed Gut-associated lymphoid tissue (GALT), the intestinal epithelium, mucus, and antimicrobial peptides all contribute to immunological protection. These mechanical and chemical barriers are classified as non-specific defense mechanisms (18). In addition to barrier formation, intestinal epithelial cells play an important role in immunological activities. As so-called non-professional APCs, they may take up luminal antigens and offer them to nave T cells via MHC-II (19). The commensal microbial species that inhabit the gut are considered to be part of the intestinal mucosal barrier. The gut microbiota can influence barrier function directly by stimulating epithelial cell proliferation and IL-8 secretion and indirectly through mediating the production of dietary metabolites such as short-chain fatty acids, which are an important energy source for colonic epithelial cells (colonocytes) (20–22). In section 1.2.4, the intestinal flora is discussed in more detail.

Introduction

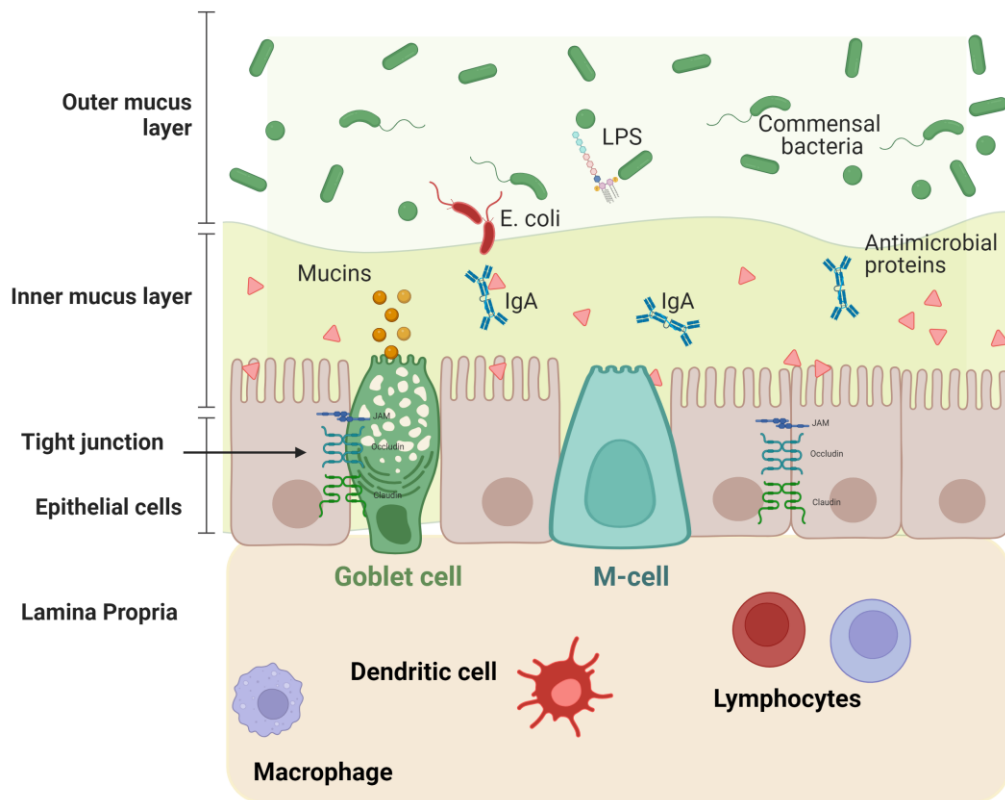


Figure 1. Schematic representation of the intestinal mucosal barrier (Created by Biorender)

1.2.1 Tight junction

The epithelium contains an important intercellular junctional complex, which includes desmosomes, adherent junctions (AJ), gap junctions (GJ), and tight junctions (23). TJs play a crucial role in the function of the intestinal barrier by connecting immune cells and sealing the space between cells to prevent the entry of toxins and pathogens (24).

These structures which are not static undergo assembly and disassembly processes depending on various factors such as exposure to bacteria and food components (25). TJs are composed of at least 50 proteins, which can be categorized into transmembrane and plaque proteins. The transmembrane proteins connect inter-epithelial cells, and they can be further divided into tetra-span proteins and single-span proteins. The tetra-span proteins include occludin, claudin, and tricellulin, while the single-span proteins include junctional adhesion molecules (JAMs) belonging to the immunoglobulin (Ig) superfamily (26, 27). Plaque proteins, on the other hand, link transmembrane proteins inside the cytoplasm. TJs constant remodelling is regulated by signalling molecules in response to external stimuli. The assembly of TJs depends on protein kinase C (28), while the

Introduction

regulation of epithelial TJs depends on myosin light-chain (MLC) phosphorylation by MLC kinase, which increases the permeability of TJs (29). Altered gut barrier components such as an impaired mucus layer, chronic hyper activation of immune cells, and dysfunctional TJs can lead to enhanced permeability and varying degrees of chronic inflammation (30). Therefore, there is an increasing interest in developing therapeutic agents that can maintain or improve gut barrier integrity.

1.2.2 Immune function of the intestine

The immune system is divided into two types, the innate and the adaptive immune system. The innate immune system is the first line of body defense against pathogens. It responds similarly to all germs and foreign substances, thus sometimes referred to as the "nonspecific" immune system. Cells of the innate immune system express PRRs that can recognize specific patterns associated with pathogens, known as pathogen-associated molecular patterns (PAMPs). This recognition triggers immune responses, including the release of cytokines and the activation of other immune cells. In the intestine, cells use specialized sensors called pathogen recognition receptors (PRRs) to identify specific patterns on microorganisms. These patterns, known as pathogen-associated molecular patterns (PAMPs), help the body distinguish potential harmful invaders from harmless microorganisms in the gut (31–35). There are several classes of PRRs in the intestine, two of them are membrane-bound toll-like receptors (TLRs), and oligomerization-domain (NOD) proteins (36–38). Host cells recognize pathogens using Toll-like receptors (TLR) and other pattern recognition molecules, functioning as sensors to detect pathogen-associated molecular patterns (PAMPs) (39). Upon activation, these sensors trigger a signalling cascade, prompting the recruitment of inflammatory cells like neutrophils to the infection site. This activation also initiates immune responses, involving the release of cytokines and the activation of additional immune cells. The mucosal adaptive immune system, which works in synergy with the innate immune system, provides a secondary level of defense by generating an antigen-specific immune response to luminal antigens. This response is orchestrated by antigen-presenting cells (APCs), which present the antigens to T cells and B cells, producing antigen-specific antibodies and developing long-term immune memory (40). It is commonly considered that macrophages and dendritic cells (DCs) are primarily responsible for innate immune responses (39, 41) while CD4⁺ T cells, including Th1, Th2, Th17, and Treg cells play a crucial role in

Introduction

adaptive immune responses (42). Depending on the subtype and location, numerous DCs with different specialized functions are present in the intestinal mucosa (41). Antigens are presented to T cells by the migration of DCs from peripheral to lymphoid tissue. Low expression of major histocompatibility complex (MHC) and co-stimulatory molecules results in immature DCs and a poorly immunogenic response (43). Dendritic cells are a critical component of the immune system that play a pivotal role in initiating and coordinating immune responses against invading pathogens (41). Immature DCs are less effective at activating T cells. However, when immature DCs encounter pathogen-associated molecular patterns or danger-associated molecular patterns (DAMPs) released by damaged or stressed cells, they undergo a process of maturation (32, 43). Mature DCs migrate to lymphoid tissues, where they interact with naïve CD4⁺ T lymphocytes, leading to the activation, clonal expansion, and differentiation of these T cell (43). The specific phenotypic characteristics of the DCs, as well as the cytokine environment, can influence the differentiation of T cells into subsets of either effector or regulatory T cells (44).

Effector T cells play a vital role in the clearance of invading pathogens by directly killing infected cells or by releasing cytokines to activate other immune cells. Regulatory T cell, on the other hand, help to maintain immune homeostasis by preventing excessive immune activation and protecting against autoimmunity (45, 46). The balance between effector T helper (Th) cells such as Th1, Th2, and Th17 cells and anti-inflammatory effector Tregs is essential in maintaining immune homeostasis and a balanced GI tract (47, 46, 45).

1.2.3 Intestinal microbiota

The human gastrointestinal tract is an inhabitant to a diverse and complex community of microorganisms, mostly bacteria, that can be classified as either indigenous or transient. Indigenous bacteria are well adapted to the extreme pH changes and other environmental conditions found throughout the GI tract and can colonize in various parts of it. Transient bacteria, on the other hand, come from external sources and are unable to survive for more than a few days in the GI tract (48, 49).

The intestinal microbiota is estimated to consist of 500 to 1000 different bacterial species, outnumbering human cells by a factor of 10 or more (50–52). Traditional methods of microbiota analysis, such as culture-based techniques, are limited in their ability to identify and study the diverse microbial communities in the GI tract. However, new culture-independent techniques, such as 16S rRNA gene sequencing and metagenomics

Introduction

sequencing, have allowed for a more comprehensive understanding of the gut microbiota (53–55). The two dominant phyla found in adult stool microbiota are Bacteroidetes and Firmicutes, which make up around 90% of the total gut microbiota, with a relative abundance of approximately 65% and 25%, respectively (56). Other phyla, such as Actinobacteria, Proteobacteria, and Verrucomicrobia, are present in smaller number and are influenced by various factors, including environmental conditions, diet, and exposure to enteropathogens. The bacterial colonization of the human gut begins shortly after birth, with exposure to maternal fecal and vaginal flora during natural delivery. The microbiota composition during early childhood is relatively simple and varies widely between individuals. However, as individuals age, their microbiota composition becomes more stable and gradually evolves into a microbiota dominated by anaerobic bacteria, such as *Bacteroides*, that are capable of digesting complex sugars and maintaining a symbiotic relationship with the host (57, 58). While microbial composition is generally stable in older adults, it can be altered in the short-term by dietary interventions, particularly changes in non-digestible carbohydrate intake. The abundance and diversity of bacterial populations in healthy adults vary along the GI tract, with the highest density of bacteria found in the colon, which is considered one of the most complex microbial ecosystems on Earth (59, 60).

1.2.4 The role of commensal bacteria in human health

Gut microbiome plays various vital roles including break down of indigestible compounds and production of hormones, amino acids, and vitamins. Microbiota plays an important role in development and homeostasis of the host immune system, proliferation and differentiation of intestinal epithelium and defense against opportunistic pathogen invasion. Commensal bacteria maintain the permeability of gut barrier by preventing pathogens from colonizing through the production of bacteriocins or by indirectly competing for nutrients (61). Human data showed a link between an imbalance in GI microbial composition, also called dysbiosis and the development of diseases such as IBD (62). Homeostasis imbalance allows bacteria to grow and leads to illness just as when commensal bacteria are depleted. A good health status may decline due to the decrease in benefits provided by commensal bacteria. According to the analysis of 16S rRNA gene amplicon sequencing, in IBD patients there was a notable decrease in the abundance of two dominant bacterial phyla, namely Firmicutes and Bacteroidetes. Conversely, the

Introduction

abundance of Enterobacteriaceae, Proteobacteria and Actinobacteria family was increase (63). Further studies revealed that decrease in Firmicutes indicates the presence of IBD and the increase in Proteobacteria indicates that the intestinal microbiota changes towards microbes which can causes inflammation.

A balanced microbial ecosystem with an appropriate level of growth and activity is one of the essential factors in not only gut health, but overall human health. Dysbiosis, or elevated activity and growth of potentially harmful bacteria can lead to a variety of diseases (64). Emerging evidence has highlighted the role of the gut microbiota and its metabolites, such as short-chain fatty acids (SCFAs), in regulation of immune homeostasis (65, 66). Acetate, propionate, and butyrate are the major SCFAs produced by bacterial fermentation of dietary fibers and resistant starch in the colon (67, 68). SCFAs are rapidly absorbed in the cecum and colon, and about 5-10% of SCFAs are excreted in the feces (68). Butyrate, has direct effects on the mucosal layer since enterocyte use it as a main source of energy (68). SCFAs also reduce the pH of the gut, thus reduce the absorption of ammonia and increasing water and mineral uptake. Additionally, SCFAs modulate inflammation-related cell signaling pathways (69). SCFAs have the potential to modify the composition of commensal bacterial populations by promoting beneficial bacterial growth while inhibiting the growth and activity of pathogen (70). For example, butyrate has been shown to promote the growth of beneficial bacteria like Bifidobacteria, and Lactobacilli (68). Moreover, butyrate can exert direct immunomodulatory and anti-inflammatory effects (69). Furthermore, commensal bacteria identification by IECs initiates the synthesis of multiple immunoregulatory molecules, thymic stromal lymphopietin (TSLP) and transforming growth factor β (TGF β) (71, 72), which subsequently promote the development of mucosal immune cells possessing tolerogenic properties. This cross-talk between commensal bacteria, Intestinal epithelial cells (IECs), and immune cells is crucial in maintaining homeostasis and restricting uncontrolled inflammation in the gastrointestinal tract (73). The health-promoting effects of probiotic bacteria and SCFAs is currently a main research focus since many chronic diseases, such as IBD, colon cancer, obesity, diabetes, and even several neurological disorders, have been linked to microbiota dysbiosis (74).

Introduction

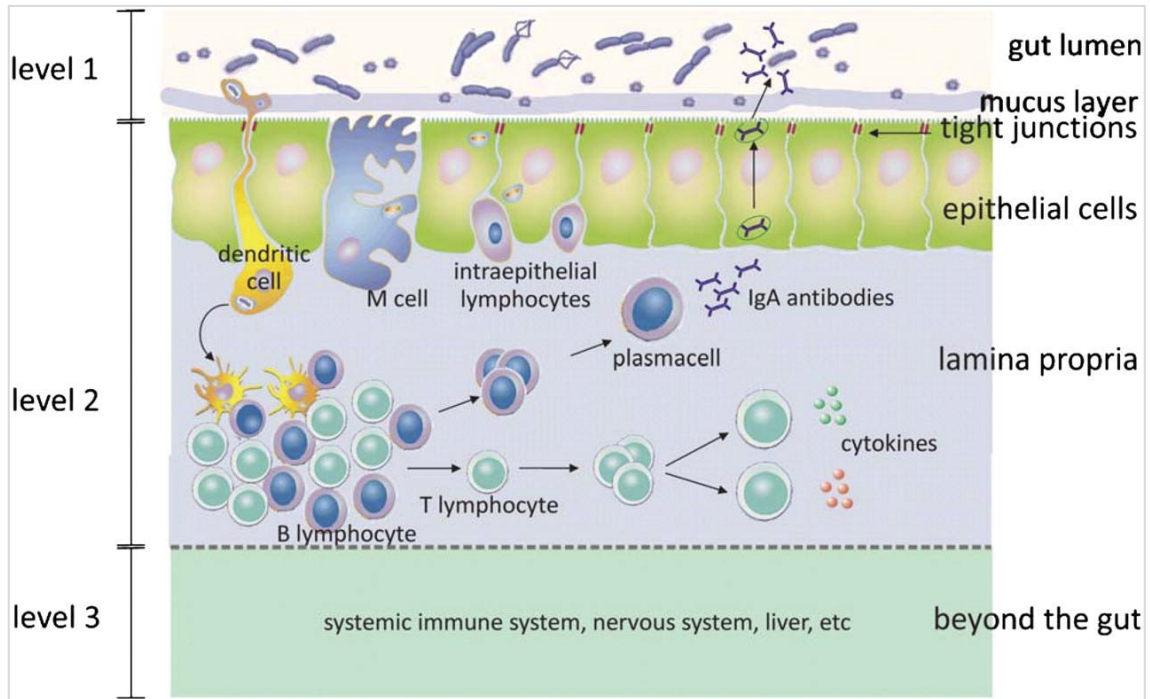


Figure 2. The health-promoting effects of probiotic bacteria ⁽⁷⁵⁾

1.3 Inflammatory bowel disease

Inflammatory bowel disease (IBD) is a series of gastrointestinal disorders characterized by chronic gut epithelial inflammation. The global prevalence of IBD is estimated to be 396 cases per 100,000 individuals annually (76). The study of IBD patients showed that there were no differences in the number of cases between men and women, although people aged 20-30 represented the group with the highest number of patients (77). Nevertheless, newborns and the elderly are also affected in significant numbers (78). Clinical symptoms of IBD include abdominal pain, diarrhea, and more general systemic symptoms, such as fatigue and weight loss (79). Crohn's disease (CD) and ulcerative colitis (UC) are the two primary types of IBD which differ in terms of the pattern involvement, type of inflammation, and therapeutic approach. CD is characterized by persistent inflammation of the bowel wall tissue at any point in the GI tract, whereas UC affects only the mucosa of the large intestine and extends from the distal to the proximal colon with varying degrees.

IBD is a complex disorder with unknown etiology which is triggered by exogenous and endogenous variables such as genetic predisposition, intestinal flora, and environmental factors (Figure 3). It induces a complicated dysfunction of the epithelial barrier and dysregulation of the mucosal immune system. Disease susceptibility is most likely driven

Introduction

by genetic predisposition, whereas environmental triggers produce inappropriate immune responses to gut microorganisms, resulting in chronic inflammation (80, 81). Various family and twin studies have revealed the impact of genetic variations. Nucleotide-binding oligomerization domain containing 2 gene (NOD2) is known as the major genetic risk factor of CD (82). A mutation on chromosome 16 leads to alterations in the NOD2 gene, which are associated with an increased risk of developing CD and IBD (83, 84). Mutations of Toll-like receptor 4 (TLR4), interleukin receptor 23 (IL-23R), signal transducer and activator of transcription 3 (STAT3), and the human antigen (HLA)-DR gene are also associated with IBD (85–87). Furthermore, there is evidence that environmental variables such as food and stress play a role (76). IBD has long been seen as a disease in developed countries, meaning that environmental variables play a significant role in its occurrence (76, 88). However, its incidence and prevalence are quickly expanding across previously underprivileged ethnicities and nationalities (89). The predominant localization of UC in the distal region of the gastrointestinal tract with the highest bacterial density suggests the involvement of the intestinal flora in the pathogenesis of this disease. It has been shown that bacterial abundance is greatly altered in an inflamed colon compared to the healthy intestinal segment. IBD, particularly UC is a complex relapsing and remitting chronic disease, which significantly increases the risk of developing colon cancer, and frequently causes extra intestinal manifestations (90). Moreover, in some cases, surgery to remove the entire colon and rectum may be recommended. After surgery, the patient is usually treated with the mentioned immunosuppressive drugs and antibiotics to prevent reappearance of symptoms. However, even with the drug treatment, a high percentage of symptom recurrence is reported in patients that underwent surgery (91, 90). Thus, it is extremely important to provide suitable therapeutic agents with the least amount of side effects which can effectively reduce the colonic inflammation and control the disease symptom.

Introduction

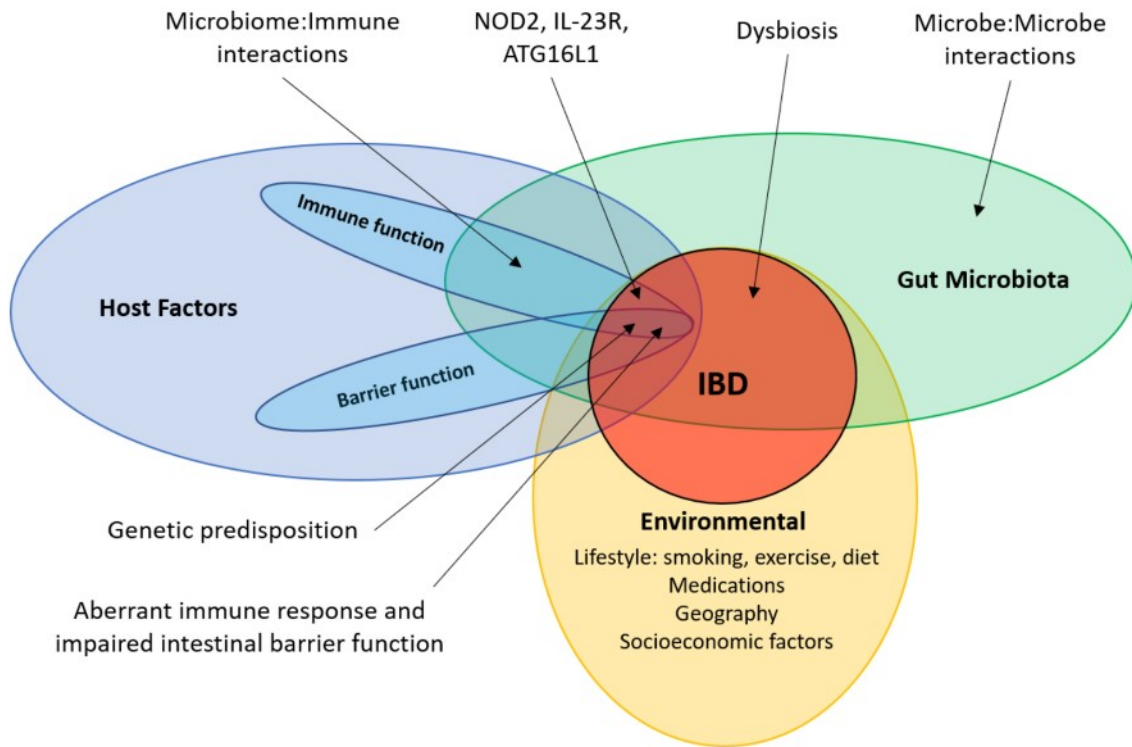


Figure 3. Interactions between the gut microbiota, host and environmental factors in the pathogenesis of IBD.⁽⁹²⁾

1.3.1 Current therapy

Treatment options for UC patients consist of long-term medical therapy to control intestinal inflammation or surgical intervention known as colectomy, which involves removing the diseased colon (93). Currently, UC patients are mainly treated symptomatically with corticosteroids, 5-aminosalicylic acid (5-ASA), immunosuppressive (e.g. azathioprine) or biologicals agent, such as monoclonal antibodies against pro-inflammatory mediators (e.g. anti-tumor necrosis factor α (TNF α) or anti-IL-12/IL-13 mAbs) to achieve a remission (94–97). However, current treatment options are focused on decreasing the course of inflammation and preserving remission. 5-ASA, also known as mesalazine (Mesalamine), is a common anti-inflammatory drug (98) used in induction and maintenance therapy of UC. However, in 10-45% of people, depending on the dose and the length of the therapy, it causes some side effects, such as diarrhoea, headache, nausea, and rash (95). The low therapeutic efficacy and substantial side effects of contemporary therapy are compelling reasons to explore an alternative effective therapeutic strategy, such as prebiotics, probiotics, and symbiotics, as complementary or alternative medicines to treat inflammatory bowel diseases (99, 96)

Introduction

Numerous randomized controlled trials have been conducted to investigate the potential therapeutic benefits of specific herbal medicines in the treatment of UC, including Kui jie qing (100), aloe vera gel (101), and wheat grass juice (102). Results from most of these studies have indicated positive effects of these herbal remedies. Furthermore, combining complementary and alternative medicine (CAM) with conventional medicine has been found to have greater therapeutic efficacy compared to either treatment alone (103). However, it should be noted that although CAMs may be effective for some UC patients, their safety cannot be assured as most herbal remedies are not regulated (104). Extensive research has been conducted on the potential therapeutic benefits of probiotics for IBD. Probiotics are live bacteria that can provide health benefits to the host when consumed in sufficient amounts. *Bifidobacterium* and *Lactobacillus* are the most commonly used probiotics and they function in several ways, such as excluding pathogenic bacteria, directly affecting the GI immune system, and producing SCFAs (105, 106). The commercial probiotic mixture VSL#3, which combines *Lactobacillus*, *Bifidobacterium* and *Streptococcus* strain, has been shown to maintain pouchitis remission and may have benefits in the induction and maintenance of remission in UC, but not CD (107–109). Recent studies suggested that certain species from the human GI microbiota, such as *Faecalibacterium prausnitzii* and *Roseburia intestinalis*, which are reduced in people with IBD, IBS, and celiac disease, could be potential candidates for a new generation of probiotics (110). Probiotics may be more effective in UC but less effective in CD due to differences in baseline microbiota, distinct disease etiology, and higher diversity in CD location and behavior.

1.3.2 Animal models of IBD

Several animal models have been developed to understand etiology and pathogenesis of IBD and to evaluate new prophylactic/therapeutic strategies. IBD animal models are characterized by chronic or relapsing inflammation of gastrointestinal tract that resembles human IBD. There are several groups of animal models relevant to IBD available. The first group of animal models involves SAMP1/ Yit and C3H/HeJBir mice which develop mucosal colitis spontaneously due to the increase of reaction between T-lymphocytes and B-lymphocytes towards antigens of the enteric microflora (111, 112). This group of animals is suitable to identify the genes involved in the onset of mucosal inflammation (113). The second group of animal models consists of animals with known genetic

Introduction

abnormalities leading to dysfunctions of cytokines receptor. These genetic dysfunctions disturb the intestinal epithelial layer, providing researchers with insight into how immunological defects or dysfunction of the epithelial barrier lead to mucosal inflammation (114). One example of this group are IL-10-deficient mice (IL-10^{-/-}), which lack the gene responsible for producing the anti-inflammatory cytokine IL-10 (115).

The third model are bacterial models, where germ-free, specific pathogen-free, or immunodeficient mice are exposed to specific bacteria, such as pathogens or commensals, to study the potential positive or negative impact of various bacterial strains in the development or treatment of IBD (116). The fourth category is using chemical compounds or immunogenic substances, such as 2,4,6-trinitrobenzenesulfonic acid (TNBS) and dextran sodium sulfate (DSS), which cause mucosal inflammation due to disruption of the epithelial barrier (117, 118). The TNBS model involves intra-rectal delivery of the substance and causes histological damage in the upper intestinal tract that resembles clinical CD. In contrast, the DSS model involves oral administration of the chemical and results in inflammation, which is similar to UC symptoms in humans. Although all these models have limitations in fully replicating human UC, they are practical and increasingly used to improve our understanding of UC pathophysiology and develop new therapeutic approaches for IBD. In this thesis study, the focus will be on the DSS-induced colitis model.

1.3.3 Dextran sodium sulfate -induced colitis

Dextran sodium sulfate (DSS) is a widely used chemical for inducing colitis in animal models and has been extensively studied in different rodents since its first use in 1985 (119). In the this model, colonic inflammation is induced by adding DSS to the drinking water, and depending on the concentration, duration, and frequency of DSS administration, acute or chronic colitis can be induced (120). Despite certain differences, the DSS model resembles the major clinical and histopathological features of human UC, including weight loss, alterations in stool consistency, blood in the stool, shortening of the colon, reduced physical activity, and decreased food and water intake (121). In terms of histological manifestations, both human and DSS-induced colitis exhibit mucosal damage, crypt distortion, and infiltration of neutrophils into the lamina propria and submucosa (122). Several molecular indicators that are common to both human UC and DSS-induced colitis include elevated myeloperoxidase (MPO) levels and increased of

Introduction

pro-inflammatory cytokines such as IL-12, IFN- γ , TNF- α , and IL-1 β (123, 124). The level of MPO, an enzyme released from neutrophils, indicates the level of neutrophil infiltration and has a direct correlation with disease severity in both IBD patients and DSS-exposed animals (123, 125). Based on the characteristics of colitis, this model is suitable for studying the effect of intestinal flora on the progression of colitis. Reduced expression of tight junction proteins (e.g., occludin) in the epithelium, as well as increased intestinal permeability for luminal bacteria, are additional significant features that both human IBD and DSS-induced colitis have in common (126).

2 Objective

The thesis objectives were to:

- Cultivate and characterize different designed microbiomes consisting of *Faecalibacterium prausnitzii*, *Roseburia intestinalis*, and *Bacteroides faecis*.
- Investigate the therapeutic potential of the three commensal bacterial species individually and in combination in an *in vitro* model of intestinal inflammation.
- Investigate the therapeutic potential of the three commensal bacterial species in an acute DSS-colitis animal model

3 Material and Methods

3.1 Materials

3.1.1 Chemicals and Reagent

Chemicals and Reagent	Manufacturer
Agar (Agar technical No.3)	Oxoid Ltd., Basingstoke, England
Acrylamid 40 %	Bio-Rad-Laboratories, Hercules CA, USA
Ammoniumpersulfat	Sigma-Aldrich Chemie GmbH, Steinheim
Bovine serum albumin	Sigma-Aldrich Chemie GmbH, Steinheim
Brain heart infusion (BHI)	Oxoid Ltd., Basingstoke, England
Cellobiose	Sigma-Aldrich Chemie GmbH, Steinheim
Cysteine	Sigma-Aldrich Chemie GmbH, Steinheim
4',6-diamidino-2-phenylindole (DAPI)	Roche, Mannheim, Germany
Dextran sodium sulfate (DSS) MW: 35,000–50,000	MP Biomedical, LLC, Santa Ana, CA, USA
Dimethylsulfoxid (DMSO)	Sigma-Aldrich Chemie GmbH, Steinheim
Dulbecco's MEM	Biochrome AG
Ethylenediaminetetraacetic acid (EDTA)	Sigma-Aldrich Chemie GmbH, Steinheim
Eosin 0.5%	Carl-Roth GmbH + Co., Karlsruhe, Germany
Ethanol (70%, 96 %)	Merck KGaA, Darmstadt, Germany
Ethidiumbromid	Sigma-Aldrich Chemie GmbH, Steinheim
Fluorescein isothiocyanate dextran	Sigma-Aldrich Chemie GmbH, Steinheim
Glycerin (99 %)	Carl-Roth GmbH + Co., Karlsruhe, Germany
Histofix 10%	Carl-Roth GmbH + Co., Karlsruhe, Germany
Hematoxyline	Carl-Roth GmbH + Co., Karlsruhe, Germany
Hemin	Sigma-Aldrich Chemie GmbH, Steinheim
Hydrogen peroxide 35 %	Merck KGaA, Darmstadt, Germany
LIVE/DEAD Cell Vitality Assay	Invitrogen, Karlsruhe, Germany
Mayer's Hämalaun	Morphisto GmbH, Germany
MEM Non-essential Amino Acid (100x)	GI BCO, Life Technologies
Methanol	J.T.Baker, Deventer, Holland
Novamine	Zentiva Pharma GmbH, Germany
Odyssey® Blocking Buffer	Licor Bioscience_GmbH
PageRuler™ Prestained Protein Ladder	ThermoFischer Scientific, Waltham, MA, USA

Material and Methods

Penicillin/Streptomycin-stock solution (1%)	Invitrogen, Life Technologies, Fisher Scientific,
Phosphate Buffered Saline (PBS) 10x	GIBCO, Life Technologies
RIPA-Lysis Buffer, 10x	Merck Millipore, Darmstadt, Deutschland
Rotiphorese®Gel 30	Carl Roth GmbH + Co. KG Deutschland
Sodium Acetate	Merck KGaA, Darmstadt, Germany
Sodiumchlorid	Carl-Roth GmbH + Co., Karlsruhe, Germany
Sodiumcitrat	Fluka Chemie AG, Buchs, Switzerland
Sodiumdihydrogenphosphat	Merck KGaA, Darmstadt, Germany
Sodiumdodecylsulfat (SDS)	Serva, GmbH, Heidelberg, Germany
Sodium acetate	Merck KGaA, Darmstadt, Germany
Trizma® base	Merck KGaA, Darmstadt, Germany
TEMED	Sigma-Aldrich Chemie GmbH, Steinheim,
Tris-Hydrochlorid (Pufferan R)	Carl-Roth GmbH + Co., Karlsruhe, Germany
Triton X-100	Carl-Roth GmbH + Co., Karlsruhe, Germany
Trypanblau	Sigma-Aldrich Chemie GmbH, Steinheim,
Trypsin EDTA (5 %)	GIBCO, Life Technologies
Tween 20	Serva, GmbH, Heidelberg, Germany
Yeast extract	Oxoid Ltd., Basingstoke, England
Xylene	J.T.Baker, Deventer, Holland
β-Mercaptoethanol	Sigma-Aldrich Chemie GmbH, Steinheim

3.1.2 Consumables

Consumable	Manufacturer
Cell culture flask (75 cm ²)	Greiner Bio-One, Kremsmünster, Österreich
Cell culture plate (6, 12, 24, 96 well-plates)	Greiner Bio-one, Kremsmunster, Osterreich
Cotton swabs	Hartmann
Cryotube (2 ml)	Biozym
Disinfectants AHD 2000	Lysoform Dr. Rosemann GmbH, Berlin
Disinfectants Bacillol® AF	Bode Chemie, Hamburg
Disposable Inoculation Loops	Greiner Bio-One, Kremsmünster, Austria
Electroporation cuvettes	peqLab Biotechnologie GmbH, Erlangen
Falcon Tube Cellstar® (15 ml, 50 ml)	Greiner Bio-One, Kremsmünster, Austria
GENbox anaer (bag)	Biometra, Göttingen
Immobilon®-FL PVDF Membran	Merck KGaA, Darmstadt, Germany
Microscope slide	Marienfeld

Material and Methods

Nitrocellulose membrane	Hybridization bottle
Hybridization bottle	Sarstedt AG & Co KG, Nümbrecht, Deutschland
Petri dish 92×16 mm with cam	Gilson, France
Pipettes (10, 20, 100, 200, 1000 µl)	Greiner Bio-One, Kremsmünster, Austria
Pipette tips (10, 20, 100, 200, 1000 µl)	Greiner Bio-One, Kremsmünster, Austria
Roti®-Nylon 0.2, pore size 0.2 µm	Carl-Roth GmbH & Co., Karlsruhe, Germany
Round bottom test tubes (12 x 75 mm)	Roche Diagnostics GmbH, Mannheim
Safe-Lock tubes (0.5, 1.5, 2 ml)	Eppendorf AG, Hamburg
Surgical suture material	Resorba, Medical GmbH, Germany
Syringes (5 ml, 10 ml, 25 ml)	Becton Dickinson.
Transwell inserts 0.4 µm pore size	Sarstedt AG & Co. Germany

3.1.3 Kits

Kits	Manufacturer
LIVE/DEAD® Viability/Cytotoxicity Kit	Invitrogen/ Thermo Fisher Scientific
LEGEND MAX™ Human IL-8 ELISA Kit	BioLegend, Koblenz, Germany
LEGEND MAX™ Human MCP-1 ELISA Kit	BioLegend, Koblenz, Germany
LEGEND MAX™ Human TNFα ELISA kit	BioLegend, Koblenz, Germany
LEGENDplex™ Mouse Th Cytokine Panel 3	BioLegend, Koblenz, Germany
Myeloperoxidase (MPO) ELISA kit	Hycult Biotech. Inc., Plymouth Meeting, PA, USA
Regulatory T cell staining kit	Miltenyi Biotech, Bergisch Gladbach, Germany
Quick-DNA Fecal/Soil Microbe Kits	Zymo Research

3.1.4 Stimulus

Stimuli	Manufacturer
Lipopolysaccharides from <i>E. coli</i> 055: B5	Sigma-Aldrich Chemie GmbH, Steinheim
Recombinant Human Interferon Gamma (IFN-γ)	ImmunoTools GmbH, Germany
Recombinant Human Interleukin 1 beta (IL-1β)	ImmunoTools GmbH, Germany
Recombinant Human Tumor Necrosis Factor alpha (TNF-α)	ImmunoTools GmbH, Germany

Material and Methods

3.1.5 Bacterial strains

Bacterial Strain	Source
<i>Faecalibacterium prausnitzii</i> A2-165 (DSM 17677)	Leibniz Institute, DSMZ-German Collection of Microorganisms and Cell Cultures GmbH
<i>Roseburia intestinalis</i> (DSM 14610)	Leibniz Institute, DSMZ-German Collection of Microorganisms and Cell Cultures GmbH
<i>Bacteroides faecis</i> (DSM 24798)	Leibniz Institute, DSMZ-German Collection of Microorganisms and Cell Cultures GmbH

3.1.6 Device

Devices	Manufacturer
Analytical balance	BP 4100S, Sartorius, Göttingen
Biological safety cabinet class II	Thermo Fisher Scientific, Waltham, USA
Confocal Laser Scanning Microscope, Zeiss LSM 510 Meta	Carl Zeiss AG, Oberkochen, Germany
Refrigerated centrifuge	Thermo Fisher Scientific, Waltham, USA
Freezer -80 °C Type Hera freeze	Heraeus, Hamburg, Germany
Horizontal electrophoresis system	Bio-Rad Laboratories GmbH, Munich, Germany
Incubator B6060	Heraeus, Hamburg, Germany
Microscope CKX41	Olympus Deutschland GmbH, Hamburg
Mini-Max anaerobic workstation	Meintrup DWS Laborgeräte GmbH, Germany
Millicell-ERS volt-ohm meter	Merck KGaA, Darmstadt, Germany
NanoDrop 1000	Thermo Scientific
Odyssey® Imager	Li-Cor Bioscience-GmbH, Bad Homburg
pH-Meter WTW Serie Type pH 720	WTW GmbH, Weilheim
Power supply Model 200/20	Bio-Rad-Laboratories GmbH, Munich
Power supply, Power Pac 3000 B	Bio-Rad-Laboratories GmbH, Munich
Spectrophotometer SmartSpec™ 3000	Bio-Rad-Laboratories GmbH, Munich
Semi-Dry Electrophoretic Transfer Cell	Bio-Rad-Laboratories GmbH, Munich
SpectraMax® M3 Multi-Mode Microplate Reader	Molecular Devices LLC
Thermomixer	Comfort Eppendorf, Hamburg
Vortex-Genie Touch Mixer	Scientific Industries, Bohemia, NY, USA

Material and Methods

3.1.7 Buffer

10 × PBS-Buffer

- KCl 2.0 g
- KH₂PO₄ 2.4 g
- Na₂HPO₄ 14.4 g
- NaCl 80.0 g
- dH₂O 1 l
- Adjust to pH 7.4

0.5% Crystal Violet

- Crystal violet powder 0.5 g
- dH₂O 80 mL
- Methanol 20 mL

1% SDS

- SDS 1g
- dH₂O 100 ml

10X Tank Buffer

- Tris-Base 30.28g
- SDS 10g
- Glycine 144.130g
- Adjust to pH 8
- Top up to 1 L with dH₂O

10× Transfer Buffer

- Tris-Base 30.28g
- Glycine 144.130g
- Adjust to pH 8
- Top up to 1 L with dH₂O
- 1X= 100ml+200 ml methanol+ 700 ml dH₂O

Material and Methods

10× TBS

- Tris-Base 30g
- NaCl 88g
- KCl 2g
- dH₂O 800ml
- pH adjust to 7.6 with HCl
- Top up to 1 L
- 1X 100ml + 900 ml dH₂O and 2 ml Tween 20

1.5 M Tris-HCl

- Tris base (18.15 g/100 ml) 27.23 g
- dH₂O 80 ml
- Adjust to pH 8.8 with 6 N HCl
- dH₂O to 150 ml

0.5 M Tris-HCl

- Tris base 6.06 g
- dH₂O 60 ml
- Adjust to pH 6.8 with HCl
- dH₂O to 100 ml

Material and Methods

3.2 *In vitro* Methods

3.2.1 Bacterial culture medium

3.2.1.1 *Anaerobic brain-heart infusion broth*

Brain-heart infusion (BHI) medium was prepared by adding various ingredients (Table 1) to 1 litre of ultra-pure water in screw-capped bottles. The medium was autoclaved at 121°C for 20 min on the same day. After autoclaving, the medium was cooled down to 55°C and the bottle was transferred into the anaerobic workstation. The medium was used within 2 weeks after preparation.

Table 1. Components used for the preparation of anaerobic brain-heart infusion broth.

Component	Amount
BHI Powder	37 g
Yeast Extract	0.5% (w/v)
Haemin	5 mg/ml
L-Cystein	0.5 mg/ml
Cellobiose	1mg/ml
Maltose	1mg/ml
dH₂O	1 L

3.2.1.2 *Anaerobic brain-heart infusion agar*

Supplemented BHI broth (YBHI) was prepared as described in section 3.2.1.1. For the preparation of anaerobic YBHI agar plates, 15 g/L of agar were added to the prepared medium before autoclaving at 121°C for 20 min. The autoclaved was medium allowed to cool, and then poured into petri dishes. The agar plates were left uncovered for at least an hour to set and dry, and once set they were stored upside down in a plastic bag inside the anaerobic workstation until use.

3.2.2 Long term storage of bacterial cultures

All three bacterial species were stored at -80°C for long term storage using glycerol as cryoprotectant. Bacterial cultures were grown in anaerobic YBHI broth. 700 µl overnight

Material and Methods

culture of the respective species was mixed with 300 μ l anaerobic glycerol (99%) and were stored at -80°C . Repeated freeze-thawing was avoided as it affected the viability of the bacteria.

3.2.3 Growth behaviour

Faecalibacterium prausnitzii (*F. prausnitzii*) strain A2–165, *Roseburia intestinalis* (*R. intestinalis*) and *Bacteroides faecis* (*B. faecis*) were routinely maintained at 37°C in the BHI medium (brain-heart infusion) supplemented with 0.5 % (w/v) yeast extract, 1mg/ml cellobiose, 1mg/ml maltose, 0.5 mg/ml L-cysteine and 5mg/ml hemin without agitation in an anaerobic atmosphere of 10 % CO_2 , 10 % H_2 , and 80 % N_2 . The same culture medium composition was used for the cultivation of *B. faecis*, however, without addition of hemin. To plot standardized growth curves of the respective bacterial species (absorbance versus time) 50 μ l of frozen bacterial stocks were inoculated into 10 ml of anaerobic YBHI medium inside an anaerobic workstation and were incubated for 24 hours (primary overnight culture). Hundred μ L of primary overnight culture were used to inoculate 10 ml of anaerobic YBHI. Samples were collected at hourly intervals over 26 hours. The optical density at a wavelength of 600 nm (OD_{600}) was measured using a spectrophotometer and recorded. Growth curves were generated using the averages of three biological replicates with three technical replicates each. The bacterial species were grown to the mid-logarithmic phase for the experiments consistency because metabolic activity differs between growth phases (127).

3.2.4 Colony forming units

CFU stands for "colony forming units" and is a measure of the number of viable bacteria present in a sample. To determine the CFU of the bacterial species, different dilution of the bacterial suspension was prepared using anaerobic PBS inside an anaerobic workstation. Twenty μ l of diluted bacteria suspension were pipetted on the anaerobic YHBI agar plate. The plates were incubated inside an anaerobic workstation for around 48 h, or until bacterial colonies were visible. The bacterial colonies per plate were counted and numbers in a range of 10 to 100 colonies were considered for the calculation of the viable CFU per millilitre. Incubation of intestinal epithelial cells with the individual bacterial species and with a three species bacterial mix was performed in an anaerobic chamber at three different multiplicity of infections (MOI) (100:1, 1000:1 and 10000:1 bacteria/cell).

Material and Methods

3.2.5 Preparation of *Faecalibacterium prausnitzii*

For each experiment, a frozen stock culture of *F. prausnitzii* was thawed in an anaerobic chamber. Twenty μL of thawed culture were plated on an agar plate for 24 to 48 hours. A single colony was then taken with an inoculating loop and used to inoculate 10 ml of anaerobic YBHI broth that was grown for 24 hours inside an anaerobic workstation (primary culture). To prepare the secondary culture, 100 μL of the primary culture were inoculated into 10 mL of fresh anaerobic YBHI broth. The inoculum in the conical tube was grown statically for 14 to 16 hours to give a mid-logarithmic phase culture.

3.2.6 Preparation of *Bacteroides faecis*

The primary culture of *B. faecis* was prepared as described in section 3.2.3. However, for this species, YBHI medium without hemin was used. One hundred μL of primary culture was inoculated into 10 mL of fresh anaerobic YBHL broth (secondary culture) and the inoculum in the conical tube was statically grown for 14 to 16 hours to give a mid-logarithmic phase culture.

3.2.7 Preparation of *Roseburia intestinalis*

The primary broth culture of *R. intestinalis* was prepared by inoculating 10 ml of anaerobic YBHI broth in a conical tube with 100 μL of frozen culture inside an anaerobic workstation. The primary cultures were incubated for 24 hours. Afterward, the secondary overnight culture was prepared by subculturing 100 μL of the primary culture into 10 ml of anaerobic YBHI broth. Bacteria in mid-logarithmic phase were obtained by incubating secondary overnight cultures for 6 hours.

3.2.8 Preparation of bacterial cultures

Secondary overnight culture of *F. prausnitzii* (section 3.2.5) and *B. faecis* (section 3.2.6) and *R. intestinalis* (section 3.2.7) were centrifuged at 3000 rpm for 7 minutes and resuspended in anaerobic cell culture medium inside an anaerobic workstation to the final concentration of 2×10^9 CFU/ml and 2×10^{10} CFU/ml by measuring absorbance at 600 nm (OD range from 0.6 to 0.8). The experiments described above were performed under strictly anaerobic conditions. The number of bacteria in the solution was calculated by counting the number of viable bacteria. To get a reasonable number of colonies to count, bacterial samples were serially diluted and plated. The number of CFU/ml was calculated by counting the colonies on each plate and multiplying them by the dilution factor as described in section 3.2.4.

Material and Methods

3.2.9 Intestinal epithelial cells

Human colon carcinoma cell lines Caco-2 and HT29-MTX were purchased from Merck (MerckCo., Darmstadt, Germany). The Caco-2 cell line originates from human colonic epithelial adenocarcinoma cells. This cell line is widely employed in gut cell biology, due to its ability to establish polarized monolayers in culture and exhibit differentiation characteristics similar to normal gut cells. HT29-MTX cells are mucus-producing goblet cells. The HT29-MTX and Caco-2 cells were used in the experiments at passages 12–30 and 10–33, respectively. All the cell culture work were done under laminar flow hood (class II biological safety cabinet).

3.2.10 Maintenance of Caco-2 and HT29-MTX

Both cell lines were grown separately in tissue culture flasks in Dulbecco's Modified Eagle Medium (DMEM) supplemented with 10% (v/v) heat-inactivated fetal bovine serum (FBS), 2 mM L-glutamine and 1% (v/v) non-essential amino acids (MEM NEAA). They were incubated in a humidified atmosphere (5% CO₂) at 37°C. Both cell lines were sub-cultured once a week at 80-90% confluence and reseeded into new culture flasks. The cell medium was replaced with fresh medium every two to three days.

3.2.11 Long term storage of Caco-2 and HT29-MTX

Each cell line was separately stored in liquid nitrogen for long-term storage. To generate frozen stocks, the cells were harvested using 0.1% Trypsin. The trypsinized cells were then centrifuged and resuspended in frozen media (FBS with 10% dimethyl sulfoxide [DMSO]). From this cell suspension, a 1 ml aliquot (1×10^5 cells/ml) was added to a cryogenic vial. The vials were transferred into a Mr. Frosty container (Nalgene, Penfield, New York, USA) and stored overnight at -80°C. The Mr. Frosty™ Freezing Container, filled with 100% isopropanol, facilitated a gradual freezing process at a cooling rate of around 1°C per minute. On the following day, the frozen stocks were moved to a liquid nitrogen tank for long-term storage.

3.2.12 Thawing of frozen cells

The cryotubes were removed from the liquid nitrogen tank and promptly thawed in a 37°C water bath. The DMSO-cell mixture was then carefully transferred to a centrifuge tube, where it was supplemented with warm DMEM to reach a volume of 5 ml. Following centrifugation (200g, 5 min, 21°C), the supernatant was discarded, and the cell pellet was resuspended in 1 ml

Material and Methods

of cell medium. The resuspended cells were then seeded into a small cell culture flask (T25), to which 9 ml of warm supplemented DMEM cell culture medium was added. The flask was subsequently placed in an incubator set at 37°C with 5% CO₂. Cells growth was monitored microscopically after 24 hours, and the cell medium was replaced after 48 hours. Upon reaching 80% confluence, the cells were transferred to a large flask for use in experimental studies.

3.2.13 Preparation of eukaryotic cell

To separate cells for experimental studies from a culture flask, adherent cells were treated with 0.1% Trypsin and incubated at 37°C. After 15 minutes of incubation, the trypsinized cells were washed with warm DMEM and the cell suspension removed. The cells were centrifuged at 300 x g for 3 minutes, and the supernatant was then aspirated. The cell pellet was re-suspended with 5 ml DMEM. To determine the number of cells, 30 µl of the cell suspension was added to 30 µl of a 0.4% trypan blue solution in a test tube, and the mixture was carefully pipetted up and down. Subsequently, 10 µl of the stained cell suspension was introduced into the Neubauer counting chamber. Four large squares were counted under the microscope, and the number of cells per ml was calculated. The average cell count from each square was then multiplied by 10,000 (10⁴). The final value represents the concentration of viable cells per mL in the original cell suspension.

3.2.14 Growing intestinal epithelial cell lines on Transwell inserts

To simulate a biological barrier similar to the epithelial cell barrier in the gastrointestinal tract, Caco-2 and HT29-MTX cells were seeded on Transwell cell culture inserts. Transwell inserts are a common technique for cultivating epithelial cells and cell differentiation (Figure 4).

Transwell inserts with semi-permeable polyester membranes create a dual compartment, where the apical medium in the insert is separated from the basal medium in the cell culture well. The cells were harvested and counted as described in section 3.2.13. The dilution needed to obtain a seeding density of 0.75×10^5 cells/ml was calculated using the counted number of live cells. The cell suspension was diluted with DMEM and 250 µL of this diluted cell suspension was seeded onto the apical compartment of each Transwell insert. The inserts were kept in 24-well cell culture plates and each well was filled with 800 µL of DMEM. The Transwell inserts in the cell culture plates were incubated at 37°C with 5% CO₂. Every second day medium was changed by carefully removing the media from the apical and basal compartments, new DMEM was added drop by drop to the apical compartment, and the basal well. For 21 days, the cells

Material and Methods

were cultured on Transwell inserts to form a differentiated cell monolayer. The co-culture experiments were carried out using these differentiated cell monolayers.

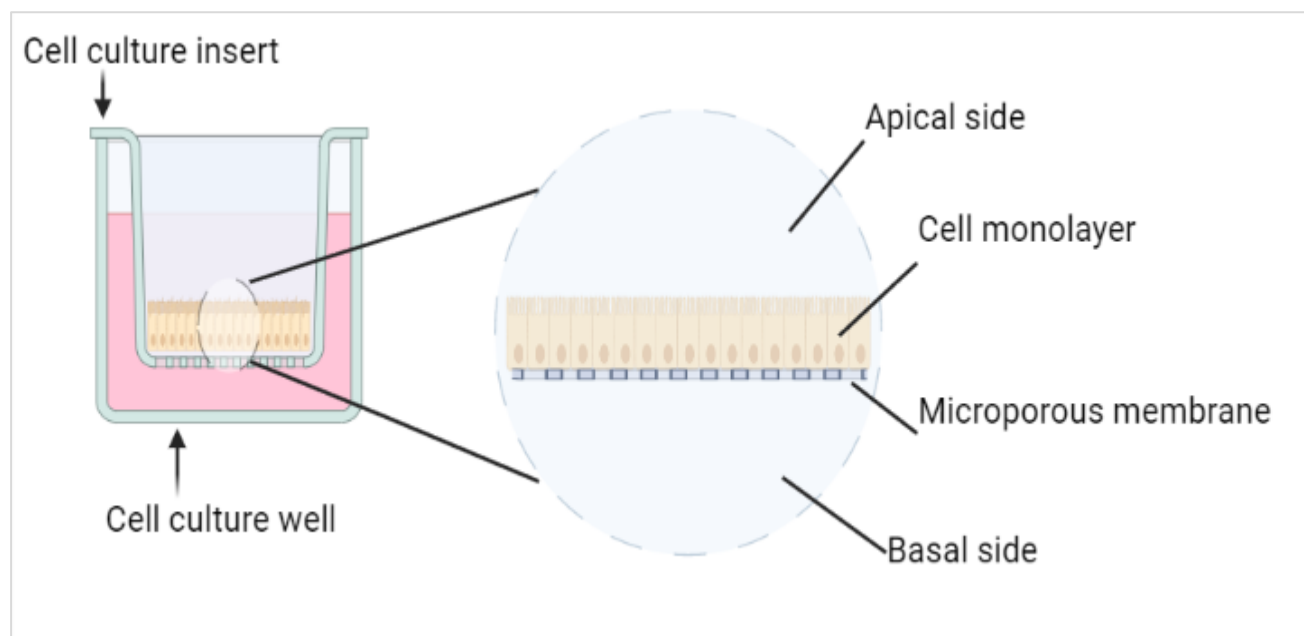


Figure 4. Illustration of a Transwell cell culture insert.

3.2.15 Transepithelial electrical resistance

Transepithelial electrical resistance (TEER) is a measurement of electrical resistance across a cellular monolayer and is a very sensitive and reliable method to confirm the integrity and permeability of the monolayer. The integrity of Caco-2 or HT29-MTX cell monolayers was assessed by measuring TEER prior to every experiment to assess if the cells seeded on the Transwell insert formed a differentiated monolayer. TEER was measured using a Millicell-ERS volt-ohm meter and a STX-2 electrode (Figure 5A). 70% ethanol was used to sterilize a STX-2 electrode. The electrodes were air dried and rinsed with cell culture medium before being connected to an EVOM voltohmmeter according to the manufacturer's instructions. As shown in Figure 5B, the electrode was placed vertically in the cell culture well, so that the tip of the longer electrode touched the bottom of the well, and the shorter electrode was above the membrane of the Transwell insert. The TEER was measured by pressing and holding the 'R' (resistance) button on the voltohmmeter for 3 seconds until the reading stabilized. In every co-culture experiment, only cell monolayers with TEER values exceeding 600 ohm/cm² were

Material and Methods

chosen. This is a commonly accepted value, indicating the presence of fully differentiated cell monolayers. An insert without cells was used as a blank. The resistance read by the voltohmmeter was converted to TEER ($\Omega \cdot \text{cm}^2$). To calculate the sample resistance (Ω), the blank value was subtracted from the total resistance of the sample. The final unit area resistance ($\Omega \cdot \text{cm}^2$) was calculated by multiplying the sample resistance by the effective area of the membrane (0.33 cm^2 for 24-well Millicell inserts).

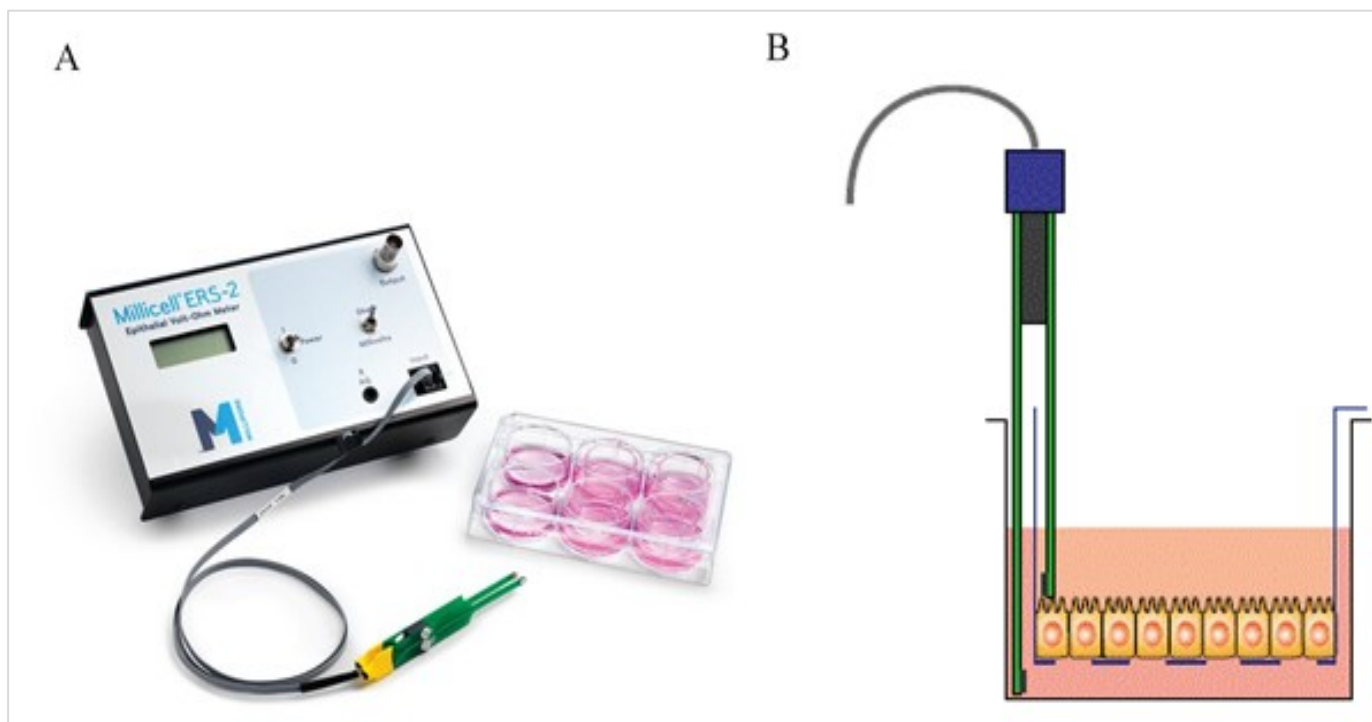


Figure 5. Transepithelial/endothelial electrical resistance (TEER) measurement using EVOM instrument.

(A) The Millicell ERS-2 unit with an STX chopstick electrode. (B) a drawing of the electrode placed in a tissue culture insert.

3.2.16 Trypan Blue staining

Cell viability was determined using trypan blue dye. Cells were seeded in 24-well plates and exposed to aerobic and anaerobic conditions for 24 hours, then trypsinized and resuspended in DMEM with 10% heat-inactivated FCS to inactivate the trypsin. The cells were stained with a 0.4% trypan blue solution in a ratio of 1:2. Trypan blue stains dead cells because the integrity of the membrane is compromised. The viable cells remain unstained. After staining, viable cells were counted using a Neubauer chamber and an inverted light microscope.

Material and Methods

3.2.17 Live/Dead staining

The live/dead assay is a common method for staining viable and dead eukaryotic cells. Live cells are characterized by their internal esterase activity, which converts the non-fluorescent calcein AM dye into highly fluorescent calcein, emitting green light. Calcein remains retained within live cells, creating a strong uniform green fluorescence. In contrast, damaged cell membranes allow the entry of ethidium homodimer-1 (EthD-1) dye, which undergoes a 40-fold fluorescence increase upon binding to nucleic acids. This results in a vivid red fluorescence in dead cells. EthD-1 is excluded by intact live cell membranes. The assessment of cell viability relies on these specific physical and biochemical properties of cells. To perform the live/dead cell vitality assay, we used the LIVE/DEAD® Viability/Cytotoxicity Kit. Briefly, Caco-2 and HT29-MTX cells were separately seeded on cover slides for 2-3 days until the cell monolayer are obtained. The cell monolayers were then incubated in an anaerobic workstation for 24 hours. The cells were then treated with live /dead staining reagent. The cells were incubated in the dark for 10 minutes and subsequently analysed with a fluorescence microscope.

3.2.18 Adhesion assay

Adhesion of *F. prausnitzii*, *B. faecis*, and *R. intestinalis* was tested using fully differentiated Caco-2 and HT29-MTX cells. Cells were seeded in 24-well plates at a density of 0.75×10^5 cells/well. The cell culture medium without antibiotics was added to the cells to prevent bacterial clumping or killing during the adhesion assay. The culture medium was changed every other day for 21 days. Bacterial strains were grown in the YBHI medium under an anaerobic condition at 37°C. For adhesion assay bacteria were washed with PBS and adjusted to OD₆₀₀ 0.5. Of this bacterial suspension a multiplicity of infection (MOIs) of 100:1, 1000:1, and 10,000:1 was added to the cell monolayers. After 4 hours incubation, the cells were washed with PBS to removed non-adherent bacteria. The cell monolayers were then detached from plate surfaces by 0.25% trypsin–EDTA solution. Detached cells were lysed by cold distilled water and plated out in serial dilution steps on the YBHI agar plate. The number of viable bacteria was assessed by counting the CFU on agar plates incubated under an anaerobic atmosphere at 37°C for 48 h. The adhesion was expressed as the percentage of the number of adhered bacteria in relation to the total bacteria used as inoculum.

Material and Methods

3.2.19 Effect of bacterial density on cell barrier permeability

To determine the effect of bacterial density on cell barrier permeability, differentiated Caco-2 and HT29-MTX cell monolayers were co-cultured with *F. prausnitzii*, *B. faecis*, and *R. intestinalis*. The culture medium was changed 24 hours before the start of the experiment. Prior to washing the cells with PBS, the TEER was measured. Cell monolayers were incubated with all three bacterial species at three different multiplicities of infection (MOI) (100:1, 1000:1, and 10000:1 bacteria/cell) in an anaerobic chamber. TEER values were measured and recorded before, directly after bacterial inoculation, and 3 and 6 hours after exposure to bacteria. The effect of the bacteria on barrier permeability was expressed as the change in TEER at each time point after the treatments were added.

3.2.20 Induction of barrier dysfunction

Pro-inflammatory cytokines produced by gut-associated immune cells and epithelial cells in response to the increased accumulation of luminal antigens contribute to the alteration of TJ protein expression thus increased permeability of the intestinal epithelium. In order to mimic chronic intestinal barrier dysfunction associated with chronic inflammation Caco-2 and HT29-MTX cells were seeded in Transwell insert as described in section 3.2.14. The differentiated Caco-2 and HT29-MTX monolayer were treated basally with a cocktail of inflammatory mediators consisting of 100 ng/ml tumor necrosis factor- α (TNF- α), 50 ng/ml Interferon γ (IFN- γ), 25 ng/mL Interleukin-1 β (IL-1 β), and 10 μ g/ml lipopolysaccharide (LPS) for 10 and 48 hours, respectively. Cells without any treatment were used as negative control.

3.2.21 Bacterial treatment

In order to investigate the therapeutic properties of *F. prausnitzii*, *B. faecis*, and *R. intestinalis* on inflamed epithelial cell monolayers, first the intact Caco-2 and HT29-MTX cell monolayer was treated with a cytomix + LPS for 10 hours and 48 hours respectively. Following cytomix + LPS stimulation TEER values of the cells were assessed. The cell monolayers were washed with HBSS and incubated apically with the individual bacterial species and with a three species bacterial mix at three different multiplicities of infections (MOI), 100:1, 1000:1 and 10.000:1 bacteria/cell, in an anaerobic chamber. Immediately after the stimulation, the TEER values were measured in the anaerobic environment. The batches were incubated anaerobically for 6 hours. This was followed by measurement of the TEER values. Thereafter, the cells and the apical and basal medium were harvested and stored at -20°C.

Material and Methods

3.2.22 Determination of paracellular permeability

Paracellular permeability was determined by the flux of the fluorescein isothiocyanate (FITC)-labeled dextran 4000 (FD-4) through differentiated Caco-2 and HT29-MTX monolayers. Cell monolayers were pre-incubated with the cytomix + LPS for 10 and 48 hours, respectively, prior to bacterial treatment for 6 hours. Following treatment, the monolayer was washed with PBS to remove any residual bacteria and cells were pre-equilibrated for 1 hour with HBSS buffered at pH 7.4 at 37 °C. Cells were carefully washed twice with PBS and 200 µL FD-4 solution (1 mg/ml in HBSS) was added to the apical side of the monolayers and incubated for 4 hours. Samples (100 µL) were collected from the basal chamber under sink conditions at 0, and 240 min and fresh HBSS solution was substituted with the same quantity. The fluorescent intensity of these basolateral aliquots was determined after sampling using a multi-mode microplate reader (SpecteraMax M3, Molecular Devices). The wavelengths of excitation and emission were 490 and 530 nm, respectively. All tests were carried out as triplicate biological experiments.

3.2.23 Immunofluorescence staining

Fully differentiated Caco-2 and HT29-MTX cell monolayers were stimulated with the pro-inflammatory cytomix + LPS cocktail. Subsequently, cells were treated with bacteria individually and in combination for 6 hours as described above. Following these treatments, monolayers of both cell lines were washed with PBS and fixed with 75% (v/v) ethanol in PBS for 30 min. Fixed monolayers were permeabilized with 75% (v/v) acetone in PBS for 3 min at -20°C. Prior to subsequent staining and detection, monolayers were washed and blocked for 40 min with 1% (w/v) bovine serum albumin (BSA) in PBS. Cells were then incubated with either mouse anti-occludin or rabbit anti-claudin-2 primary antibodies overnight at 4 °C. Cells were rinsed again with washing buffer (PBS+0.05% Tween-20) for 3 times each five minutes, followed by incubation with the Alexa Fluor 488 goat anti-mouse secondary antibody (1:500) and Alexa Fluor 488 goat anti-rabbit secondary antibody (1:500) for 1 hour at room temperature. Cells were rinsed again with washing buffer, and finally incubated with 1µg/ml Hoechst 33342 for 10 minutes to stain all nuclei. The membranes were separated from the Transwell insert using a scalpel. The permeable support membrane was then mounted cell side up between a slide and coverslip with mounting medium. Microscopy of the mounted membranes was performed on a Zeiss LSM 510 Meta Confocal Laser Scanning Microscope.

Material and Methods

3.2.24 Western Blot analysis

Cell monolayers were grown on 24-mm Transwell inserts at a density of 2×10^5 cells/well and cultured for 21 days. Caco-2 and HT29-MTX cell monolayers were treated with the cytomix + LPS cocktail and bacteria (MOI 1000:1) as described before. Cells were lysed with lysis buffer containing phenylmethylsulfonyl fluoride (PMSF), sodium orthovanadate and a phosphatase inhibitor cocktail. After 30 minutes incubation in ice, cell lysates were centrifuged at 12,000 g for 30 minutes at 4°C. The supernatant was removed, and the protein concentration was measured by a bicinchoninic acid (BCA) protein assay kit. This assay relies on a colorimetric technique that detects total protein concentration through observable color changes. The color alteration results from a chemical reaction between the sodium salt of bicinchoninic acid and the cuprous ion produced by the biuret reaction under alkaline conditions. This standard assay proves effective for determining protein concentrations in each homogenized sample. Approximately 25 µg of each sample were denatured, separated by SDS-PAGE, and transferred to nitrocellulose membranes using a Bio-Rad Semidry transfer apparatus. Transfers were conducted at 15 V for 30 minutes. Membranes were subsequently washed with tris-buffered saline/ 1% Tween-20 (TBS-T) and blocked in 5% BSA for 1 hour following by incubation with primary antibody (anti-claudin-2 and anti-occludin) diluted 1:1000 in 5% BSA at 4°C overnight. Membrane was washed and then incubated with IRDye® 800CW Goat anti-Mouse and IRDye® 800CW Goat anti-Rabbit IgG secondary antibody (diluted 1:10000) in 5% BSA for 30 minutes at room temperature. After an additional round of washing, bands were visualized and analysed using an Odyssey imaging system (Li-Cor).

3.2.25 Determination of cytokine secretion by ELISA

The culture supernatants were collected from the basal chamber of cytokine-stimulated cells incubated w/o commensal bacteria, centrifuged (10 min 600× g at 4 °C) and then were analyzed for IL-8 cytokine and MCP-1 chemokine secretion level using Enzyme-linked Immunosorbent Assay (ELISA). ELISA is a common biochemical assay used for the measurement of specific analytes in liquid samples. It was performed on a microwell plate and consists of various steps that include sequentially added, incubated, and washed liquid reagents. First, a primary antibody was introduced to the plate and allowed to bond specifically overnight. To prevent nonspecific binding, the surface of the plate wells was then blocked using a blocking buffer. Cell-free supernatant samples containing the analyte of interest, along with standards featuring a specific analyte content, were added to the wells and underwent

Material and Methods

incubation. Throughout this incubation period, the analyte selectively binds to the capture antibody. To identify the antibody-antigen complex, a second detection antibody, linked to an enzyme was added to each well. The enzyme catalyzed the conversion of a chemical substance added in the next step, resulting in a color signal. To stop this reaction, a stop solution (Sulfuric acid) was subsequently added to the wells. Following this final step, the absorbance was read at 450 nm using spectrophotometry.

Material and Methods

3.3 *In vivo* methods

3.3.1 Study design and bacteria treatment

Male BALB/c mice (specific pathogen-free, SPF) aged 9-11 weeks (19-25 g) were originally purchased from Charles River Laboratories (Sulzfeld, Germany). The animals were housed in a temperature-controlled environment ($22\pm 2^{\circ}\text{C}$) with a 12-h day/night light cycle, a relative humidity of 50-60%, and *ad libitum* access to rodent chow and drinking water. Individual body weights were assessed daily for eight days. All animal experiments were performed under the German animal protection law and the EU Guideline and approved by the German local authority (72221.3-1-039/19). Experimental mice were randomly assigned into eleven groups as illustrated in Figure 6. Acute colitis was induced by adding 3.5% (w/v) DSS to the drinking water for 8 days, and the control group received normal drinking water. *F. prausnitzii*, *B. faecis*, and *R. intestinalis*, and the mixture of all three bacterial species at two concentrations of 10^9 and 10^{10} CFU per 100 μl were administered by oral gavage simultaneously with DSS treatment for up to 7 days. Animals in the positive control group were orally administered mesalazine (200 mg/kg). Animals in the control and DSS groups were gavaged with normal PBS every day. At the end of the experimental period on day 8, the mice were anesthetized with an intraperitoneal injection of ketamine/xylazine cocktail to collect blood samples, followed by cervical dislocation. The colon, stool, and spleen were collected for further analysis.

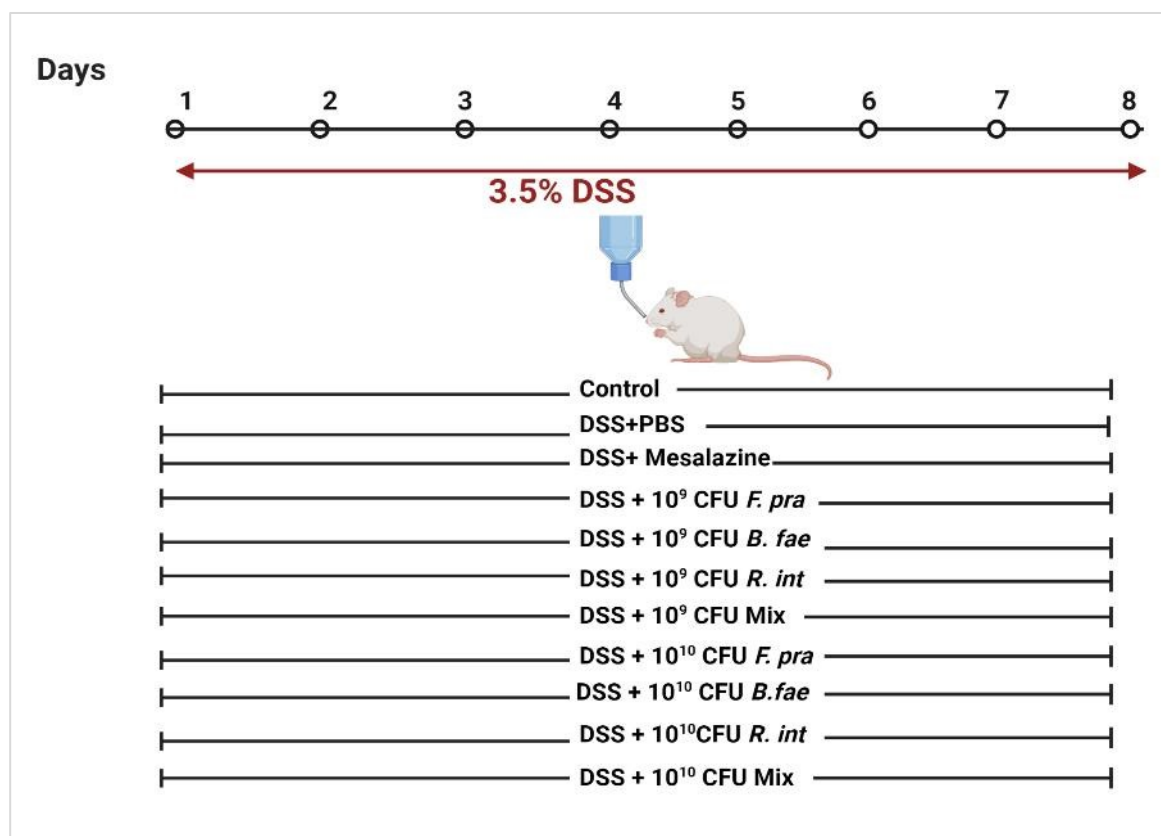


Figure 6. Experimental design for acute colitis induction

3.3.2 Organ removal and tissue preservation

At the end of experiment, mice were euthanized by cervical dislocation, the peritoneum was opened with a median longitudinal incision. Subsequently, the colon segment was removed intact from the ileocecal junction to the distal rectum region. The colon contents were removed, and its weight and length were measured. A portion of the tissue (2×1cm) were transferred to cryotube and snap-frozen in liquid nitrogen and stored at -80°C for later protein (distal colon) extraction.

3.3.3 Clinical scoring of colitis

The body weight of each animal was assessed during the DSS induction, and the faeces were collected daily. The disease activity index (DAI) of mice was calculated daily using the scoring system described by Cooper et al.(128) with minor modifications as shown in Table.2. The DAI includes three aspects: weight change, blood in the stool, and stool consistency. A HemoCARE occult blood detection kit was used to detect blood in faeces. The body weight change was

Material and Methods

calculated relative to day 1. The sum of the weight loss, diarrhea, and bloody stool scores served as the clinical disease score.

Table 2. Disease activity index (DAI) score parameters

Weight Loss	Stool Consistency	Visible Blood in Faeces	Score
<1%	Normal	None	0
1%-5%	Slightly Loose	Slightly Bleeding	1
6%-15%	Loose	Bleeding	2
16%-20%	Diarrhea	Severe Bleeding	3
>20%	–	–	4

3.3.4 Histological analysis

For microscopic histological evaluation, colon segments were kept in Roti®-Histofix 10 % for 24 hours before embedding in paraffin and sectioning (5 µm) with a rotary microtome. Slides were stained with hematoxylin and eosin for microscopic evaluation as per standard methods. Tissue sections were assessed based on extent of inflammation, crypt damage, and neutrophil infiltration (Table 3). The total histological score was generated by adding the single scores to a maximum value of 25. Each section of colon was analysed blinded to the experimental group. Alcian blue staining was done on separate sections to assess the number of mucus producing goblet cells. Briefly, the 5µm colonic paraffin sections were dewaxed in xylene and rehydrated through 95%, 80%, 70%, and 50% ethanol. Sections were then incubated with Alcian blue (1%) pH 2.5 for 30 minutes following by 3 minutes incubation with 3% acetic acid. Next, sections were incubated with nuclear fast red solution (0.1%) and rinsed with dH₂O and were counter-stained using Mayer's hematoxylin solution. Images were obtained using a model BX53 light microscope.

Material and Methods

Table 3. Histological score to quantify the degree of colitis.

Score	Inflammation	Extend	Regeneration	Crypt Damage	% Involvement
0	None	None	-	None	0%
1	Slight	Mucosa	Almost complete regeneration	Basal1/3 damaged	1%-25%
2	Moderate	Mucosa+ Submucosa	Regeneration with crypt depletion	Basal2/3 damaged	26%-50%
3	Severe	Transmural	Surface epithelium not intact	Entire crypt and epithelium lost	51%-75%
4			No tissue repair		76-100%

3.3.5 Intestinal permeability assay

On the last day of the experiment, mice were deprived of food and water for four hours before orally gavaged with fluorescein isothiocyanate (FITC)-dextran solution (4 kDa, 600 mg/kg). Three hours later, blood was collected by retro-orbital bleeding, and serum was isolated. Fluorescence intensity in the plasma of the mice was measured using a multi-mode microplate reader at an excitation/emission wavelength of 490/530 nm. Standard curves for calculating the FITC-dextran concentration were obtained by diluting FITC-dextran in PBS.

Material and Methods

3.3.6 Homogenization of the tissue

Snap frozen distal colon samples were homogenized in tubes containing lysis buffer and 5 × 2.8 mm ceramic beads at 3500 rpm for 20 sec. The lysis buffer contained 200 mM NaCl, 500 mM EDTA, 10mM Trisma HCl, 10% glycerine, 28µg/ml aprotinin, 1 µg/ml leupeptin and 1mM phenylmethylsulfonyl fluoride. Homogenization was followed by 3 rounds of centrifugation (at 4 °C and 15,000 g for 15 min) to eliminate cellular debris. The protein concentration was assessed by a Bio-Rad protein assay kit. The absorbance was read at 595nm using microplate reader.

3.3.7 Myeloperoxidase activity assay

Myeloperoxidase (MPO) level was measured as a biomarker of neutrophil infiltration. Colon tissue samples were homogenized as described in section 3.3.6. The homogenates were centrifuged at 15,000 × g for 15 min at 4°C, and the MPO concentration in the supernatant was measured using an ELISA kit (Hycult Biotech. Inc., Plymouth Meeting, PA, USA) according to the manufacturer's instructions. Briefly, 100 µl of standards and each sample, were transferred into a pre-coated 96-well plate. The plate was incubated for 1 hour in room temperature, followed by four washes with a wash buffer. Subsequently, 100 µl of diluted tracer was introduced to each well, and after an additional 1-hour incubation, 100 µl of diluted streptavidin-peroxidase was applied, followed by another hour of incubation. The plate was washed again before the addition of 100 µl of TMB substrate to each well. After a 30-minute incubation, the stop solution was introduced to each well, and the plate's absorbance was read at 450 nm using a microplate reader.

3.3.8 Measurement of cytokines

The expression level of inflammatory cytokines in colonic tissue was determined using a multiplex mouse T helper cytokine magnetic bead panel following the manufacturer's instructions. The colon tissue homogenate was centrifuged at 15,000 g for 15 minutes at 4°C. The supernatant was used to detect the levels of T helper associated cytokines including IL-2, 4, 5, 6, 9, 10, 13, 17A, 17F, 22, IFN-γ, and TNF-α. The analysis was performed using the BD FACSVerse™ Flow Cytometer, and LEGENDplex™ Data Analysis Software evaluated the data.

Material and Methods

3.3.9 Immunohistochemistry analysis

Immunohistological examinations were performed on 5 μ m thick frozen sections of the colon segment. The sections were dewaxed in xylene 2 times for 10 minutes and dehydrated in a series of graded ethanol solutions (100%, 100%, 95%, 70% and 50% 3 min/solution). The sections were then incubated for antigen retrieval using the heat-induced epitope retrieval method for 20 minutes, followed by endogenous peroxidase inactivation with 3% H₂O₂ in methanol for 10 minutes. Non-specific binding sites were blocked for 1 hour at room temperature in 5% bovine serum albumin (BSA) in PBS. The primary and secondary antibodies were diluted with blocking serum. Then the tissue sections were incubated with the appropriate primary antibodies (Table 4) overnight at 4°C. The following day, the sections were washed three times with PBS and were incubated with the corresponding secondary antibodies conjugated with horseradish peroxidase (HRP) for 1 hour at room temperature. The slides were again washed three times with TBS-T and incubated with the liquid DAB+ 2-component system. This was followed by nuclear staining using Mayer's hematoxylin solution. Histological images were acquired using a microscope. All incubation steps were performed in a humid chamber at room temperature.

Table 4. Primary and secondary antibodies used for immunohistochemical staining.

Primary antibody	Dilution	Secondary antibody	Dilution
Anti-claudin-2 (Rabbit polyclonal) #ab53032 Abcam	1:200	Goat anti-Mouse Secondary Antibody, HRP	1:50
Anti-occludin (Mouse monoclonal) Santa Cruz Biotechnology, #sc-133256	1:50		
E-cadherin (Rabbit monoclonal) #3195T (Cell Signalling Technology, Inc).	1:450	Goat anti-Rabbit IgG Secondary Antibody, HRP	1:50

Material and Methods

3.3.10 Western Blot assay

The colonic tissue was weighed and homogenized in 300 μ l of cold RIPA lysis buffer supplemented with a protease inhibitor. The homogenate protein content was determined using the PierceTMBCA protein assay kit. The proteins, which were previously separated by 10% SDS-polyacrylamide gel electrophoresis according to their molecular weight, were transferred to a polyvinylidene difluoride (PVDF) membrane by Western Blot and detected using specific antibodies. For this purpose, the semi-dry transfer method was used. First, the PVDF membrane was pre-treated with methanol for 2 min then floated in transfer buffer. Afterwards, gels and membranes were sandwiched between buffer-wetted filter papers that are in direct contact with flat-plate electrodes. The membrane was then blocked for 1 hour with 5% BSA before being incubated overnight at 4 °C with the appropriate primary antibody (Table 5). The blot was then washed at least five times for 5 min with 0.1% (v/v) Tween-20 in PBS and incubated for 1 hour at RT with the fluorescent secondary antibodies. After an additional round of washing, the bands were visualized and analysed using the Odyssey[®] CLx Imaging System. Quantification was also performed using Image Studio software.

Table 5. Primary and secondary antibodies used for Western Blot

Primary antibody	Dilution	Secondary antibody	Dilution
Anti-claudin-2 (Rabbit polyclonal) #ab53032 Abcam	1:1.000	IRDye [®] 680RD goat (polyclonal) anti-rabbit IgG (H+L) (LI-COR Biosciences, Lincoln, Nebraska, USA)	1:10.000
Anti-occludin (Rabbit monoclonal) #ab216327 Abcam	1:500		
E-cadherin (Rabbit monoclonal) #3195T Cell Signalling Technology, Inc).	1:1.000		
Anti-β-Aktin (Rabbit monoclonal) (Cell Signaling Technology, Cambridge,UK)	1:10.000		

Material and Methods

3.3.11 Analysis of Treg cells in spleen

To determine Treg subset levels, the spleen from each mouse was collected and carefully crashed to obtain cell suspension. The cell suspensions were passed through a cell strainer (70 μm pore diameter) to obtain single-cell suspensions. The isolated cells were stained with CD4+CD25+ Foxp3+ regulatory T cell staining kit following the manufacturer's instructions. These cell suspensions were centrifuged at 300g for 10 minutes. The supernatant was aspirated, and the cell pellet was resuspended in fresh cell culture medium (DMEM). Next, 1×10^6 splenocytes were incubated with 2 μL of CD4-VioBlue and 2 μL of CD25 antibody for 10 minutes in the dark at 2-8 $^{\circ}\text{C}$. The cells were washed and resuspended in 1 ml of cold and freshly prepared fixation/permeabilization solution, then incubated in the dark for 30 minutes at 2-8 $^{\circ}\text{C}$. Afterward, the cells were washed with cold permeabilization buffer twice before incubated with 2 μL of the Anti-FoxP3 antibody. Following a 30-minute incubation, the cells were washed and centrifuged at 300xg for 5 minutes at 4 $^{\circ}\text{C}$. The supernatant was completely aspirated, and the cell pellet was resuspended in 200 μL of 1 \times permeabilization buffer and proceeded to flow cytometry analysis. Flow cytometry analysis was performed using the BD FACSVerserTM Flow Cytometer. The numbers of Tregs in the spleens were quantified and were expressed as percentages of the CD4 cell population. Post-acquisition analyses were performed using FlowJo software. In flow cytometry analysis, a meticulous gating strategy was employed to discern and quantify specific immune cell subsets, with a particular focus on regulatory T cells (Tregs). The initial gating steps involved singlet and live cell selection to ensure the examination of individual and viable cells. Subsequent gates were set to identify CD4+ cells, indicative of helper T cells, followed by a gate within the CD4+ population to isolate cells expressing CD25, a marker associated with activated T cells. The final gate targeted cells expressing Foxp3 within the CD4+CD25+ subset, pinpointing regulatory T cells. This strategy allowed for the precise identification and quantification of Tregs,

3.3.12 Microbial DNA extraction

To explore the distinct impacts of the treatments on the gut microbiome, fecal samples were collected on the final day of the experiment (day 8) and preserved at -80°C . Subsequently, total genomic DNA was extracted from approximately 50 mg of the fecal sample using *Quick-DNA* Fecal/Soil Microbe Kits (Zymo Research), following the manufacturer's instructions. The purity of the extracted DNA was assessed by measuring the A260/230 and A260/280 ratio using Nanodrop, and the DNA was stored at -20°C until further analysis.

Material and Methods

3.3.13 16S rRNA gene sequencing

For each sample, genomic DNA was isolated and amplified using primers targeting the hypervariable V4 region of the included bacterial 16S rDNA with the following bacterial 16S ribosomal RNA (rRNA) specific primer sequences: 515 F (TCG-TCG-GCA-GCG-TCA-GAT-GTG-TAT-AAG-AGA-CAG-GTG-CCA-GCM-GCC-GCG-GTA-A) and 806R (GTC-TCG-TGG-GCT-CGG-AGA-TGT-GTA-TAA-GAG-ACA-GGG-ACT-ACH-VGG-GTW-TCT-AAT). The amplicon PCR and index PCR, a quantity and quality control, and sequencing of the individual libraries as a pool in one Illumina MiSeq run were performed as described in the Illumina “16S Metagenomic Sequencing Library Preparation” manual. Sequencing on the MiSeq platform using the MiSeq Reagent Kit 600 v3 resulted in 58.090 to 368.468 paired-end reads per individual sample with the length of 300 nt. After quality control with Cutadapt (Version 2.8, Dortmund, Germany) (129) the microbiome analysis was executed using Mothur (Version 1.46.1, Ann Arbor, MI, USA) (130). In brief, paired-end reads were joined, filtered and the primer sequences were removed. Reads were aligned to the SILVA ribosomal RNA gene database (131) and trimmed to the hypervariable region V4. After chimera removal, reads were clustered into a total of 17.588 OTUs representing between 24.517 and 246.192 paired-end reads. Next, OTUs were classified against the SILVA ribosomal RNA gene database and subsampled to 24.000 reads per sample. Graphs were created using GraphPad Prism software version 8.0 (GraphPad Software Ltd, La Jolla, California, United States of America) and Microsoft Excel (Version 2017, Redmond, WA, USA).

3.4 Statistical analysis

Results are expressed as the means \pm SD. For the TEER measurement, the change overtime in TEER values between the different groups were compared using the Mann–Whitney U test. One-way ANOVA was used for statistical analysis of ELISA and Western Blot. A p-value of less than 0.05 was accepted as the level of statistical significance. The *in vivo* results are expressed as the mean \pm SEM. Statistical differences between the groups were evaluated using one-way analysis of variance (ANOVA) followed by Tukey's post hoc tests. In addition, two-way ANOVA followed by Tukey's post hoc test was used to analyze DAI and body weight changes during the experimental period. Differences with $P < 0.05$ were considered significant. All the analyses were performed with Graph-Pad Prism software (GraphPad Prism Inc., San Diego, CA, USA).

4 Results

4.1 Monitoring bacterial growth

The bacterial growth behaviour was studied for 26 hours in an anaerobic chamber using BHI medium supplemented with yeast extract, cellobiose, maltose, L-cysteine, and hemin (Table 1). *F. prausnitzii* and *B. faecis* reached mid-logarithmic phase between 14 and 16 hours of incubation, while *R. intestinalis* already reached stationary phase after 6 to 8 hours (Figure 6). However, for operational reasons (i.e. subculture bacteria at night), the 16-hour old secondary cultures of *F. prausnitzii* and *B. faecis*, as well as the 6-hour old secondary culture of *R. intestinalis*, were deemed to be at mid-logarithmic phase and prepared for the experiments described in the following sections.

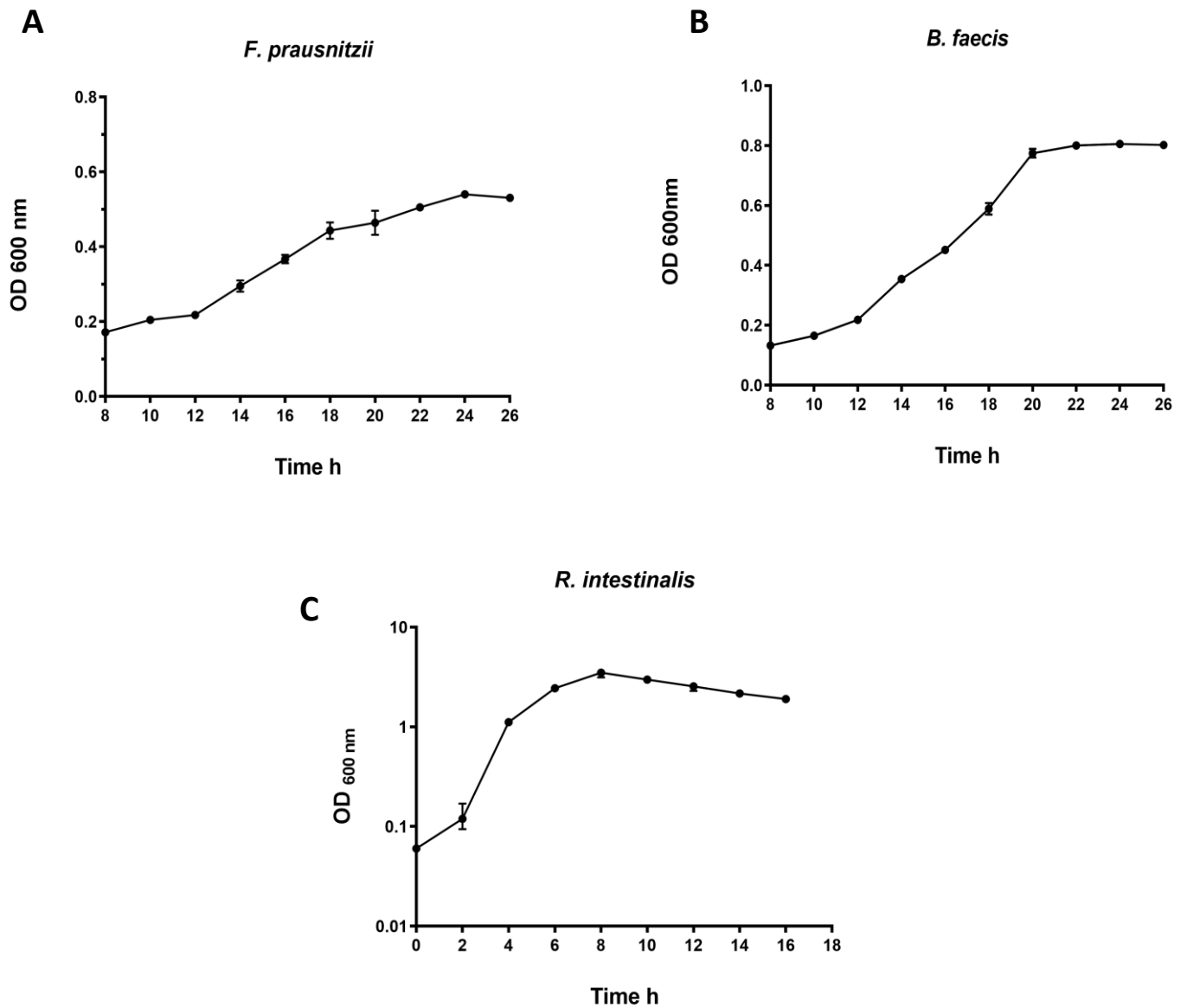


Figure 6. The growth curve of *F. prausnitzii*, *B. faecis*, and *R. intestinalis*. Each curve depicts the mean \pm SD, OD₆₀₀ nm over time (h). The three bacterial species were cultured in supplemented BHI medium at 37°C in an anaerobic chamber, and optical density was measured at 600nm every hour for 18 to 26 hours.

4.2 Viability of the commensal bacteria in cell culture medium

The growth behaviour of *F. prausnitzii*, *B. faecis*, and *R. intestinalis* was studied in anaerobic cell culture medium. The prerequisite for bacterial-cell co-culture experiments was the survival of bacteria in the cell culture medium. Eukaryotic cells cannot survive in bacteria-adapted media like supplemented brain heart infusion (BHI).

Result

The ability of these commensal species to survive in anaerobic cell culture medium (DMEM + NEAA) at 37°C in an anaerobic chamber was determined. The cell culture medium (DMEM) was placed into the anaerobic chamber 48 hours before the start of the experiment. To enable bacterial growth when co-cultured with eukaryotic cells, no antibiotics were added to anaerobic DMEM medium. The culture optical density (OD₆₀₀ nm) was measured over 12 hours. After 6 hours of incubation in cell culture media, all three bacterial species showed a decrease in OD₆₀₀ nm compared to earlier time periods. In contrast, incubation in supplemented yeast brain heart infusion (YBHI) medium did not result in a decrease in OD₆₀₀ nm (Figure 7). Based on these experimental results, DMEM was used for co-cultivation of commensal microorganisms and eukaryotic cells within a maximum time frame of 6 hours for the following in vitro experiments.

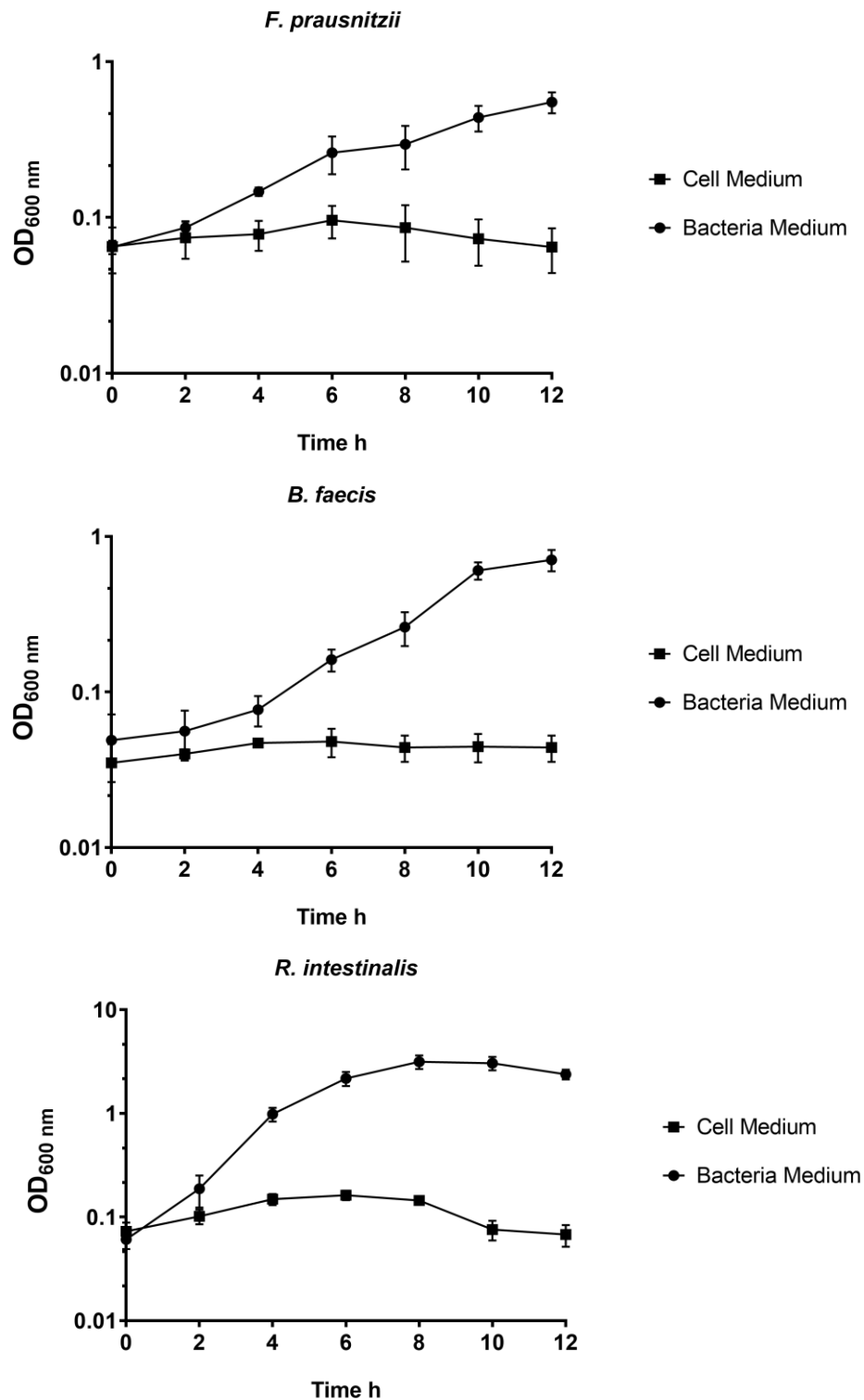


Figure 7. Growth curve for *F. prausnitzii*, *B. faecis*, and *R. intestinalis* in anaerobic cell culture medium and bacteria culture medium.

Each graphs show the growth behavior of *F. prausnitzii*, *B. faecis*, and *R. intestinalis* in anaerobic cell medium and anaerobic bacteria medium for a period of 12 hours, determined at OD 600 nm. (mean \pm SD; n = 3).

4.3 Cultivation of eukaryotic cells under anaerobic conditions

In the first series of the experiments, the viability of cell monolayer under anaerobic conditions was analyzed. Therefore, the number of viable cells between samples were compared following incubation in aerobic or anaerobic atmosphere.

Compared to aerobic conditions, all cells exhibited decreased survival in anaerobic conditions. Nevertheless, Caco-2 and HT29-MTX cells were able to survive in anaerobic conditions for up to 24 hours, with survival rates of nearly 70% and 50%, respectively (Figure 8 A and Figure 9 A). A decrease in viability for both differentiated epithelial cell lines indicated that Caco-2 and HT29-MTX cells have a limited ability to tolerate anoxic conditions. The fact that both cell lines were able to survive in anaerobic conditions for at least 24 hours is interesting, as it suggests that these cells have some ability to tolerate low-oxygen environments. However, the decrease in viability indicates that their tolerance is limited. To confirm these results and visually document the cellular behavior, cells were stained with Live/Dead dye and monitored via fluorescence microscopy. Cells incubated in an aerobic environment for 24 hours show a high level of green, fluorescent calcein AM staining, which proves the viability of the cells. However, both cell lines show noticeable increased EthD-1 staining after 24 h of incubation in an anaerobic workstation (Figure 8 B and Figure 9 B). This leads to the conclusion that the majority of cells are dead. The microscopic images fully support the results of the viability assay. It is important to note that these results may vary depending on the specific experimental conditions, such as the duration of anaerobic exposure, the cell culture medium used, and the specific cell line being studied.

Result

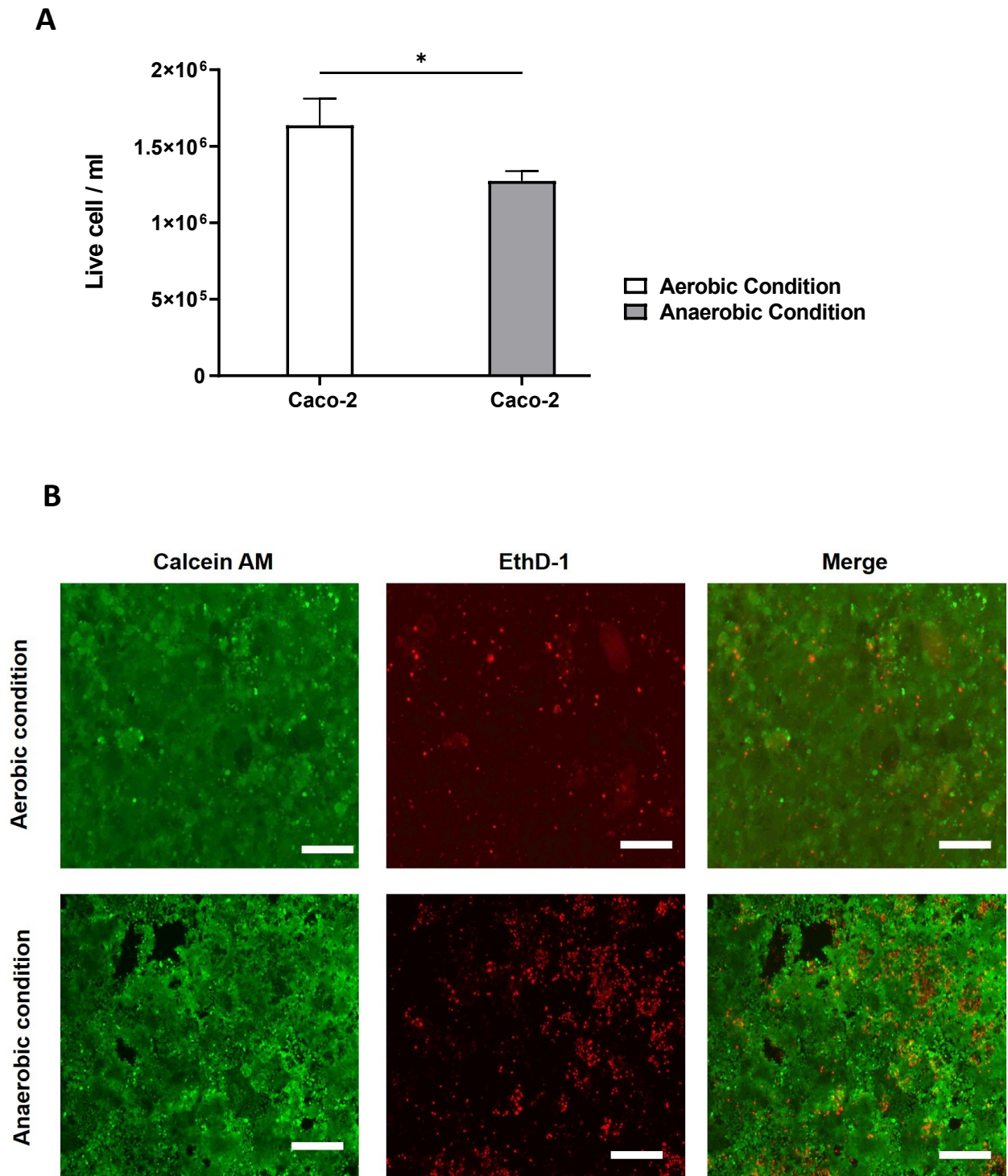


Figure 8. Survival of differentiated Caco-2 under aerobic and anaerobic conditions. (A) shows the number of viable cells per milliliter compared between aerobic and anaerobic cultivation conditions. Data were analyzed with the Mann–Whitney-U test, $*P < 0.05$. (B) Immunofluorescence images of Caco-2 cells stained with Live/Dead dyes after 24 h in aerobic and anaerobic conditions. Calcein AM (green) visualizes live cells, and EthD-1 (red) marks dead cells. Scale bar: 200 μm .

Result

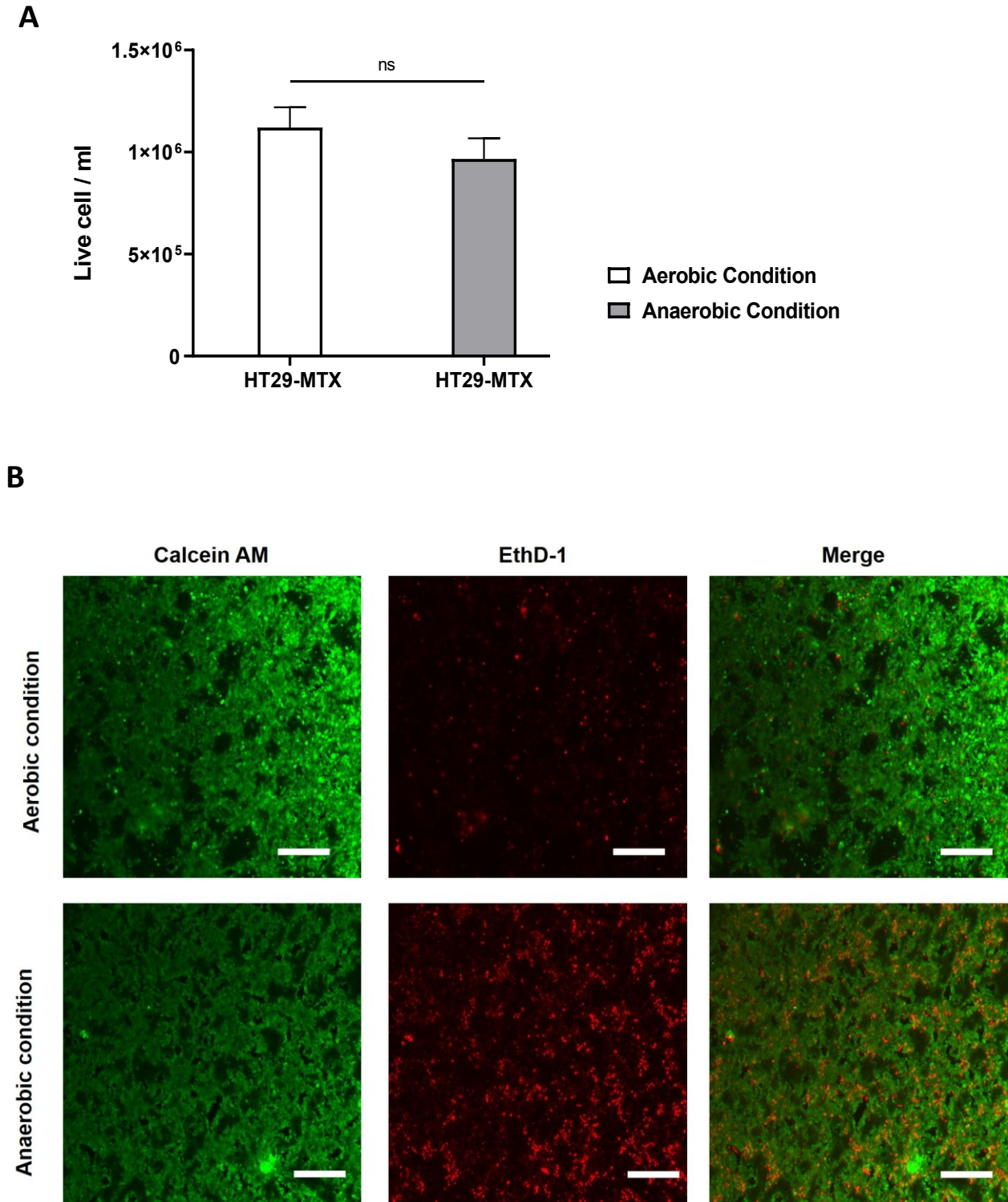


Figure 9. Survival of differentiated HT29-MTX under aerobic and anaerobic conditions. (A) shows the number of viable cells per milliliter compared between aerobic and anaerobic cultivation conditions. Data were analyzed with the Mann–Whitney-U test, ns= not significant. (B) Immunofluorescence images of HT29-MTX cells stained with Live/Dead dyes after 24 h in aerobic and anaerobic conditions. Calcein AM (green) visualizes live cells, and EthD-1 (red) marks dead cells. Scale bar: 200 μ m.

Result

4.4 Bacterial adherence to intestinal epithelial cells

Exploring the adhesive properties of commensal bacteria to host cells is a crucial aspect in assessing the colonization potential of a probiotic strain. Therefore, we quantified the adhesion capability of *F. prausnitzii*, *B. faecis*, and *R. intestinalis* to the intestinal epithelial cells Caco-2 and HT29-MTX under anaerobic condition. The differentiated epithelial cells were separately challenged with live *F. prausnitzii*, *B. faecis*, and *R. Intestinalis* using multiplicity of infection (MOI) values ranging from 100 to 10000 in an anaerobic chamber. The results, presented in Table 6, compare both cell lines incubated with each commensal bacterium. The number of adhering bacteria was dependent on the density of inoculum. All the species tested at a low MOI of 100:1 adherence to the Caco-2 and HT29-MTX cells reached values below the detection limit of this assay. However, the maximum adhesion to both cell lines was shown at MOI of 1000:1. Among all three bacterial species, *B. faecis* showed the highest adhesion to the Caco-2 and HT29-MTX with values of 2.49 ± 1.14 and 6.40 ± 1.46 percent of the inoculum attached to the cells, respectively. *F. prausnitzii* also adhered to both target cell lines; however, the capacity was not as pronounced compared to *B. faecis* (1.51 ± 0.65 and $1.32 \pm 0.94\%$, respectively). Only very small numbers of *R. intestinalis* adhered to both cell lines, making it the least adhesive species among all three tested ($0.11 \pm 0.07\%$ and $0.06 \pm 0.01\%$ to Caco-2 and HT29-MTX cell lines, respectively). To sum up, the findings affirm that each species exhibits the ability to adhere to polarized epithelial cell layers in a manner unique to its species. Notably, the most efficient ratio was found to be an MOI of 1000:1, with lower or higher bacterial numbers per cell failing to yield further improvements in the results.

Result

Table 6. Adhesion of *F. prausnitzii*, *B. faecis*, and *R. intestinalis* to differentiated intestinal epithelial cell monolayers.

Caco-2 and HT29-MTX incubated with the commensal bacteria at three different multiplicity of infections (MOIs). Results are represented as the mean of triplicate experiments \pm SD. ND not detected.

Bacterial species	MOI	Relative adhesion (% of inoculum)	
		Caco-2	HT29-MTX
<i>F. prausnitzii</i>	100:1	ND	ND
<i>B. faecis</i>	100:1	ND	ND
<i>R. intestinalis</i>	100:1	ND	ND
<i>F. prausnitzii</i>	1000:1	1.51 \pm 0.65	1.32 \pm 0.94
<i>B. faecis</i>	1000:1	2.49 \pm 1.14	6.40 \pm 1.46
<i>R. intestinalis</i>	1000:1	0.11 \pm 0.07	0.06 \pm 0.01
<i>F. prausnitzii</i>	10000:1	1.07 \pm 0.50	0.02 \pm 0.00
<i>B. faecis</i>	10000:1	4.87 \pm 2.69	5.39 \pm 2.37
<i>R. intestinalis</i>	10000:1	0.01 \pm 0.00	0.01 \pm 0.00

4.5 Effects of commensal bacteria on healthy polarized epithelial monolayers

This series of experiments attempted to study the influence of *F. prausnitzii*, *B. faecis*, and *R. intestinalis* on intact and non-stressed or damaged Caco-2 and HT29-MTX polarized monolayers. Incubation of cells and bacteria is described in section 2.6.2. The co-culture of commensal bacteria and epithelial cell monolayers was performed at two time points of 3 hours and 6 hours. Changes in TEER values after bacterial contact were used as a readout parameter for potential effects. We tested different MOIs (100:1, 1000:1 and 10000:1) for each bacterial strain at two different incubation time points (3 and 6 hour). Cell monolayers without bacterial incubation were considered as a control group. TEER was immediately measured after inoculation of Caco-2 and HT29-MTX with viable *F. prausnitzii*, *B. faecis*, and *R. intestinalis*. As shown in Figure 10 A-F, when differentiated Caco-2 and HT29-MTX cells were exposed to a low MOI of 100:1,

Result

the TEER values after 3 and 6 hours of co-incubation did not differ significantly compared to the control. At a higher MOI of 1000:1, the TEER value of Caco-2 cells incubated with *F. prausnitzii*, *B. faecis*, and *R. intestinalis* showed a significant increase with corresponding values of 24.7%, 14.3% and 18.3% after 6 hours of incubation, respectively. For HT29-MTX, parallel outcomes were observed. After a 3-hour co-incubation with *F. prausnitzii*, *B. faecis*, and *R. intestinalis*, an elevation in TEER was evident, reaching values of 29.4%, 23.4%, and 10% compared to the control in the 6-hour incubation experiment, respectively. Nevertheless, the changes in TEER induced by *R. intestinalis* treatment did not achieve statistical significance. These experiments collectively highlight a time-dependent positive impact, primarily attributed to *F. prausnitzii* and *B. faecis*, on the TEER of polarized epithelial cells. The effects were more pronounced after a 6-hour incubation period. Notably, the MOI of 1000:1 emerged as the most efficient ratio, with higher bacterial numbers per cell failing to yield further enhancements in the results.

Result

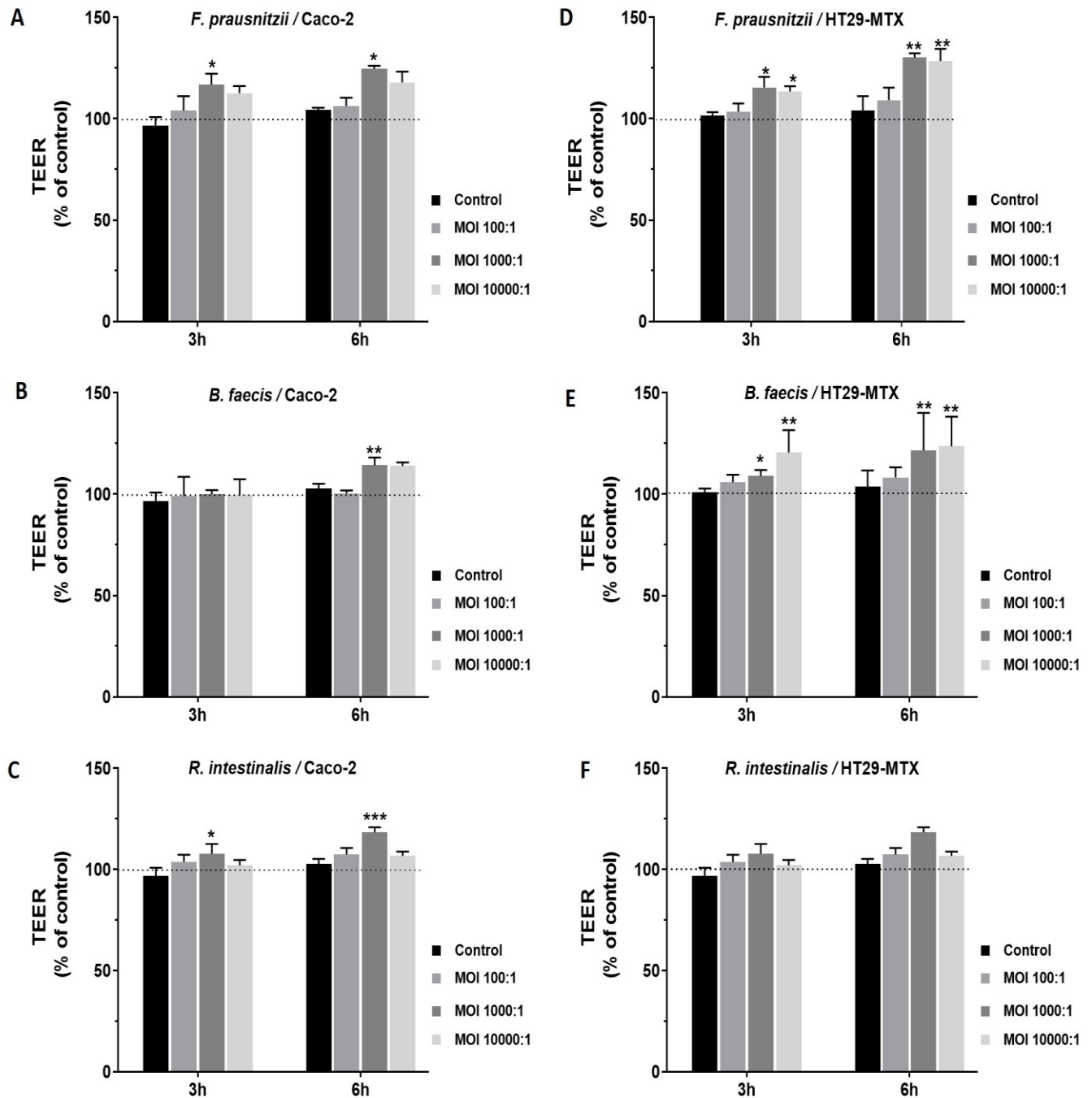


Figure 10. Effect of the commensal bacteria on the transepithelial electrical resistance (TEER) of differentiated Caco-2 and HT29-MTX cell monolayers.

(A, B, C) TEER value of Caco-2 after incubation with the commensal at three different MOI. (D, E, F) TEER value of HT29-MTX after incubation with the commensal at three different MOI. Results are represented as the means \pm SD ($n \geq 5$). Data were analyzed with the Mann-Whitney-U test, * $P < 0.05$, ** $P < 0.01$, *** $P < 0.001$ vs control.

4.6 Effects of commensal bacteria on inflamed intestinal epithelial cell function

In this phase of experiments, our investigation delved into understanding the impact of three bacterial species on inflamed epithelial cell monolayers, with a primary goal of assessing whether these commensal species could contribute to the healing and recovery of stressed and damaged cell monolayers. The experimental protocol began with the treatment of intact monolayers using a cytomix + LPS cocktail, as detailed in Section 3.2.20. Subsequent to this treatment, damage was quantified through TEER measurements. Following the initial damage assessment, we introduced *F. prausnitzii*, *B. faecis*, and *R. intestinalis* at MOIs of 1000:1 and 10000:1. The TEER values were recorded at 3 and 6 hours after bacterial inoculation. As shown in Figure 11 A-H, the untreated monolayer (control) consistently maintained their TEER level over the course of the experiment in the anaerobic chamber. Conversely, the treated monolayer, subjected to cytomix + LPS stimulation, exhibited a substantial reduction in the resistance of Caco-2 cells by 48.75% after 48 hours and HT29-MTX cells by 56.25% after 10 hours compared to untreated controls. Notably, cells stimulated with the cytomix + LPS cocktail did not display an increase in the TEER value after transitioning to fresh medium without inflammatory cytokines, strongly suggesting a lack of spontaneous recovery in monolayer TJ function. Further observations revealed that both monolayer cell lines stimulated with cytomix + LPS exhibited a significant increase in TEER value after 3 hours of incubation with *F. prausnitzii*, *B. faecis*, and *R. intestinalis* at MOIs of 1000 and 10000. This effect was sustained at 6 hours post-incubation. Treatment of cell monolayers with the bacterial three-species mixture (MOI 1000:1) significantly restored cytomix + LPS-induced barrier disruption at both time points (HT29-MTX 34.0±24.3% and Caco-2 35.0±11.55%) compared to cytomix + LPS-challenged epithelia in the absence of bacteria.

These results collectively highlight that all three bacterial species, individually and in combination, have the potential to mitigate disruption of the epithelial barrier function induced by inflammatory cytokines and LPS in both Caco-2 and HT29-MTX cell lines.

Result

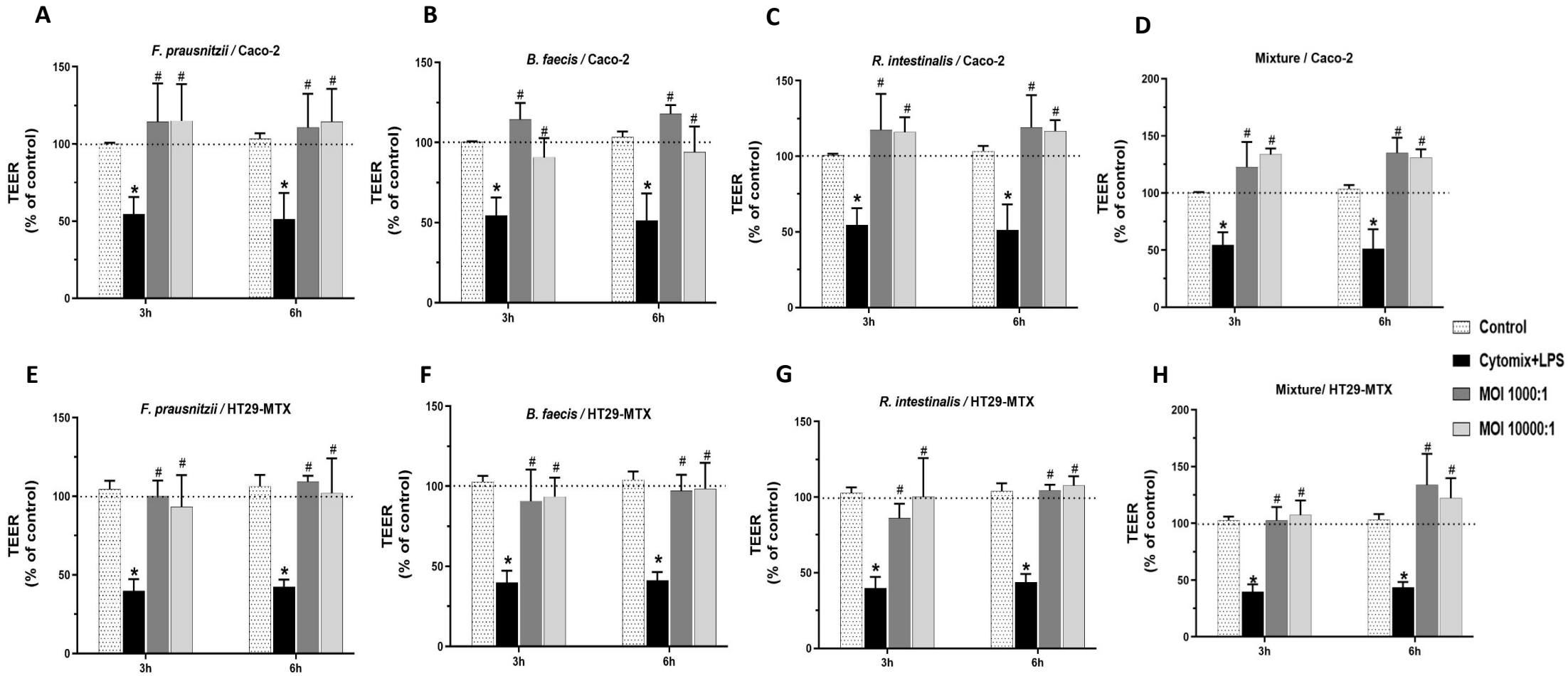


Figure 11. Effect of *F. prausnitzii*, *B. faecis*, and *R. intestinalis* individually and in combination on TEER in inflamed epithelial barrier. The effect of *F. prausnitzii*, *B. faecis*, and *R. intestinalis* individually and in combination on TEER in inflamed Caco-2 (A-D) and HT29-MTX (E-H) cell monolayers were investigated. Data are presented as means \pm SD ($n \geq 5$). * $P < 0.05$ cytomix + LPS compared to control and # $P < 0.05$ treated groups compared to cytomix + LPS, as determined by Mann–Whitney U test.

4.7 The paracellular permeability of epithelial cell monolayers

In examining changes in paracellular permeability, we employed FITC-dextran (FD-4) diffusion as a widely accepted indicator for monitoring and quantifying these processes. The measurement of FD-4 flux provided insights into the protective effect of bacteria on epithelial monolayer integrity (Figure 12 A, B). Consistent with TEER values, Caco-2 and HT29-MTX cell monolayers subjected to cytomix + LPS exhibited a substantial increase in FD-4 diffusion and flux (3 and 5-fold, respectively) compared to controls. This confirmed severe barrier damage following pro-inflammatory treatment. Inflamed and damaged HT29-MTX cells displayed a significant reduction in FT-4 flux after single-species incubation with *F. prausnitzii* ($65.34 \pm 22.35\%$), *B. faecis* ($65.04 \pm 2.61\%$), and *R. intestinalis* ($55.79 \pm 2.87\%$) compared to cytomix + LPS-stimulated cells without bacterial treatment. A similar trend was observed in Caco-2 cell monolayers. The inflammatory cytokine and LPS mixture elevated the paracellular flux of 4-KDa FITC-dextran, and this increase in permeability was significantly restored by *F. prausnitzii* treatment at both 1000:1 and 10000:1 MOIs ($55.48 \pm 23.51\%$ and $42.41 \pm 18.90\%$, respectively). Furthermore, *B. faecis* treatment of inflamed and damaged Caco-2 cells led to a significant reduction in barrier permeability by $48.38 \pm 24.81\%$ and $49.47 \pm 13.90\%$, for MOIs of 1000:1 and 10000:1, respectively. Additionally, a significant decrease in paracellular permeability was observed in cells incubated with *R. intestinalis*, relative to stimulated cells without bacterial incubation (MOI 1000:1 = $32.63 \pm 11.40\%$ & MOI 10000:1 = $38.46 \pm 12.40\%$). Co-administration of viable *F. prausnitzii*, *B. faecis*, and *R. intestinalis* as a mixture significantly attenuated the increase in paracellular FITC-dextran transport induced by the inflammatory stimuli treatment in both Caco-2 (MOI 1000:1 = $48.46 \pm 29.10\%$ & MOI 10000:1 = $41.45 \pm 27.10\%$) and HT29-MTX (MOI 1000:1 = $38.40 \pm 93.5.10\%$ & MOI 10000:1 = $32.27 \pm 34.85\%$) cell monolayers compared to the appropriate controls without bacterial presence. Therefore, beyond the positive effects observed on TEER, these bacterial species demonstrate significant beneficial recovery effects on paracellular leakage induced by inflammation.

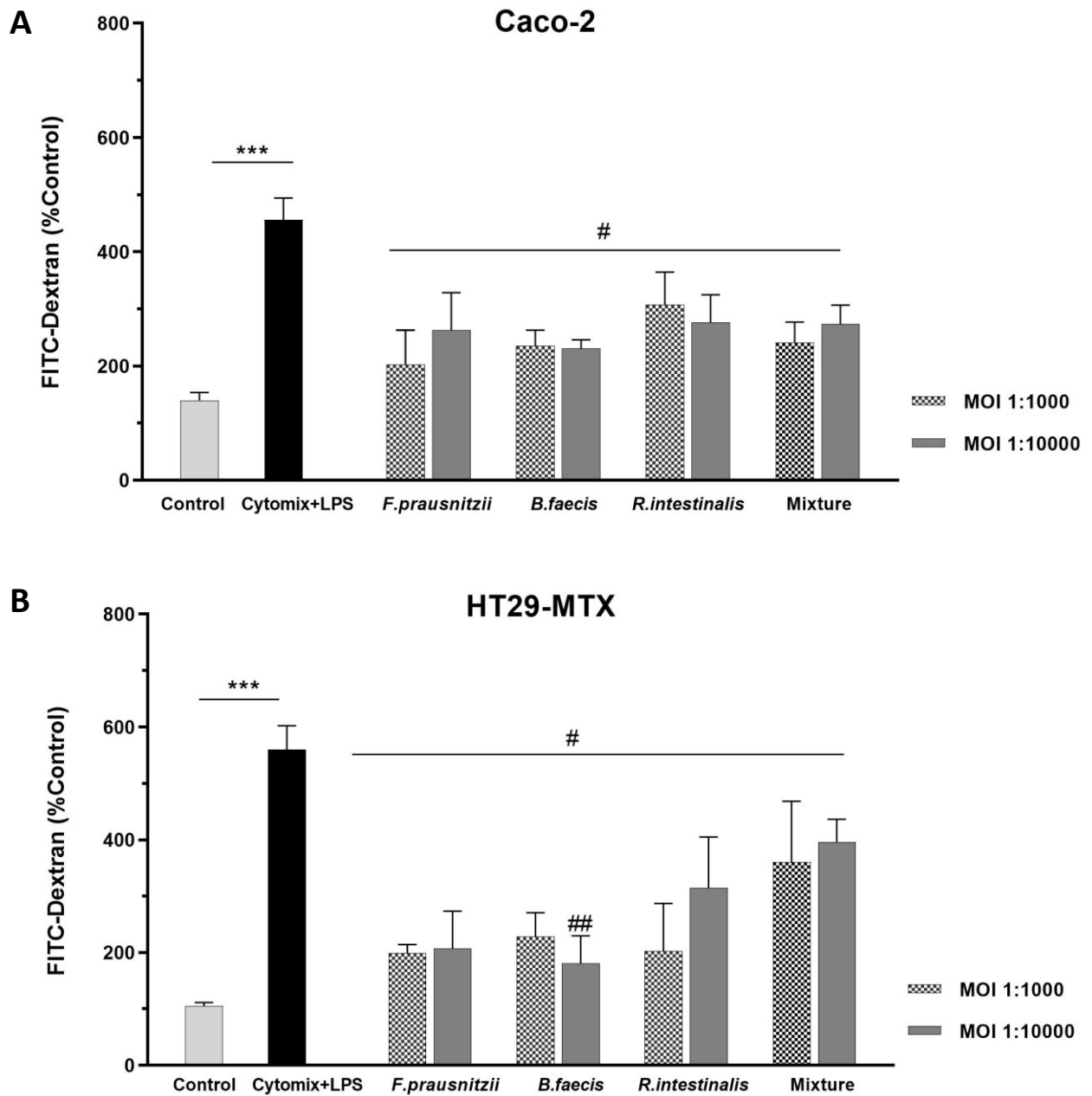


Figure 12. Effect of *F. prausnitzii*, *B. faecis* and *R. intestinalis* on paracellular permeability. Paracellular permeability was determined by the flux of FITC–dextran through the differentiated Caco-2 (A) and HT29-MTX (B) cell monolayers. Cell monolayers were incubated with cytomix + LPS followed by 6 h incubation with bacteria individually and in combination, the flux of FITC–dextran was measured. The control group received culture media. Data are presented as the means \pm SD (n = 4). *** P < 0.001 cytomix+LPS group compared to control group and # P < 0.05, ## P < 0.01 treated groups compared to cytomix+LPS group, as determined by the Mann–Whitney U test.

Result

4.8 Bacterial effects on host cell cytokine secretion

In the subsequent experimental phase, our focus shifted towards assessing whether the three commensal bacterial strains exerted a protective effect on cells by influencing the secretion of inflammatory mediators. Following a 6-hour co-culture of cytomix + LPS stimulated Caco-2 and HT29-MTX cells with live *F. prausnitzii*, *B. faecis*, and *R. intestinalis* (at MOIs 1000:1 and 10000:1), we quantified the inflammatory chemokines IL-8 and MCP-1 in the supernatant of both cell lines using ELISA. Our findings, illustrated in Figure 13 A-D, revealed that stimulation of both cell lines with the cytomix + LPS cocktail led to a significant increase in the production of IL-8 and MCP-1 compared to non-stimulated control cultures ($****P \leq 0.0001$). Interestingly, treatment of Caco-2 monolayers with all three bacterial species resulted in a noteworthy decrease in the levels of both chemokines in the basolateral media at both MOIs ($####P \leq 0.0001$) (Figure 13 A, B). However, while there were low levels of MCP-1 secretion in HT29-MTX supernatants co-incubated with all three species, statistical significance was not achieved for treatment with *F. prausnitzii* (MOI 1000:1, $P < 0.0921$ and MOI 10000:1) and *B. faecis* (MOI 1000:1) (Figure 13 C). Additionally, the IL-8 secretion levels in HT29-MTX cells co-incubated with the three bacterial species showed a substantial approximately 3.5-fold reduction compared to cytomix + LPS-stimulated cell monolayers. Furthermore, simultaneous treatment of both cell lines with the three bacterial species resulted in a significant decrease in the detection levels of both IL-8 and MCP-1. However, it is noteworthy that the reduction in MCP-1 levels in HT29-MTX cells was not statistically significant. These findings suggest that the tested bacterial species significantly reducing the elevated levels of pro-inflammatory chemokines induced by pro-inflammatory stimuli. This indicates their immunomodulatory potential by which they protect the monolayers from further damage.

Result

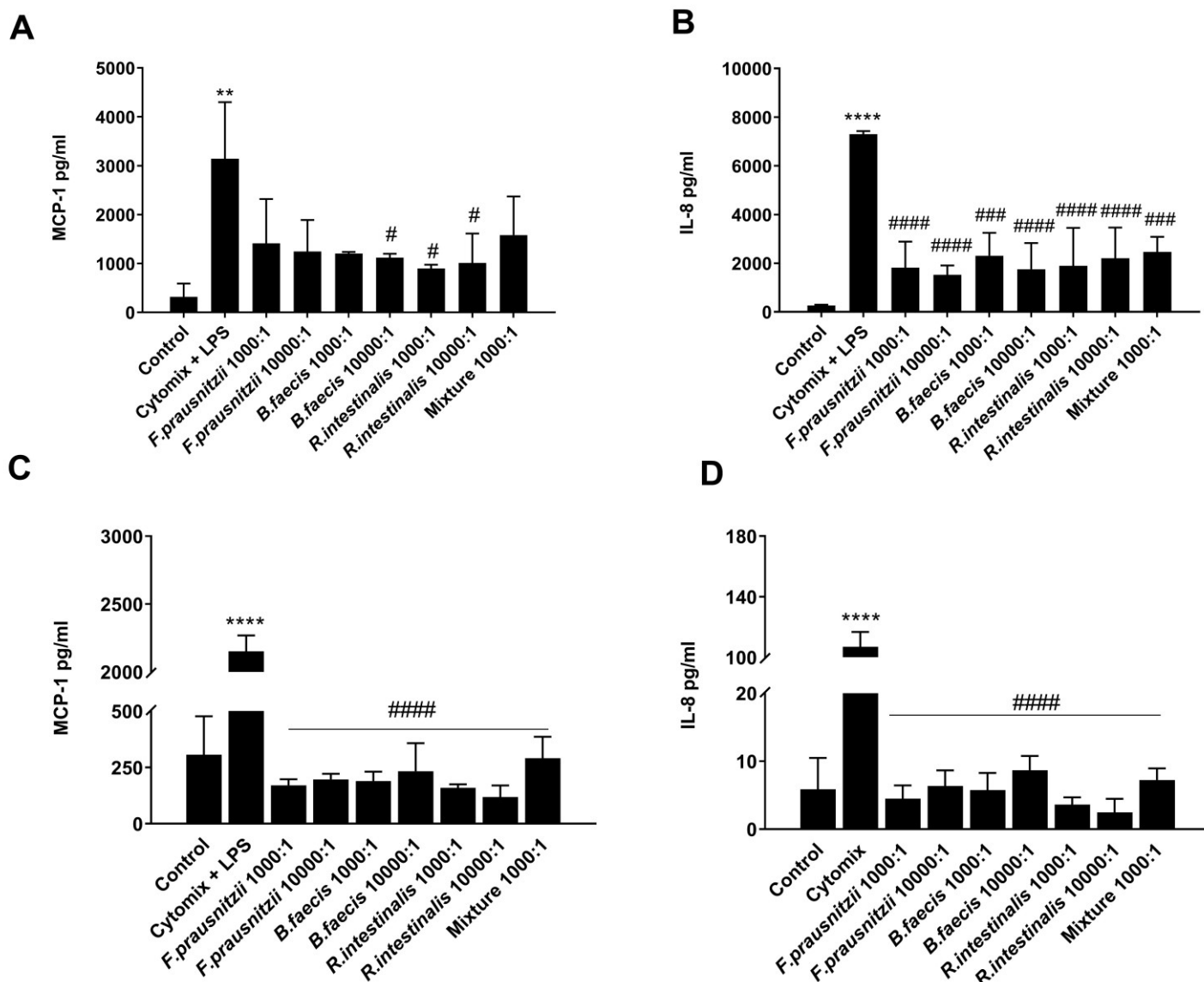


Figure 13. IL-8 and MCP-1 secretion by differentiated Caco-2 and HT29-MTX cells expose to inflammatory cytokine and LPS.

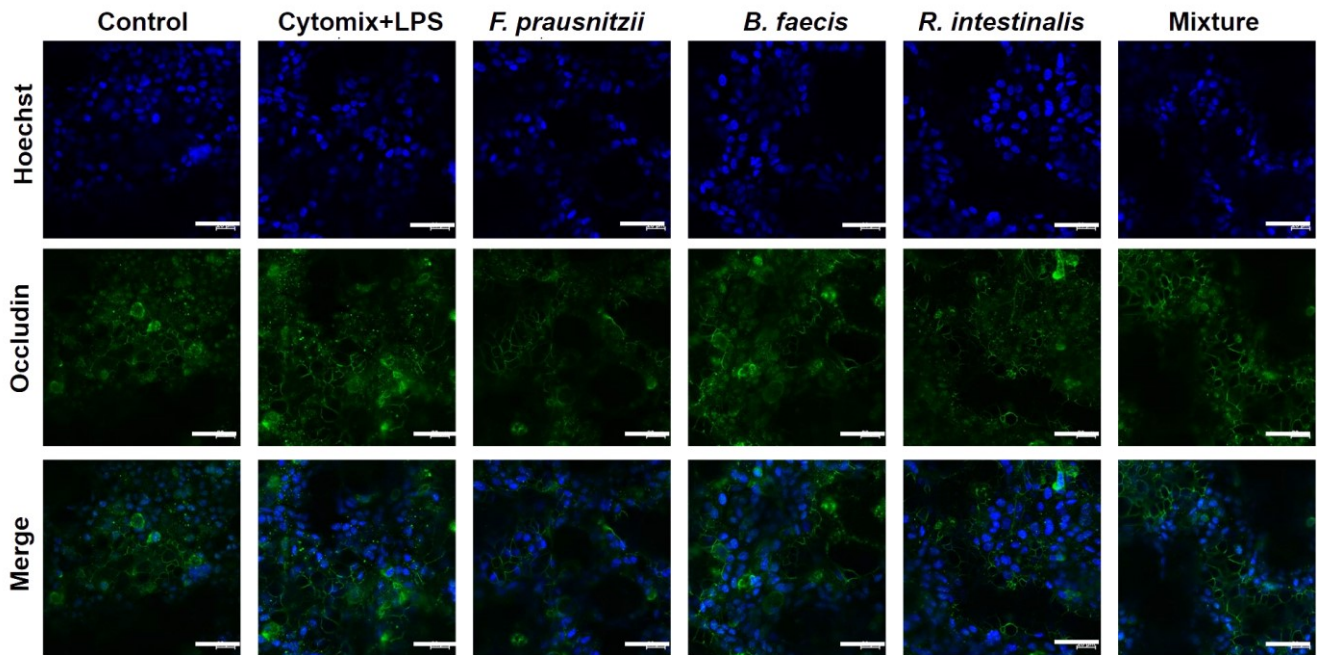
Epithelial cell monolayers were treated with cytomix + LPS following incubation with bacteria individually or in a mixture for 6 hours. The control group received culture medium. Culture media sample was collected from the basal compartment. The concentration of IL-8 and MCP-1 secreted by Caco-2 (A-B) and HT29-MTX (C-D) cells were measured by enzyme-linked immunosorbent assay. ** $P < 0.01$, **** $P < 0.0001$ compared to control, # $P < 0.05$, ### $P < 0.001$, #### $P < 0.0001$, compared to cytomix + LPS, as determined by One-way ANOVA and presented as means \pm SD (n=3).

4.9 Immunofluorescence microscopic localization of tight junction proteins

In our investigation, we assess the expression and localization of tight junction proteins through immunofluorescence staining. As shown in Figure 14 A, B in control samples from both epithelial cell lines, the occludin staining showed a characteristic localization at areas of cell contact, forming a discernible cobblestone pattern. However, the introduction of the pro-inflammatory cytokine + LPS cocktail led to a notable shift in occludin localization, moving away from the cell surface and causing a reduction in the immunofluorescence signal an indication of tight junction disruption. The intriguing aspect arises when we consider the subsequent incubation of cytomix + LPS-stimulated monolayers with *F. prausnitzii*, *B. faecis*, and *R. intestinalis*, either individually or in combination. This intervention effectively restored occludin localization to the areas of cell contact (Figure 14 A, B). Notably, occludin expression in HT29-MTX cells was notably reduced, hinting at potential effects on its synthesis.

A parallel phenomenon was observed concerning claudin-2 expression. Stimulation with the cytomix + LPS cocktail resulted in an upregulation of claudin-2 expression in both epithelial cell lines, in contrast to control cells. However, the treatment with all three bacterial species in inflamed Caco-2 and HT29-MTX cells successfully mitigated the heightened expression of claudin-2 induced by the inflammatory cytokine and LPS (Figure 15 A, B). This set of results underscores a significant observation - the function of intestinal epithelial tight junctions was compromised upon stimulation with the inflammatory cocktail. However, the intervention with all three bacterial species, either individually or in combination, demonstrated the remarkable ability to partially restore this disrupted phenotypic state. This finding suggests opportunities to investigate the intricate relationship between beneficial bacteria and the preservation of the intestinal barrier's integrity during inflammatory situations.

A) Caco-2



B) HT29-MTX

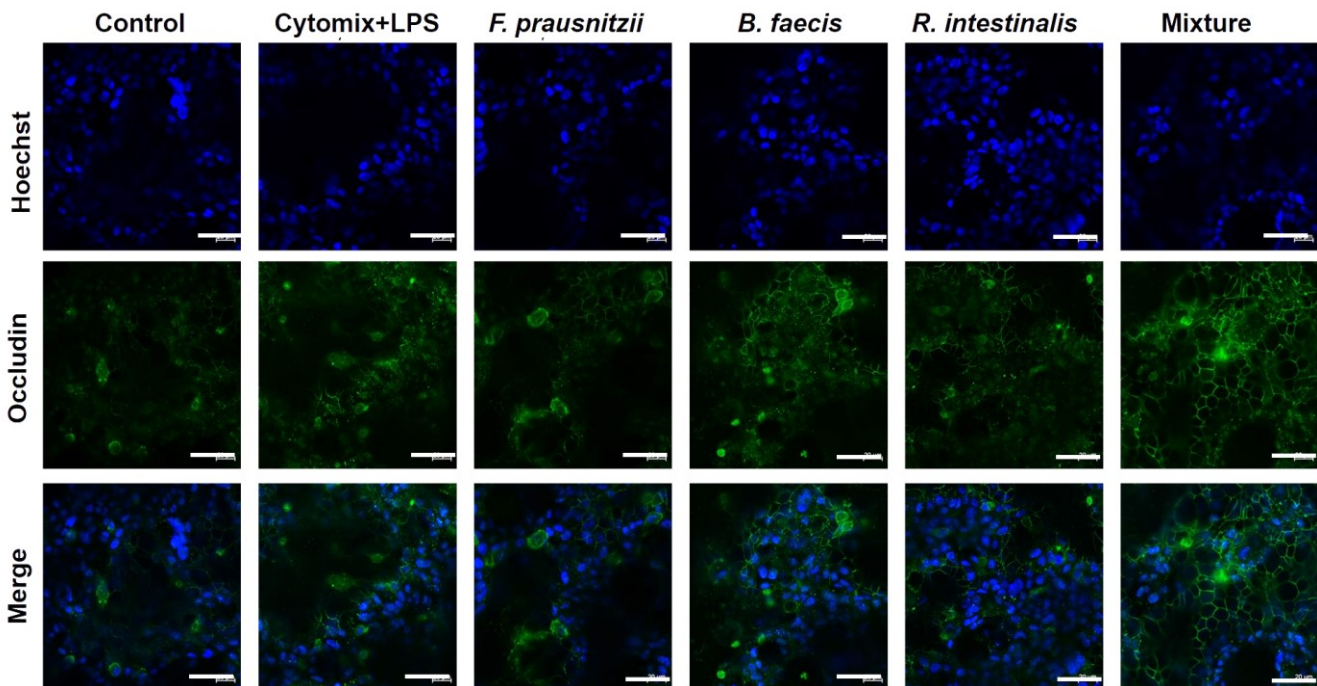
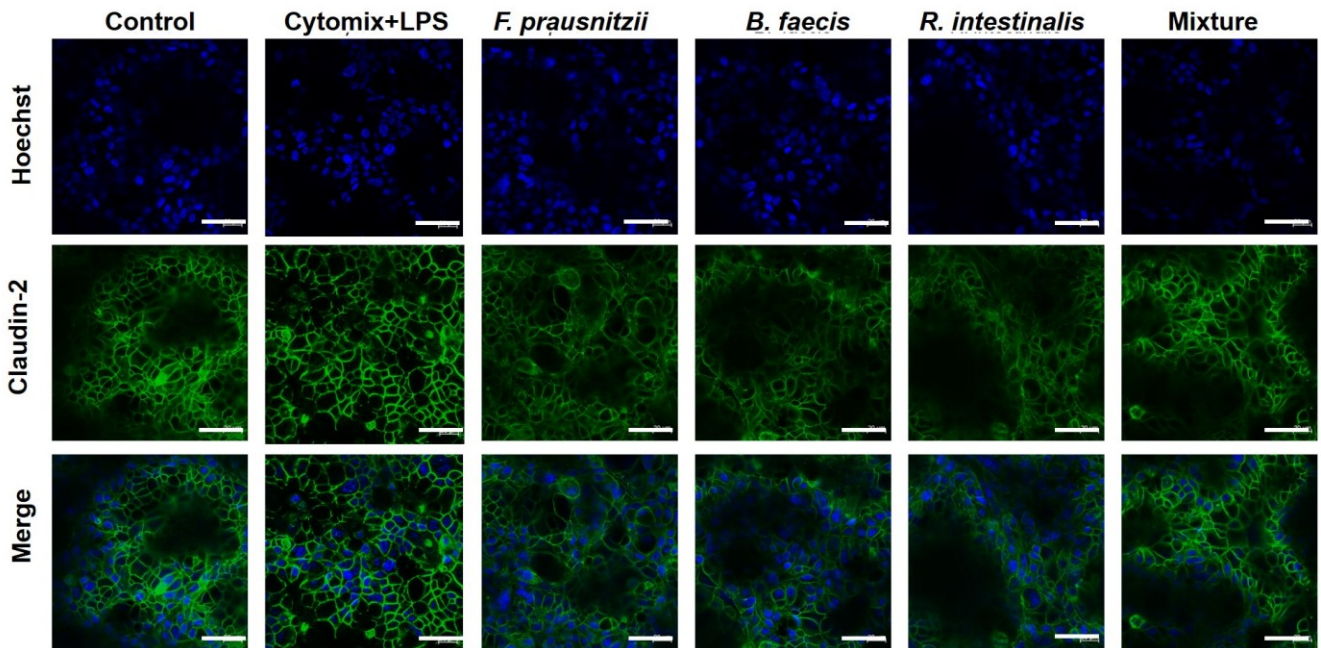


Figure 14. Immunofluorescence localization of the tight junction protein occludin in Caco-2 and HT29-MTX epithelial cells.

Differentiated Caco-2 (A) and HT29-MTX (B) cells were subjected to three conditions: growth media (Control), cytomix + LPS, and exposure to the tested commensal bacteria. Subsequently, cell monolayers were stained using anti-occludin antibodies (green) and Hoechst (blue) and visualized through confocal microscopy. The images were captured at 40x magnification, and the scale bar represents 20 μ m.

A) Caco-2



B) HT29- MTX

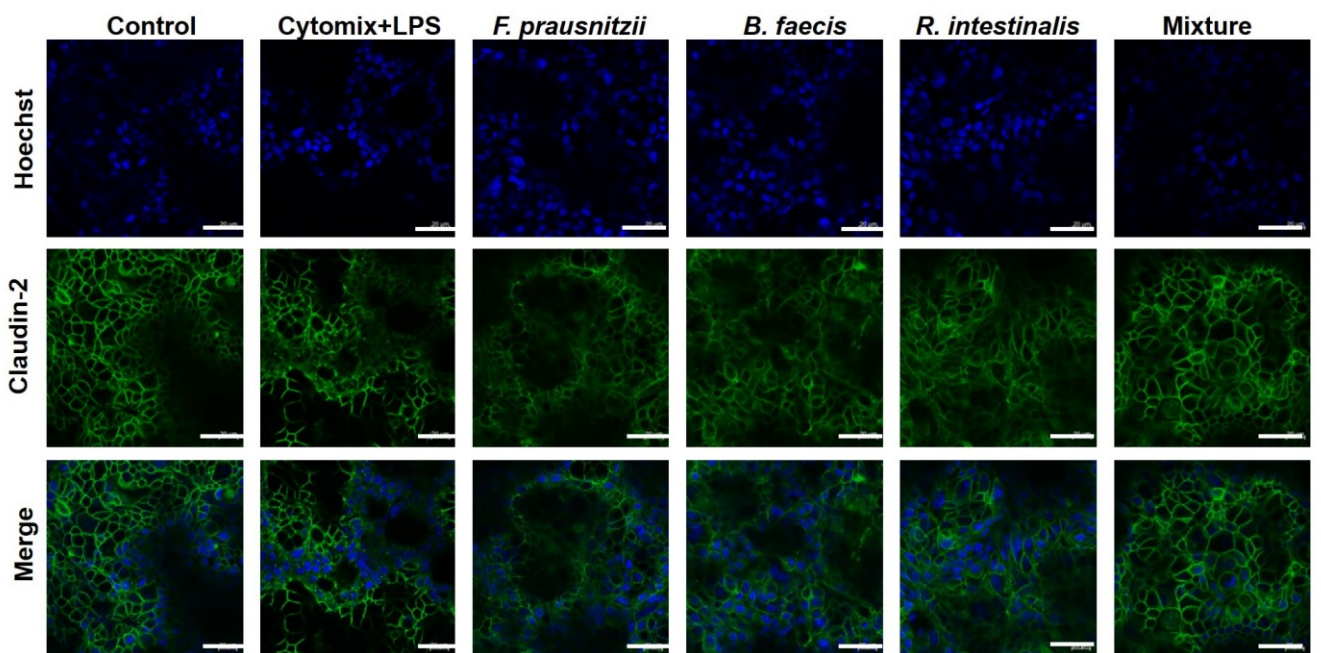


Figure 15. Immunofluorescence localization of the tight junction proteins claudin-2 in Caco-2 and HT29-MTX epithelial cells.

Differentiated Caco-2 (A) and HT29-MTX (B) cells were subjected to three conditions: growth media (Control), cytomix + LPS, and exposure to the tested commensal bacteria. Subsequently, cell monolayers were stained using anti-claudin-2 antibodies (green) and Hoechst (blue) and visualized through confocal microscopy. The images were captured at 40x magnification, and the scale bar represents 20 μ m.

Result

4.10 Effects of bacteria on tight junction protein expression in epithelial cell monolayers

To investigate whether the changes in paracellular permeability on epithelial cell monolayers following inflammatory cytokines+LPS cocktail and *F. prausnitzii*, *B. faecis*, and *R. intestinalis* treatments were associated with modifications in TJ protein expression, protein levels of the claudin-2 and occludin were quantified by Western Blot analysis. As shown in Figure 16 A Caco-2 cells, the stimulation with inflammatory cytokines and LPS led to a substantial decrease in occludin expression (0.55 ± 0.14 -fold) and a marked increase in claudin-2 expression (1.32 ± 0.67 -fold). This dysregulation hinted at a compromised tight junction structure, potentially contributing to increased paracellular permeability. The subsequent 6-hour incubation with *F. prausnitzii*, *B. faecis*, and *R. intestinalis* individually demonstrated their ability to attenuate the reduction in occludin levels (1.60 ± 0.28 -fold, 1.91 ± 0.21 -fold, and 1.31 ± 0.44 -fold, respectively). These findings imply a protective role of the bacterial species in preserving the integrity of tight junctions against inflammatory insults. Similarly, claudin-2 expression was downregulated by the bacterial treatments (*F. prausnitzii*: 0.50 ± 0.22 -fold, *B. faecis*: 0.53 ± 0.35 -fold, and *R. intestinalis*: 0.32 ± 0.22 -fold), further supporting their potential in mitigating inflammatory-induced disruptions. The co-administration of the three bacterial species as a mixture significantly increased occludin levels ($P < 0.05$), suggesting a cooperative effect in restoring tight junction integrity in Caco-2 cells.

In HT29-MTX cells, exposure to inflammatory cytokines and LPS prompted a noteworthy decrease in occludin expression (0.58 ± 0.13 -fold), coupled with a notable increase in claudin-2 levels (0.75 ± 0.18 -fold) (Figure 16 B). This alteration indicated a disturbance in tight junction integrity, potentially compromising the epithelial barrier function. Subsequent incubation with *F. prausnitzii*, *B. faecis*, and *R. intestinalis* individually demonstrated a restorative effect on occludin levels (1.91 ± 0.21 -fold, 1.31 ± 0.44 -fold, and 1.45 ± 0.20 -fold, respectively), as illustrated in Figure 16B, suggesting their potential in mitigating the impact of inflammatory stimuli on tight junction proteins. While the increases in occludin levels induced by *R. intestinalis* and *B. faecis* were not statistically significant, the combined administration of the three bacterial species significantly elevated occludin levels ($P \leq 0.05$), as indicated in Figure 16B, emphasizing a synergistic effect. In summary, the observed effects on tight

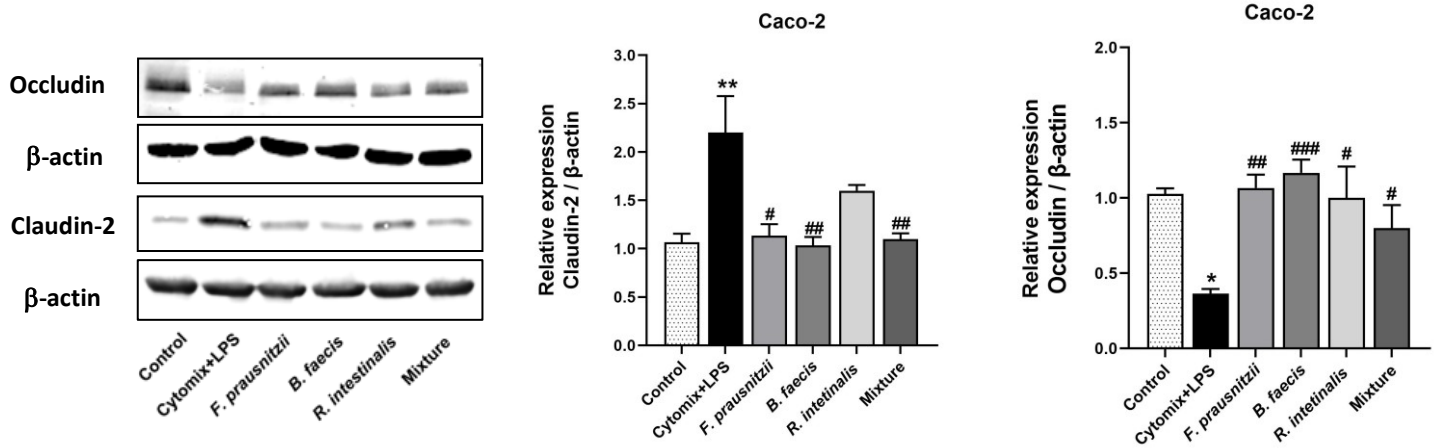
Result

junction protein expression in both HT29-MTX and Caco-2 cells indicate the potential of *F. prausnitzii*, *B. faecis*, and *R. intestinalis* to counteract the detrimental impact of inflammatory stimuli. This supports the hypothesis that these commensal bacteria possess protective properties, contributing to the maintenance of epithelial barrier function in the face of inflammatory challenges.

Result

A)

Caco-2



B)

HT29-MTX

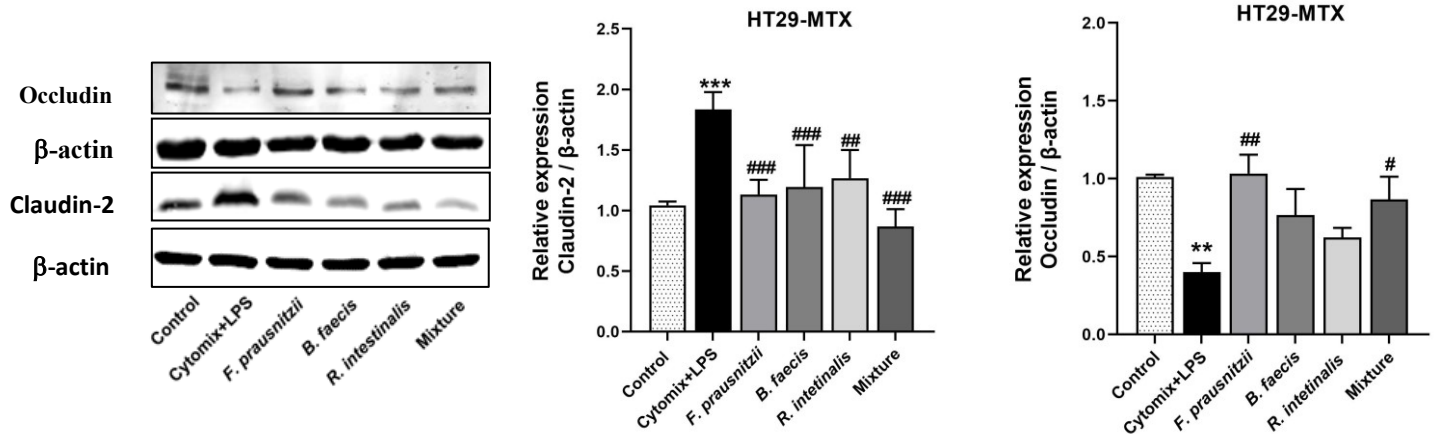


Figure 16. Western blot analysis of claudin-2 and occludin expression after treatment with *F. prausnitzii*, *B. faecis*, and *R. intestinalis*, alone and in combination.

Caco-2 and HT29-MTX cells were grown for 21 days and exposed to cytomix + LPS and the tested commensal bacteria individually and in mixture. The cell lysates were used for immunoblotting for claudin-2, occludin, and β -actin. The diagrams show quantification of the intensity of bands, normalized to the intensity of the β -actin bands. All data represent the results of three different experiments (mean \pm SD). * P < 0.05, ** P < 0.01 compared to control group. # P < 0.05, ## P < 0.01, ### P < 0.001 compared to cytomix+LPS group, as determined by one-way ANOVA.

4.11 The effects of the commensal bacteria on acute colonic inflammation in mice

A mouse model of UC was used to investigate the effects of the three commensal bacterial species individually and in combination on acute colitis development. The mice drinking water was supplemented with 3.5% DSS for seven days. Disease progression in mice was assessed using classic colitis symptoms, such as weight loss, hematochezia, and diarrhea. Mice treated with DSS exhibited progressive weight loss compared to control mice which reached almost 10% of the initial body weight on last day of experiment. However, in the groups treated with *F. prausnitzii*, *B. faecis*, and *R. intestinalis* and the mixture of all three bacterial species, there was a significant reduction in weight loss at 10^9 CFU/100 ($P = 0.002$, $P = 0.006$, $P = 0.636$ and $P = 0.040$, respectively) and 10^{10} CFU ($P = 0.009$, $P = 0.586$, $P = 0.001$ and $P = 0.003$, respectively) relative to the DSS group (Figure 17 A). The results of the commensal bacteria treatment groups were comparable to those of mesalazine, which also significantly prevented weight loss following DSS administration. Moreover, *B. faecis* administration at 10^{10} CFU led to an increase in body weight on day 3 of the experiment, even under DSS treatment, and generally kept the body weight close to the values of the untreated control group. As demonstrated in Figure 17B-E, exposure to DSS significantly increased the DAI score of the DSS group, reaching a maximum at the end of the experiment (9.36 ± 1.80 , $P < 0.0001$). However, the DAI scores of mice treated with mesalazine, *F. prausnitzii*, *R. intestinalis*, *B. faecis*, and the mixture at both doses were significantly reduced (6.00 ± 2.10 , 4.54 ± 1.92 , 3.36 ± 0.64 , 6.45 ± 2.90 , 4.18 ± 0.93 at 10^9 CFU and 4.81 ± 1.79 , 5.18 ± 1.58 , 4.72 ± 2.21 , 4.81 ± 2.24 at 10^{10} CFU, respectively) compared to those of the DSS group. Colon length serves as an established marker for assessing colonic tissue inflammation induced by dextran sulfate sodium (DSS). Moreover, as shown in Figure 17 G the colon length in the DSS group was significantly reduced relative to that in the control group (6.41 ± 0.36 cm vs. 8.70 ± 1.0 cm, $P < 0.001$). Of note, DSS mice treated with bacteria (individually and in combination) exhibited longer colon lengths than DSS-treated mice at 10^9 CFU (*F. prausnitzii*: 7.49 ± 0.47 cm, $P = 0.006$; *R. intestinalis*: 7.25 ± 0.71 cm, $P = 0.056$; *B. faecis*: 7.10 ± 0.51 cm, $P = 0.179$; and mixture: 7.50 ± 0.45 cm, $P = 0.190$) and at 10^{10} CFU (*F. prausnitzii*: 7.40 ± 0.56 cm, $P = 0.014$; *R. intestinalis*:

Result

7.23 ± 1.16 cm, $P = 0.065$; *B. faecis*: 7.16 ± 0.76 cm, $P = 0.254$; and mixture: 8.00 ± 0.50 cm, $P = 0.007$). The mesalazine treatment in DSS animals exhibited comparable efficacy to all bacterial interventions.

Result

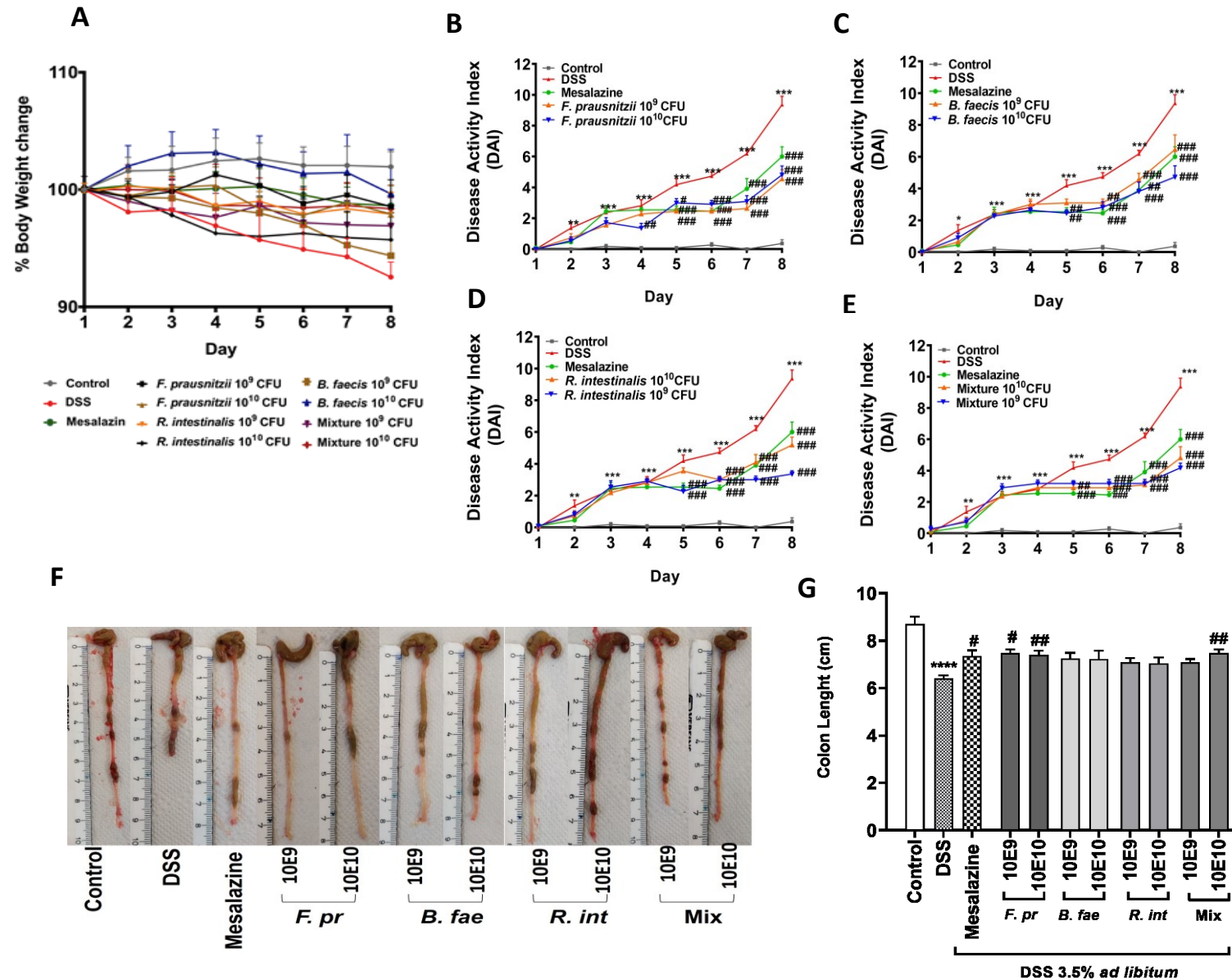


Figure 17. Impact of *F. prausnitzii*, *B. faecis*, and *R. intestinalis* on DSS-induced colitis.

(A) The body weight of mice was evaluated throughout the experiment, and the values are expressed as the percentage change from the initial value measured before DSS administration (n=11/per group). (B-E) The disease activity index was evaluated at the end of the experiment.

(F) colon lengths were evaluated at the end of the experiment. (G) Representative pictures of colons from mice of each treatment group. The terms 10E9 and 10E10 refer to CFUs of 10⁹ and 10¹⁰, respectively. Graphs show the mean ± SEM. Statistical analysis was performed with two-way ANOVA for multiple comparison followed by the Dunnett test for comparison of the untreated control group versus the DSS group (***P* < 0.01, ****P* < 0.001, *****P* < 0.0001) and the mesalazine- and bacterial species-treated groups versus the DSS group (# *P* < 0.05, ## *P* < 0.01, ### *P* < 0.001).

4.12 Myeloperoxidase activity assay

As a next step neutrophil infiltration in colonic tissue was assessed by quantifying the level of myeloperoxidase (MPO). As shown in Figure 18, the MPO activity increased nearly 22-fold compared to control mice ($p < 0.001$), which was markedly reduced by the treatment with mesalazine (32.0 ± 1.92 U/mg), *F. prausnitzii* (26.4 ± 2.15 & 26.4 ± 2.15 U/mg at 10^9 CFU/ml and 10^{10} CFU/ml, respectively), *R. intestinalis* (17.2 ± 1.62 and 18.4 ± 1.16 U/mg at 10^9 CFU/ml and 10^{10} CFU/ml, respectively), *B. faecis* (23.2 ± 1.64 and 24.3 ± 1.43 U/mg at 10^9 CFU/ml and 10^{10} CFU/ml, respectively) and the bacterial mixture (17.1 ± 0.97 and 20.6 ± 2.01 U/mg at 10^9 CFU/ml and 10^{10} CFU/ml, respectively). This result revealed a positive correlation with histopathologic features and suggested that compared to mesalazine treatment, the three tested commensal bacterial species individually and in combination can equally relieve the symptoms of experimental colitis by decreasing the infiltration of neutrophils.

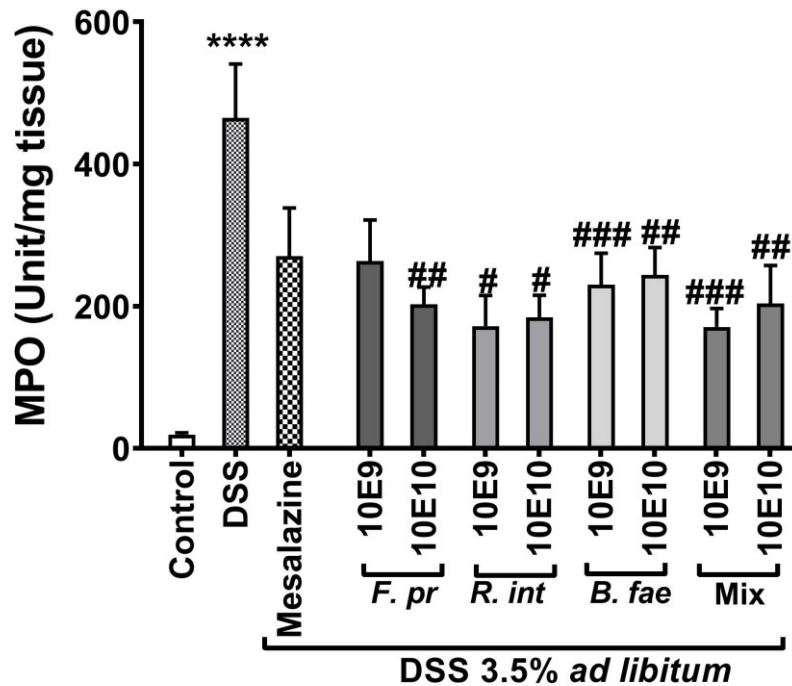


Figure 18. Effect of *F. prausnitzii*, *B. faecis*, and *R. intestinalis* on MPO activity. The level of MPO in colonic tissue from mice with DSS-induced colitis was measured by ELISA. Data are presented as the mean \pm SEM. The terms 10E9 and 10E10 refer to CFUs of 10^9 and 10^{10} , respectively. Statistical analysis was performed with one-way ANOVA for comparison of the control group versus the DSS group (**** $P < 0.0001$) and the mesalazine- and bacterial species-treated groups versus the DSS group (# $P < 0.05$, ## $P < 0.01$, ### $P < 0.001$).

4.13 Histological analysis

The histological and morphological changes in the colon of all groups were subsequently examined by Hematoxylin and eosin (H&E) staining (Figure 19 A, B). The colon structure was intact and the mucosa with the crypt was physiologically distinct without sign of inflammation in the control group animals. However, the colon of DSS mice exhibited superficial ulcerations, loss of goblet cells, neutrophil infiltration, and extensive epithelial and goblet cell damage, resulting in an overall histological score of 11.50 ± 3.21 ($P < 0.0001$). In contrast, relative to that of DSS-treated mice, the colon tissue of DSS mice treated with mesalazine, *F. prausnitzii*, *R. intestinalis*, and *B. faecis* separately and in combination at both CFUs revealed significantly less loss of goblet cells, less distortion of the crypt, and decreased neutrophil infiltration in the colonic mucosa. This resulted in a lower histological

Result

damage score (7.20 ± 3.61 , 6.55 ± 3.37 , 2.27 ± 1.68 , 5.27 ± 5.68 , 5.45 ± 2.30 , respectively, at 10^9 CFU, and 4.82 ± 6.24 , 6.18 ± 4.83 , 9.27 ± 4.03 , 5.55 ± 3.93 , respectively, at 10^{10} CFU). Concerning the attenuation of severe histological damage, mesalazine was less efficient than nearly all the bacterial treatments. Additionally, Alcian blue staining was performed to determine the number of goblet cells (Figure 19 C). The oral administration of all three bacterial species individually and in combination markedly attenuated the depletion of goblet cells. Collectively, these results proved the efficacy of all three commensal bacterial species (both individually and in combination) in attenuating clinical symptoms in mice with DSS-induced colitis. Moreover, application of the commensal bacterial species outperformed mesalazine therapy in alleviating and healing all evaluated types of histological damage.

Result

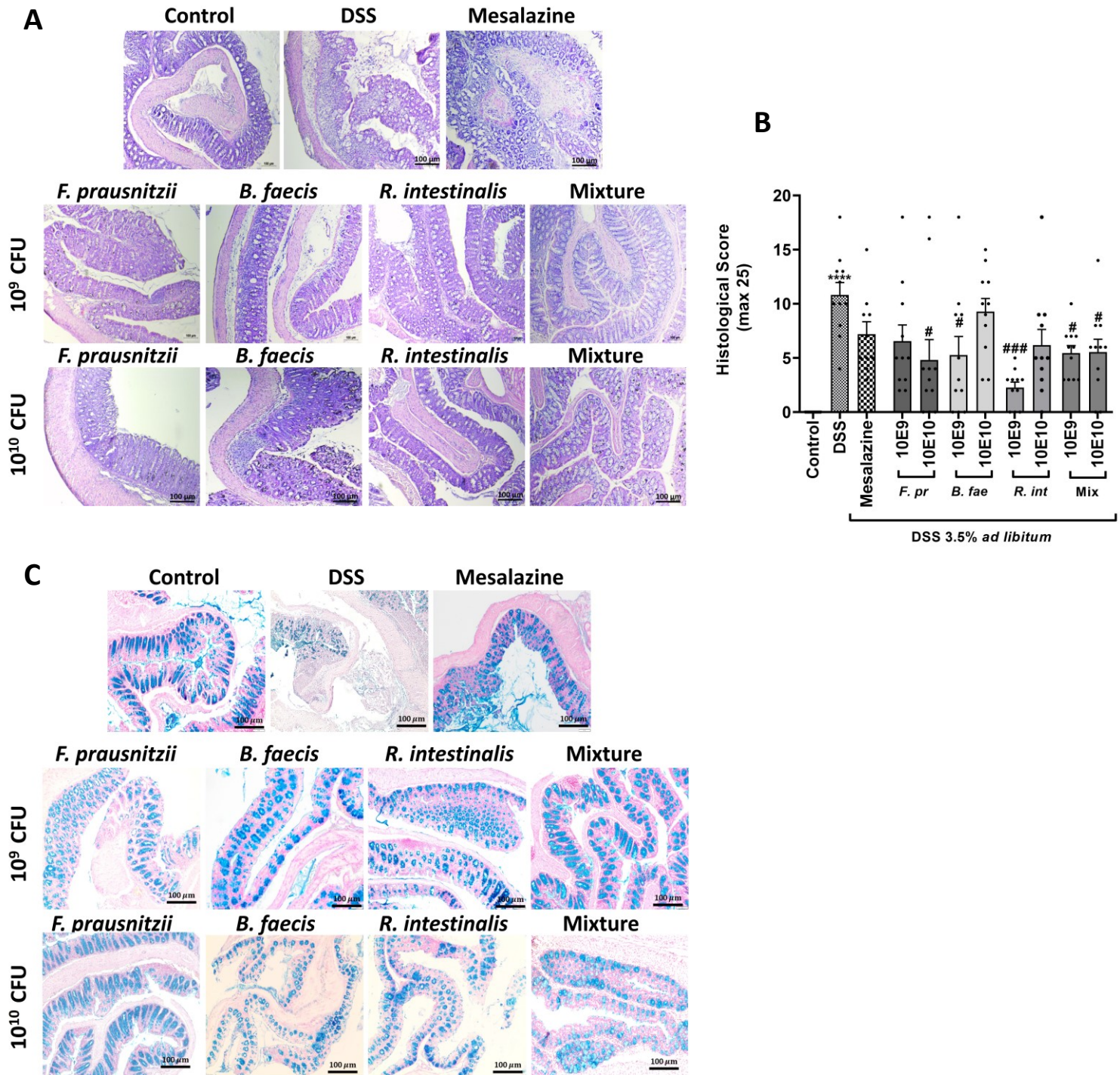


Figure 19. Impact of *F. prausnitzii*, *B. faecis*, and *R. intestinalis* on histopathological features and goblet cells of DSS-induced colitis mice.

(A) Representative images of H&E staining of colon tissues. (B) Histological scores based on H&E-stained sections per mouse ($n = 11$). The terms 10E9 and 10E10 refer to CFUs of 10^9 and 10^{10} , respectively. (C) Representative images of alcian blue staining of colon tissues. Graphs show the mean \pm SEM. Statistical analysis was performed with two-way ANOVA for multiple comparison followed by the Dunnett test for comparison of the untreated control group versus the DSS group (** $P < 0.01$, *** $P < 0.001$, **** $P < 0.0001$) and the mesalazine- and bacterial species-treated groups versus the DSS group (# $P < 0.05$, ## $P < 0.01$, ### $P < 0.001$).

4.14 Intestinal barrier function in DSS-induced colitis mice

Increased intestinal permeability is linked to intestinal barrier dysfunction. In animal models of colitis and human IBD, TJ protein expression has been shown to play a vital role in the development of intestinal inflammation. Therefore, we determined whether the administration of *F. prausnitzii*, *R. intestinalis*, and *B. faecis* individually and in combination can protect the intestinal barrier against damage induced by DSS. FITC-dextran was administered by gavage, and the intensity of fluorescence in the serum was measured 4 hours later. As shown in Figure 20, the level of FITC-dextran in the serum of mice with DSS-induced colitis was significantly increased compared to that in the control mice ($P < 0.001$). In addition, *F. prausnitzii*, *R. intestinalis*, *B. faecis* and the mixture treatment induced significant reductions in FITC-dextran levels in mouse plasma ($P = 0.011$, $P = 0.037$, $P = 0.007$, $P = 0.001$, respectively, at 10^9 CFU) and ($P = 0.018$, $P = 0.006$, $P = 0.037$, $P = 0.027$, respectively, at 10^{10} CFU). Of note, the commensal bacterial treatments had positive protective effects comparable to those of the standard mesalazine therapy in our DSS mouse model.

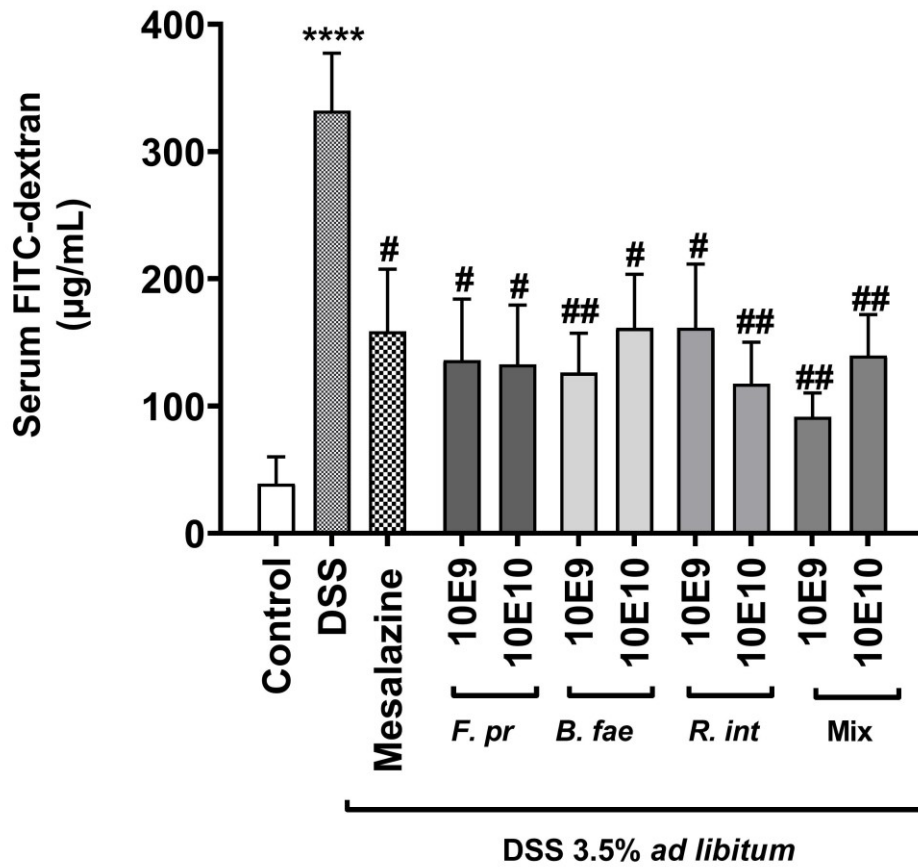


Figure 20. Levels of FITC dextran in the serum of mice with DSS induced colitis. Administered FITC-dextran were measured as an indicator of intestinal permeability (n=6-10/animal per group). The terms 10E9 and 10E10 refer to CFUs of 10^9 and 10^{10} , respectively. Data are presented as the mean \pm SEM. Statistical analysis was performed with one-way ANOVA for multiple comparison followed by the Dunnett test for comparison of the untreated control group versus the DSS group ($*P < 0.05$, $****P < 0.0001$) and the mesalazine- and bacterial species-treated groups versus the DSS group ($\# P < 0.05$, $##P < 0.01$).

4.15 Tight junction protein expression in acute DSS-induced colitis

An investigation was conducted to assess the potential correlation between shifts in intestinal permeability induced by DSS and bacterial species treatments and modifications in the expression of tight junction proteins. The protein levels of occludin, E-cadherin, and claudin-2 were examined by Western blotting and immunohistochemistry. As indicated in Figure 21 A-D, the expression levels of colonic E-cadherin and occludin decreased in the DSS induced colitis group compared to the control group ($P = 0.042$ and $P = 0.461$). However, administration of mesalazine, *F. prausnitzii*, *B. faecis*, *R. intestinalis*, and the mixture protected mice against the loss of occludin expression (by 14.26-fold \pm 0.67, 15.62-fold \pm 0.9, 8.98-fold \pm 1.33, 10.43-fold \pm 1.16, and 12.68-fold \pm 0.67, respectively) and the loss of E-cadherin expression (by 3.66-fold \pm 0.64, 4.79-fold \pm 0.97, 5.49-fold \pm 0.60, 6.30-fold \pm 0.85, and 4.09-fold \pm 0.70, respectively). Furthermore, claudin-2 protein expression levels were markedly increased (by 1.32-fold \pm 0.36, $P = 0.461$) in the DSS group compared to the control group. Following the administration of *F. prausnitzii*, *B. faecis*, and *R. intestinalis* individually and in combination, a significant decrease in claudin-2 expression was noted, with corresponding decreases of 0.60-fold \pm 0.21, 0.41-fold \pm 0.14, 0.60-fold \pm 0.27, 0.35-fold \pm 0.11, and 0.43-fold \pm 0.2, respectively, compared to the DSS group. Overall, some of the commensal bacterial treatments showed stronger protective effects than the mesalazine standard therapy. Supporting the TJ protein Western blot results, immunohistochemistry experiments (Figure 22) also showed that the substantial decrease in occludin and E-cadherin protein levels was prevented in mice treated with the bacterial species. Moreover, compared to DSS treatment alone, administration of all three bacterial species alleviated the altered expression of claudin-2 in the cell membrane and cytoplasm of enterocytes and glandular epithelial cells. These findings suggested that the three tested commensal bacterial species individually and in combination could ameliorate the disruption of intestinal barrier function in DSS-treated mice by reducing intestinal epithelial permeability and preventing the loss of tight junction proteins.

Result

A

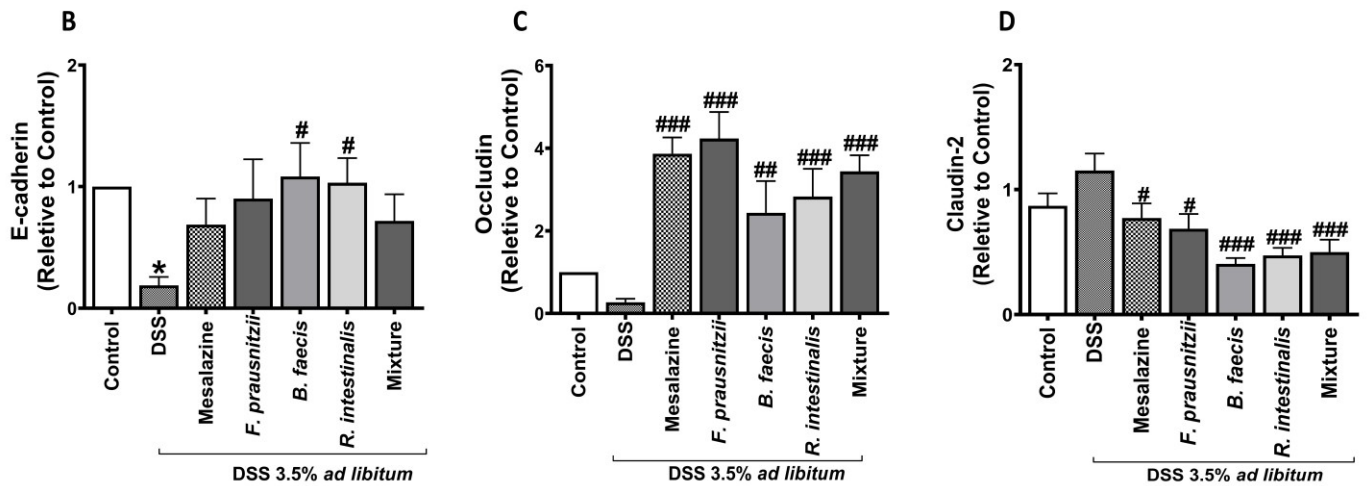
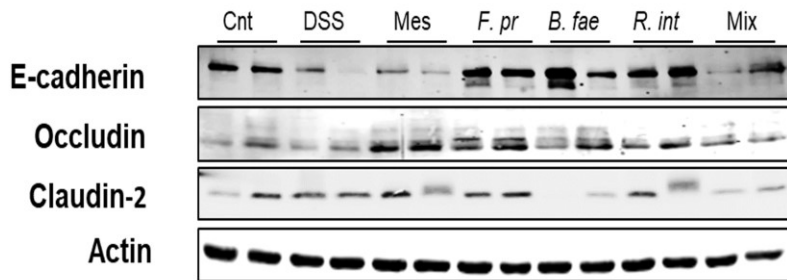


Figure 21. Effect of *F. prausnitzii*, *B. faecis*, and *R. intestinalis* alone and in combination on epithelial tight junction protein expression.

Homogenates of colon tissue were analyzed by western blotting to detect the expression levels of tight junction proteins. (A) Representative blots from 2 samples from three independent experiments are shown, and β -actin was used as a loading control. The levels of (B) E-cadherin, (C) occludin, and (D) claudin-2 expression were subsequently quantified.

Statistical analysis was performed with one-way ANOVA for multiple comparison followed by the Dunnett test for comparison of the untreated control group versus the DSS group ($*P < 0.05$) and the mesalazine- and bacterial species-treated groups versus the DSS group ($\#P < 0.05$, $\#\#\#P < 0.001$).

Result

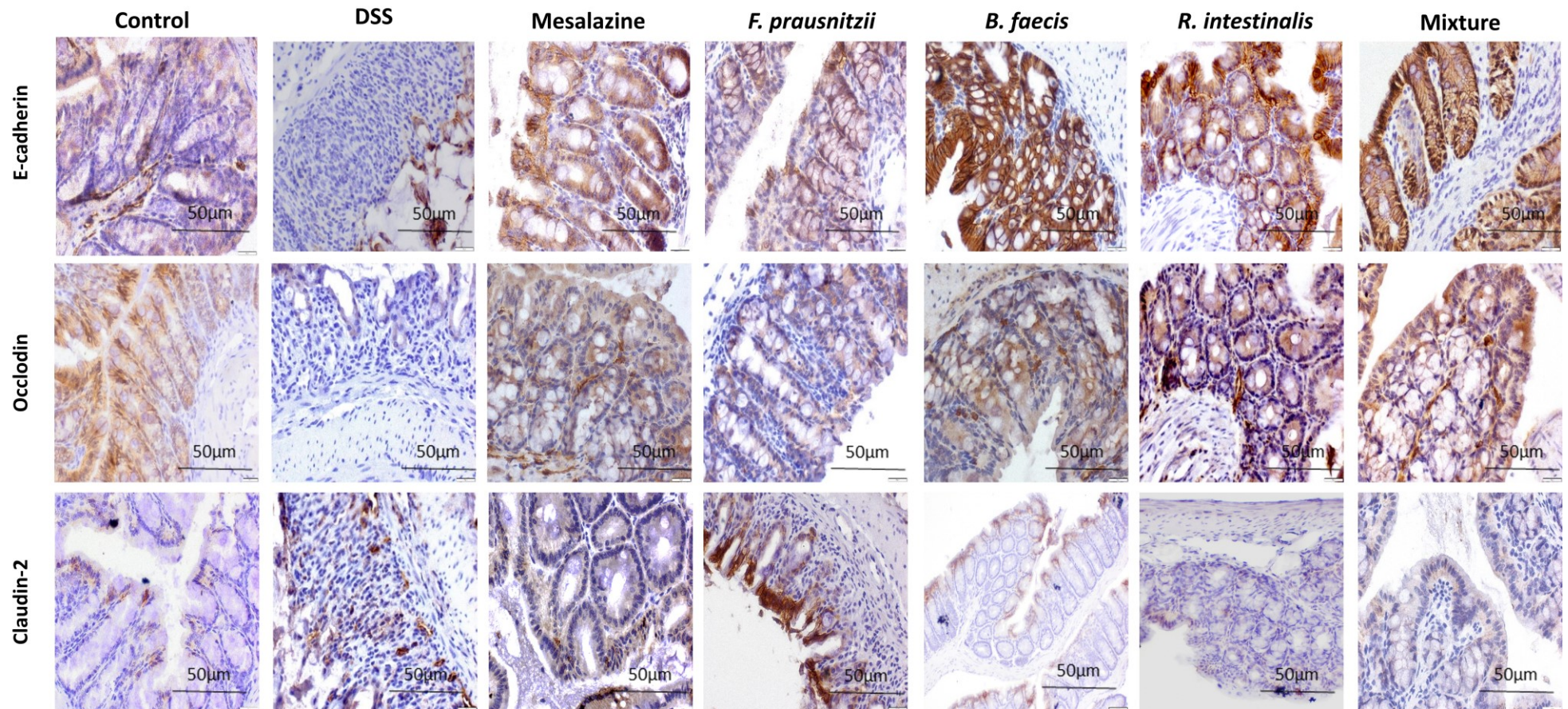


Figure 22. Immunohistochemically staining of tight junction proteins.

Immunohistochemical expression patterns of the E-cadherin, occludin and claudin-2 proteins in colon tissue. Magnification: 20 ×, scale bar: 50 μm.

4.16 Cytokine levels in colonic tissue in acute DSS-induced colitis

Infiltration of inflammatory cells in the colon increases mucosal production of cytokines. Pro-inflammatory cytokines play a crucial role in the progression of DSS-induced colitis. We measured Th1, Th2, and Th17-type cytokine in distal colon tissue to investigate the effectiveness of the three commensal bacterial species individually and in combination in alleviating colitis by modulating the secretion of inflammatory mediators. As shown in Figure 23 A-H, the levels of Th1-type (IFN- γ), Th2-type (IL-13), and Th17-type (TNF- α , IL-6, IL-17A, IL17F, and IL-22) cytokines were significantly enhanced only in DSS treated animals in comparison with the control group. The colon tissue from mice treated with either a single species or the combination of all three species at both CFUs significantly reduced the levels of IFN- γ , IL-13, TNF- α , IL-6, 17A, 17F, and IL-22 compared with the DSS group mice. In contrast, the Th2-type anti-inflammatory cytokine IL-10 secretion slightly increased in the bacteria treated groups compared with the DSS mice (Figure 23 E). Notably, this increase was statistically significant in the groups treated with *F. prausnitzii* and *R. intestinalis* in both CFU level. Mesalazine was exclusively superior to all bacterial treatments in the reduction of IL-13 levels (Figure 23 H). These findings suggested that oral administration of all three tested commensal bacteria individually and in combination at both CFUs attenuates the development of colonic inflammation in the DSS-induced colitis model via changes in Th1-type, Th2-type, and Th17-type cytokine secretion. Moreover, the bacterial treatment regimen was comparable to mesalazine treatment in reducing cytokine levels.

Result

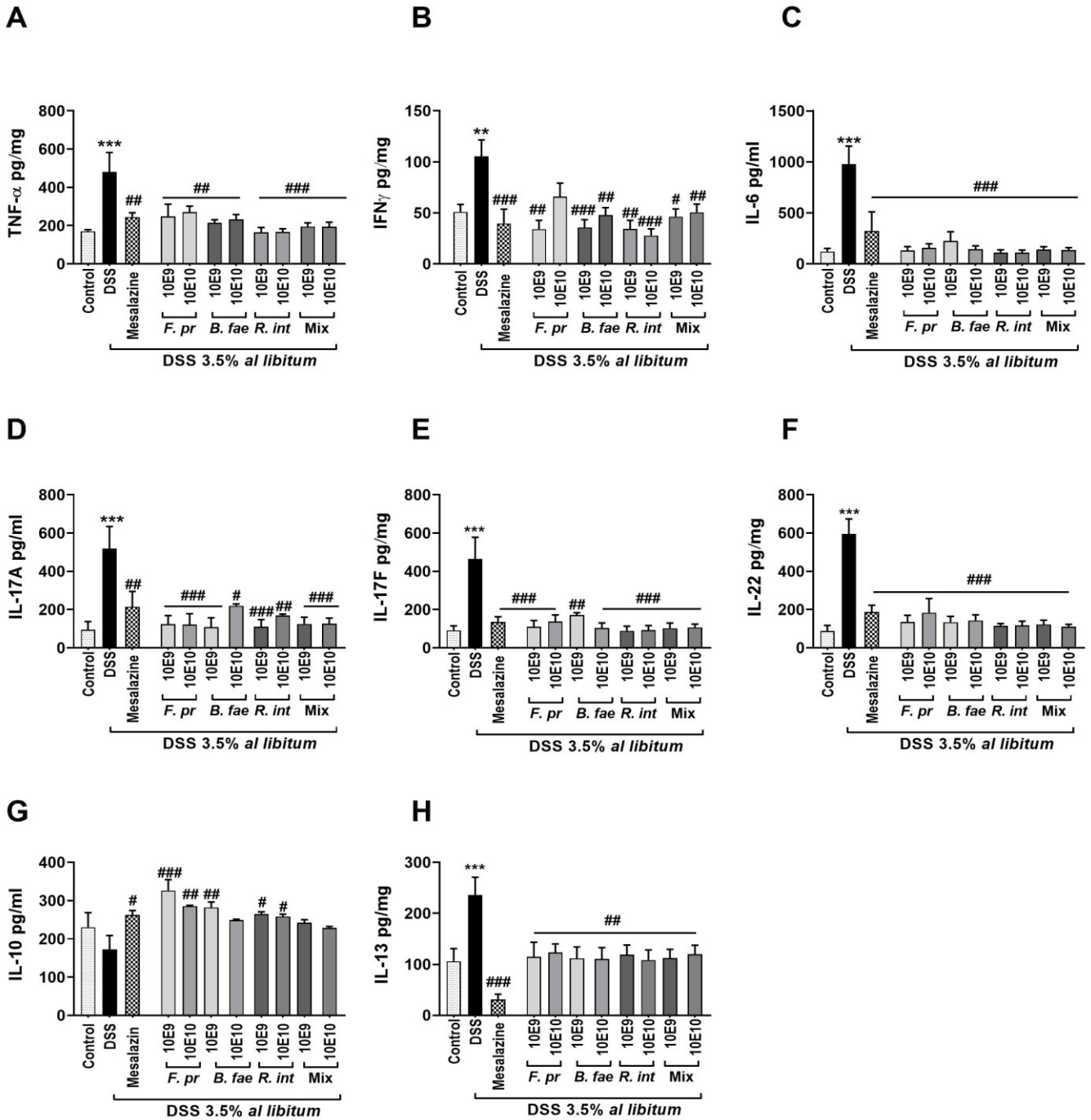


Figure 23. Regulation of the innate immune response in the colon by *F. prausnitzii*, *B. faecis*, and *R. intestinalis*.

The expression levels of the cytokines IFN- γ , TNF- α , IL-6, IL-17F, IL17A, IL-22 IL-13, and IL-10 in colon tissue were detected by multiplex ELISA. Data are shown as the means \pm SEMs (n=11). The terms 10E9 and 10E10 refer to CFUs of 10^9 and 10^{10} , respectively. Statistical analysis was performed with one-way ANOVA followed by the Dunnet test for comparison of the untreated control group versus the DSS group (** $P < 0.01$, *** $P < 0.001$) and the mesalazine- and bacterial species-treated groups versus the DSS group (# $P < 0.05$, ## $P < 0.01$, ### $P < 0.001$).

4.17 Treg percentages in mice with DSS-induced colitis

Regulatory T cells (Tregs) are a distinct subset of helper T cells that play a pivotal role in immune homeostasis and peripheral tolerance. Dysregulation of Treg function leads to the development of inflammatory disorders, including IBD (132). To examine the effects of mesalazine and the selected bacterial species individually and in combination on Treg subset abundance in mice with DSS-induced colitis, we isolated cells from the spleens of BALB/C mice. The isolated cells were stained with fluorochrome-conjugated mAbs against the CD4, CD25, and Foxp3 markers before analysis by flow cytometry. As shown in Figure 24 A, B, co-administration of all three bacterial species significantly elevated the percentage of CD4⁺CD25⁺Foxp3⁺ T cells at 10⁹ CFU (15.90 ± 1.80) and 10¹⁰ CFU (14.91 ± 2.89) compared to DSS treated group. Moreover, the expression level of CD4⁺CD25⁺Foxp3⁺ T cell population increased in the groups treated with *F. prausnitzii*, *B. faecis*, and *R. intestinalis* individually; however, the observed increase did not reach statistical significance. These findings suggest that a combination of all tested commensal bacteria has a protective effect against acute DSS-induced colitis, which could partly be mediated by an increase in Treg percentages. Mesalazine therapy was comparable to the bacterial mixture in terms of Treg modulation.

Result

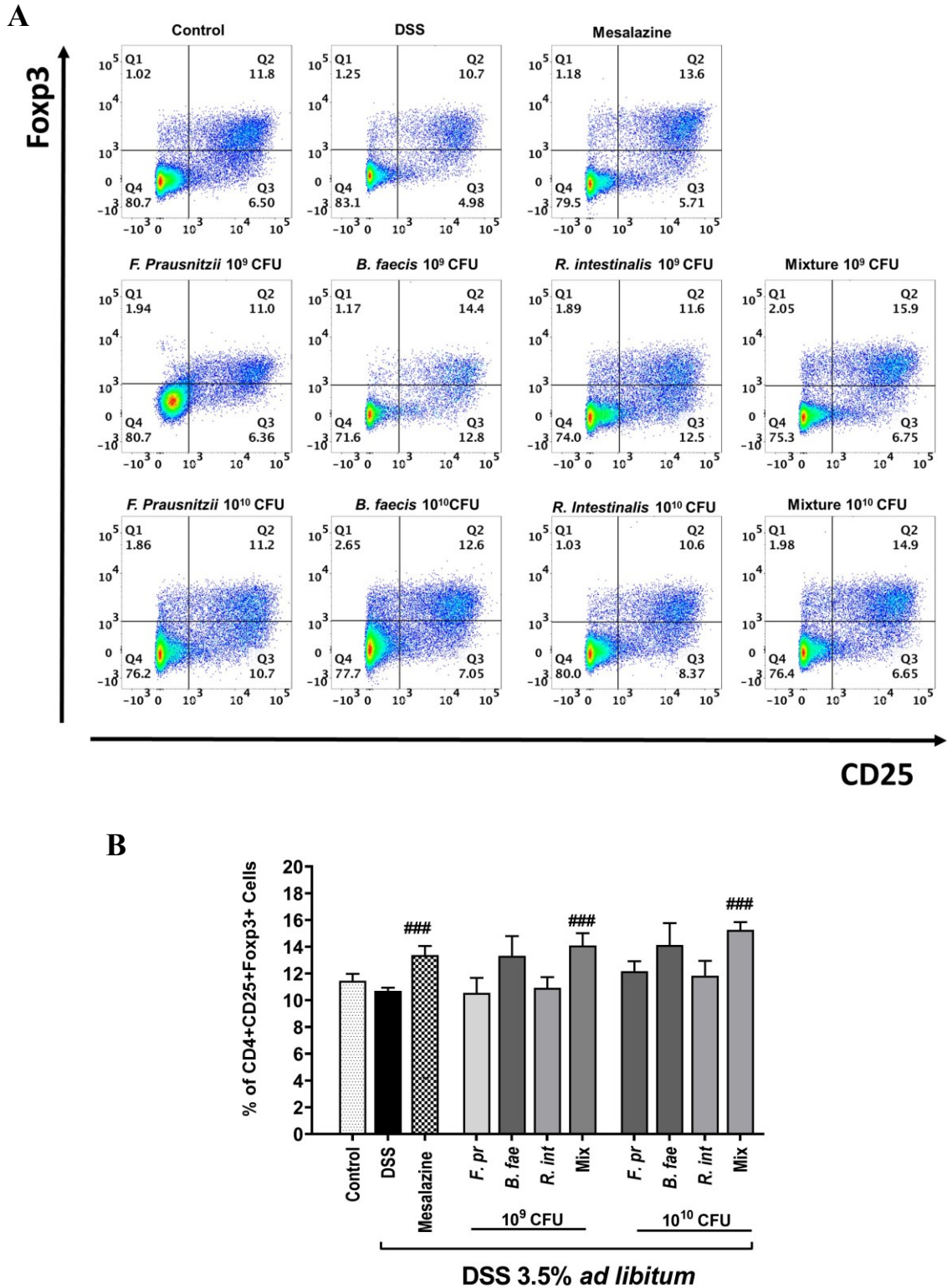


Figure 24. *F. prausnitzii*, *B. faecis*, and *R. intestinalis* alone and in combination expand the Treg population in mice with experimental colitis.

The mice were sacrificed, and their spleens were isolated. To detect Tregs, the spleens were stained with anti-mouse CD4, CD25, and Foxp3 mAbs. Treg percentages were analyzed by FACS. (A) Representative dot plots from spleen. (B) The percentage of Treg cell population. Data are shown as the means \pm SEMs ($n=11$). Statistical analysis was performed by the Mann–Whitney U test versus the DSS group (### $P < 0.001$).

4.18 Influence of bacteria treatments on the gut microbiome composition

Considering safety and the potential for disruption and dysbiosis in the gut microbiome with oral treatment of mesalazine and high doses of commensal gut microbial species in DSS-treated mice, we conducted a microbiome analysis at the experiment's endpoint. The results revealed a substantial reduction in bacterial community richness in the DSS group compared to the control group ($P < 0.0001$) (Figure 25 A). The groups treated with mesalazine and the eight bacterial treatments did not exhibit notable variations in richness when compared to the DSS group.

The analysis identified a total of 16 phyla, with Bacteroidota and Firmicutes collectively representing around 90% of the fecal microbiome in the experiment (Figure 25 B). At the phylum level, the administration of *R. intestinalis* (10^{10} CFU) and *B. faecis* resulted in a reduction in the proportion of *Proteobacteria*, like the observed effect in the mesalazine-treated group.

At the genus level, we observed 231 bacterial genera. The majority of the 15 most abundant genera were typical fecal commensals with similar abundances across all treatment groups. Of note is the higher abundance of *Pelomonas* and *Methylobacterium* in all bacterial treatment groups and the mesalazine group compared to the DSS group. Treatment with *F. prausnitzii*, the bacterial mixture (10^{10} CFU) and mesalazine slightly increased the abundance of *Lactobacillus*. Furthermore, the abundance of *Escherichia-Shigella* was decreased in all bacterial treatment groups and the mesalazine group (Figure 25 C). As a final observation regarding the microbiome data, we could not detect the presence of *F. prausnitzii*, *R. intestinalis*, or *B. faecis* in the bacterial treatment groups, suggesting that the microbiome was nearly unaltered, and that the bacterial species used for treatment were present only transiently.

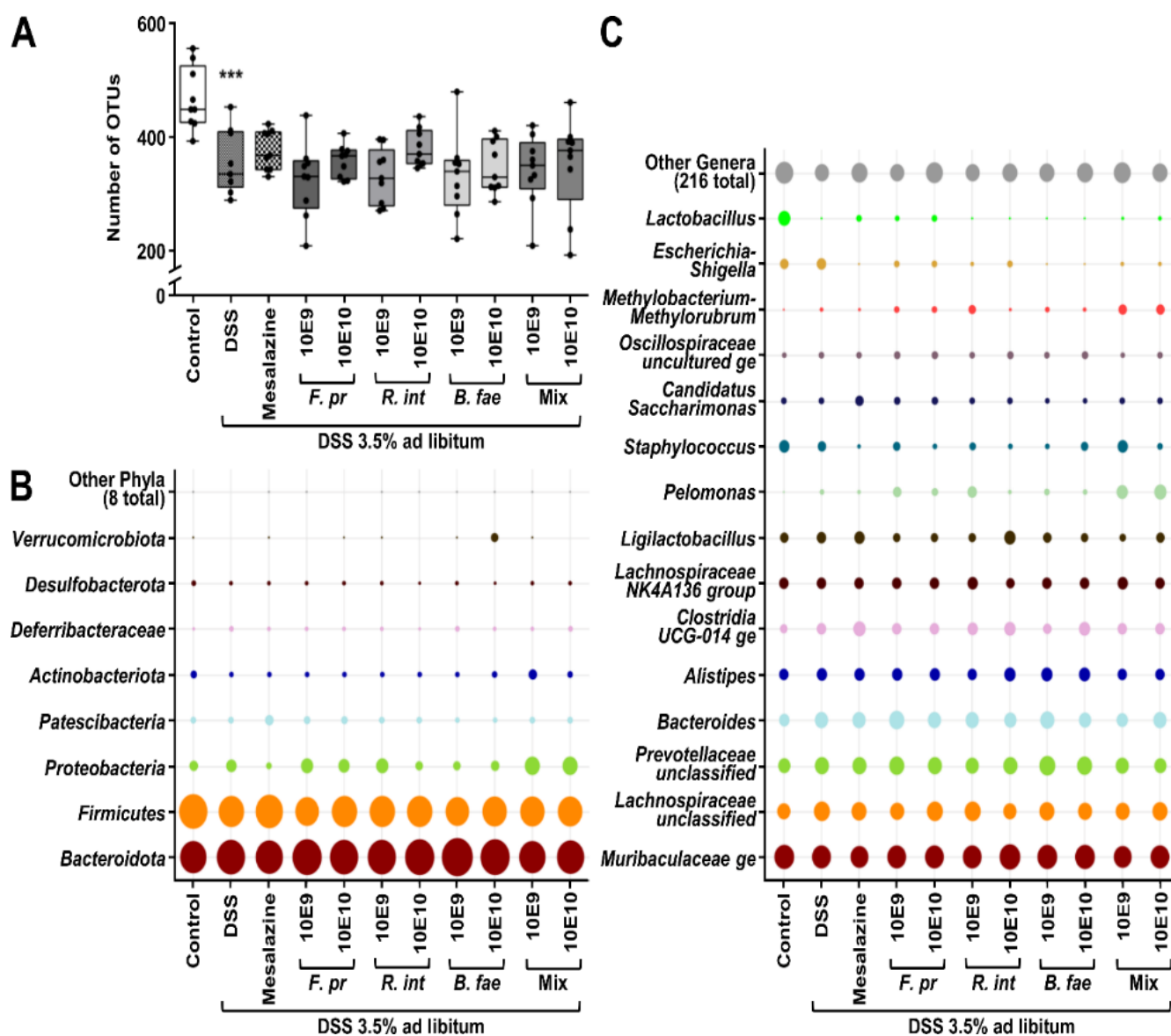


Figure 25. Alterations of the fecal microbiome due to DSS and bacterial treatments.

(A) Number of distinct Operational Taxonomic Units (OTUs) observed in the different treatment groups. (B) Phyla found in the fecal microbiome with at least 1 % relative abundance. (C) Top 15 genera by overall relative abundance found in the eleven treatment groups. The terms 10E9 and 10E10 refer to CFUs of 10^9 and 10^{10} , respectively.

5 Discussion

5.1 The influence of commensal bacteria on intestinal inflammation *in vitro*

The human gastrointestinal tract is home to a large number of microorganisms, collectively known as the gut microbiota. These microorganisms play crucial roles in the regulation of various host physiological functions, including immune modulation, metabolism, and gut barrier integrity. Commensal bacteria, which are non-pathogenic bacteria that coexist with their host, are known to provide protective effects against pathogenic microbes and maintain a healthy gut microbiota. Therefore, there has been significant interest in developing strategies to promote the growth and colonization of beneficial commensal bacteria within the gut. In this study, we investigated the barrier protection and recovery effects of three commensals, *F. prausnitzii*, *B. faecis*, and *R. intestinalis*, on differentiated intestinal epithelial cells (IECs). For this purpose, it is necessary to elucidate the interaction between these commensal bacterial species and the cells of the gastrointestinal system. To this end, the conditions for co-culture experiments for both bacterial and eukaryotic cells were optimized.

The centrifugation and resuspension of bacterial cells in a mammalian cell culture medium is a well-established approach in bacterial-mammalian cell co-culture research (133, 25, 134). Studies have shown that some species, such as *E. coli*, *S. typhimurium*, and *Lactobacillus fructosus*, are able to maintain equivalent viability in both mammalian and bacterial culture medium (134). However, in our experiment none of the three commensal bacteria demonstrated growth in the anaerobic mammalian cell culture medium DMEM for over 6 hours. This could be due to the inadequate concentration of essential nutrients and substrates in the DMEM medium for bacterial survival. The growth of the commensals may require the use of complex media. For instance, *F. prausnitzii* A2-165 did not grow without the addition of yeast extract to the bacterial culture medium, YCFAG (135). Additionally, iron is a crucial factor for bacterial growth, and its presence in adequate amounts is vital for the survival of microorganisms (136, 135). Bacterial culture media commonly provide hemin as a source of iron, which is a more suitable iron source for commensals compared to ferric nitrate, the sole iron source in the cell culture medium. Our experimental results revealed that, while the use of complex media enriched with appropriate levels of nutrients and substrates is critical for

Discussion

the cultivation of commensal bacteria in co-culture experiments, the tested commensal bacteria demonstrated normal growth behavior up to 6 hours of incubation in DMEM medium, albeit at a slower rate compared to that observed in bacterial medium.

On the other hand, the TEER measurement of differentiated Caco-2 and HT29-MTX cells treated with supplemented YBHI media under anaerobic conditions showed a significant decline, reaching approximately 300 cm². The TEER of differentiated epithelial cells has been reported to be within a range of 500 to 1100 cm² (137). Hence, the TEER values of Caco-2 and HT29-MTX cell monolayers treated with bacterial culture medium were lower than those of differentiated epithelial cells treated with pure cell culture medium. This suggests that the treatment of the cell monolayers with bacterial culture medium had an impact on the TEER values, which is an important measure of epithelial barrier function. Based on these findings, the choice of DMEM medium as the culture medium was deemed appropriate as it did not negatively affect the viability or barrier integrity of the Caco-2 and HT29-MTX cells and allowed for the growth of all three tested commensal species up to 6 hours of incubation. These results indicate that DMEM is a suitable choice for co-culture experiments with commensal bacteria and epithelial cells, as it provides a balance between supporting cell growth and maintaining cellular functionality.

Adherence to the intestinal surface is a crucial characteristic of probiotics, which can be direct attachment to intestinal epithelial cells (IECs) or temporary colonization within the intestine (138). While there are a number of studies assessing the adhesion of probiotic bacteria quantitatively (139–141) to date only very few have investigated adhesion of these organisms from a mechanistic point of view. Most mechanistic studies on adhesion to IECs were performed for pathogenic bacteria such as enteropathogenic *E. coli* (EPEC), *Salmonella enterica*, *Streptococcus salivarius*, *Yersinia enterocolitica*, and *Listeria monocytogenes* (142–145). Nevertheless, a few *in vitro* studies have been performed to evaluate the species and strain-specific adherence of probiotics to IECs, utilizing model systems such as mono-cultures of Caco-2 cells (146), and HT29 (147), as well as co-cultures of Caco-2:HT29-MTX cells (148). The results of these investigations suggest that the adherence of probiotics to IECs can be highly influenced by both the species and strain of the used probiotic (149). The adhesion capability of bacteria to intestinal epithelial cells promotes the residence time and affects the ability of probiotic strains to regulate the immune response. However, little is known, as to how the adhesion ability is

Discussion

correlated with immunomodulation (150), there are indications that the adherence of some probiotic bacteria to the gastrointestinal mucosa might be essential to stimulate the host immune system (151). Many studies have used Caco-2 and mucus-secreting HT29-MTX cell lines to assess the adhesion ability of putative probiotic strains (152). *Lactobacillus* spp and *Bifidobacterium* spp are the most common probiotics, and their adhesion properties to intestinal epithelial cells have been studied extensively (153, 141). In the present study, the Caco-2 and HT29-MTX cell lines were selected to determine the adhesion behavior of *F. prausnitzii*, *R. intestinalis*, and *B. faecis*. All species showed adhesion to the used cell lines, however, the adhesion level of *B. faecis* and *R. intestinalis* were more pronounced to HT29-MTX cell line. These data correspond with the finding by Schillinger et al. (154), who showed that the adhesion of all probiotic strains varies among strains, though high adhesion rates to HT29-MTX compared to other cell lines were observed. Gopal et al. (155) used HT-29, Caco-2 and HT29-MTX cells to assess the adherence ability of two *L. acidophilus* and two *L. rhamnosus* strains and reported the higher affinity of bacteria to adhere to the latter cell line. Moreover, they hypothesized that this behavior might be due the physical entrapment of bacteria in the mucus layer rather than the higher association of this cell line for strains. In our study, *F. prausnitzii* exhibited similar adherence percentages to both the Caco-2 and HT29-MTX cell lines, with adhesion values of 1.51 ± 0.65 and 1.32 ± 0.94 , respectively. This is in contrast to the findings of Martin et al. who reported no adherence of *F. prausnitzii* to HT-29 cell lines, but observed up to a 20% adhesion level (relative to *Lactobacillus rhamnosus GG*) when mucin was added to the HT-29 cell line (156).

Bacterial adhesion is a complex process, affected by several factors such as nonspecific and specific interactions, which include hydrophobic interactions, cation-bridging, receptor–ligand binding (157), and also the environmental conditions (158). For instance, the adhesion of strain *B. bifidum* MIMBb75 to Caco-2 and HT29 cells, is depending on pH and the presence of sugars and bile salts (159). While adhesion might play an important role in establishing administered probiotic bacteria in the intestinal tract of the host, to date no direct correlation between the health-promoting properties of probiotics and their adhesion to IECs and/or mucus has been demonstrated.

Discussion

Many intestinal inflammatory diseases, including IBD, have been associated with impaired intestinal barrier function (59). Intestinal barrier consists of a single epithelial cell layer and an intraepithelial tight junction (TJ) complex is considered to be the first line of defense against the hostile luminal environment (160).

The barrier function and integrity depend on the regulation of intercellular tight junctions. TJ proteins such as claudins (CLDs), occludin, the zonula occludens (ZO), junctional adhesion molecule (JAM), and the adherence junction protein E-cadherin, are located at the apical-lateral membrane (161, 162). These proteins regulate the passage of solutes and macromolecules through the paracellular pathway, thereby playing a vital role in regulating intestinal barrier function (160). In principle, intestinal permeability reflects the state of the epithelial TJ (163). Dysregulation of intracellular TJs contributes to the uncontrolled translocation of microorganisms, pathogens, and antigens throughout the epithelium, resulting in an overactive mucosal immune response that subsequently leads to chronic inflammation, as in the case of IBD (30).

In our study, we analyzed several parameters to examine the effect of *F. prausnitzii*, *R. intestinalis*, and *B. faecis* on integrity of epithelial cells. One way to measure the integrity of an epithelial layer is to measure its trans-epithelial electrical resistance (TEER). TEER is a measure of the electrical resistance across the epithelial layer, which is related to the tightness of the TJ complex. When the TJ complex is intact, the TEER is high, indicating low ion flux through the pore pathway regulated by the TJ complex. Conversely, when the TJ complex is disrupted, the TEER is low, indicating high ion flux.

Our results show significant alterations in the expression of claudin-2 and occludin, as well as in TEER (a marker for tight junction integrity) and FITC dextran flux, induced by a pro-inflammatory cytokine cocktail and LPS treatment. This disturbance is attributed to an increased ion flux through the pore route regulated by the tight junction (TJ) complex. However, Intervention with *F. prausnitzii*, *B. faecis*, and *R. intestinalis* restored the expression of both TJ proteins, leading to an improvement in barrier function, as shown by TEER and FITC dextran experiments, along with immunofluorescence staining. These findings reveal that all three tested commensal species markedly enhanced cell-to-cell integrity. Our findings are consistent with the findings of previous studies which demonstrated that a high occludin expression and a decrease in the abundance of claudin-2 are associated with increased TEER values following treatment with probiotic strains (164–168). These observations prompted us to hypothesize that increased occludin and

Discussion

decreased claudin-2 expression may contribute to the ability of the commensal species to strengthen the epithelial barrier. Several recent research studies have explored the potential impact of commensal microbiota on the presence of tight junctions. In a study conducted by Karczewski et al. (166), *L. plantarum* was administered to human subjects for six hours. Following this, the authors collected biopsies of the duodenum and performed immunostaining on the tight junction proteins ZO-1 and occludin. The results indicated that abundance of both ZO-1 and occludin was increased in intestinal epithelial cells (IECs), suggesting that *L. plantarum* could potentially enhance the strength of TJs, reduce gut permeability, and improve barrier protection (166).

A microbial metabolite might promote the expression of TJ proteins like claudins and occludin, increasing the amount of TJ strands and strengthening the seal between cells. Shimada et al. (169) investigated the potential benefits of indole, a quorum-sensing molecule found in commensal bacteria, on intestinal barrier function. They showed that germ-free (GF) mice, express fewer TJ-associated molecules. However, after indole treatment, GF mice regained higher mRNA expression of the same TJ molecules. This finding clearly shows that intestinal epithelium integrity is increased by indole, a product of commensal bacteria, by upregulating TJ molecules. Further, a study by Singh et al. (170) found that the TJ proteins ZO-1, claudin-4, and occludin are highly upregulated in an epithelial cell line after exposure to the microbial metabolite urolithin A, demonstrating the beneficial effects of commensal bacteria in enhancing barrier defense (170).

Further, immunostaining and Western blot analysis were performed to validate the impact of the tested commensals on tight junction expression and localization. The findings indicated that the disruption of the epithelial barrier function was linked to the depletion and redistribution of the tight junction proteins occludin and claudin-2. This finding is in line with previous research which found that the expression of claudin isoforms, particularly claudin-2, have an impact on TEER and ion permeability. Claudin-2 induces channel formation within the TJ, and is mostly expressed in leaky epithelia like the proximal intestine (171). The influence on the expression of other TJ proteins not measured in this study may also be a possible mechanism of our commensal species as it is known from various probiotic strains that the enhancement of the intestinal barrier is mediated by the activation of several signaling pathways (MAPK, ERK), resulting in a reorganization and increase of TJ proteins (172–174).

Discussion

The pathogenesis of IBD involves an imbalance between pro- and anti-inflammatory mediators produced by various immune and non-immune cells (175). In this study, we investigated the anti-inflammatory potential of three commensal species on pro-inflammatory and LPS mixture stimulated Caco-2 and HT29-MTX cells. Our findings demonstrated that treatment with all tested commensal species significantly inhibited the secretion of IL-8 and MCP-1, two key pro-inflammatory mediators, reducing their values to basal levels. IL-8 is a chemokine that attracts neutrophils to sites of inflammation (176), while MCP-1 is a chemokine that attracts monocytes and T cells (177). The suppression of these pro-inflammatory cytokines by the tested commensal species implies their potential application as therapeutic agents for inflammatory bowel disease (IBD). These findings correspond with previous research on the immunosuppressive effects of commensal and probiotic bacteria. Earlier studies have shown that *L. acidophilus* and various strains of *Bifidobacteria*, *Lactobacillus*, and *E. coli* are also able to reduce the secretion of pro-inflammatory cytokines, such as MCP-1 and IL-8 (175, 178–180). Moreover, IL-8 production in IL-1 β stimulated Caco-2 and TNF- α stimulated HT29 cells was reduced by *F. prausnitzii* supernatant (91, 181). *R. intestinalis* was able to increase the secretion of TGF β in LPS-stimulated Caco-2 cells (182).

Our study also demonstrates that commensal species have the potential to enhance the intestinal epithelial barrier. The *in vivo* application of live *F. prausnitzii* or the cell-free supernatant in experimental gut inflammation models has been shown to attenuate the severity of inflammation and enhance the intestinal epithelial barrier (91, 182, 183). Similarly, *R. intestinalis* has been shown to have similar effects in a murine model of acute colitis (184).

The transcription factor NF- κ B and its downstream pathway play a crucial role in the pro-inflammatory immune response, and its activation by pro-inflammatory stimuli has been implicated in IBD pathogenesis (185, 186). Inhibition of the NF- κ B signaling pathway was shown to have a pivotal influence on downstream mechanisms, resulting in enhanced TEER and alterations in tight junction expression (187, 188). It is likely that the observed immunosuppressive effect of commensal species is mediated via the NF- κ B pathway, as has been shown for other enteric bacteria (189, 190).

In conclusion, this *in vitro* study provides evidence for the immunosuppressive potential of commensal species in IBD. The ability of commensal species to suppress pro-inflammatory cytokines and enhance the intestinal epithelial barrier suggests their

potential use as therapeutic agents for IBD. However, their effect needs to be elucidated in an *in vivo* animal model to reveal the mechanisms underlying their immunosuppressive effects and their potential use in clinical practice.

5.2 The influence of commensal bacteria on intestinal inflammation *in vivo*

There is increasing evidence that some of the commensal bacteria may have a profound influence on the immune system under certain conditions. Several probiotic strains, mostly isolated from the normal human intestinal microbiota, have already been tested for application against gastro-intestinal inflammatory disorders, such as IBD (191, 192). Since the properties of a probiotic appear to be strain-specific (193), probiotic strains differ in their mode of action and therefore their potential applications (194). In the present study we aimed to investigate the therapeutic effects of *F. prausnitzii*, *R. intestinalis*, and *B. faecis* on intestinal inflammation in a DSS-induced murine colitis model. Mesalazine, a conventional treatment for ulcerative colitis (195), was used as a positive control.

IBD represents a multifactorial disease and is based on complex interactions between different cell populations. To understand the etiology and pathogenesis of IBD, several animal models have been developed based on genetic, immunological, bacterial, and chemical principles (196, 197). However, no single model can fully replicate all the features of UC. Instead, each model can mimic specific UC characteristics, allowing researchers to investigate its pathogenesis and develop potential treatments. In genetic models, animals with genetically modified backgrounds, such as gene knockout or transgenic models, are used to study specific genetic factors involved in IBD susceptibility and disease progression. For example, IL-10-deficient mice (IL-10^{-/-}) spontaneously develop inflammation that modifies the immune system and resembles UC in humans (115). In immunological models, specific subtypes of immune cells are introduced to immunodeficient mice to investigate their roles and effects in disease progression or treatment (197). To study the possible positive or negative impacts of various bacterial species in the development or treatment of IBD, bacterial models are used in which germ-free, specific pathogen-free, or immunodeficient mice are exposed to particular bacteria, such as pathogens or commensals (116, 198). Chemical models, such as TNBS and DSS-induced colitis models, are the most widely used experimental models due to their simplicity, reliability, and applicability (117).

Discussion

Among these models, DSS-induced colitis mimics the major clinical and histopathological features of human IBD (199), including diarrhea, rectal bleeding, crypt destruction, infiltration with granulocytes, edema and ulceration of colon tissue (200). The toxic agents mediate a toxic effect on intestinal epithelial cells, leading to a loss of barrier integrity and exposing immune cells to antigens, subsequently triggering an immune response. Based on the characteristics of colitis, this model is suitable for studying the effect of intestinal flora on the progression of colitis. Reduced expression of tight junction proteins (e.g., occludin) in the epithelium, as well as increased intestinal permeability for luminal bacteria, are additional significant features that both human IBD and DSS-induced colitis have in common.

In this study, mice were given 3.5% DSS in their drinking water for 7 days, which resulted in weight loss, increased DAI score, intestinal ulceration, increased neutrophil infiltration, and secretion of colonic pro-inflammatory cytokines. These findings indicate the successful induction of ulcerative colitis-like pathology in our colonic colitis model.

However, administration of *F. prausnitzii*, *R. intestinalis*, and *B. faecis*, and their combination, at both doses, attenuated the severity of DSS-induced colitis in mice, which is evidenced by significant improvements in clinical symptoms, including, body weight loss, stool consistency, bleeding and consequently, reduced disease activity index (DAI) scores in mice treated with DSS. Moreover, the macroscopic and microscopic analysis revealed that the tested bacteria significantly reduced colon shortening. According to the literature, patients with active IBD experience histopathological damage characterized by inflammation in the colonic mucosa. In a colitis colon, inflamed tissue can involve the infiltration of immune cells, such as macrophages and neutrophils, into the submucosal region, as well as the destruction or loss of colonic crypts, ulceration in the crypts, and depletion of mucosal goblet cells (201). This recurrent epithelial damage results in the disruption of the intestinal barrier (202). Our study showed that intervention with *F. prausnitzii*, *R. intestinalis*, and *B. faecis* reduced crypt disruption, goblet cell loss, submucosal edema, and epithelial damage. Additionally, reduced MPO activity in DSS-induced mice treated with bacteria was noted. It is well known that MPO activity is one of the key indicators of neutrophil infiltration into colonic tissues and is used as a potential biomarker to study the progression of colitis (203, 204). Taken together, the sum of attenuated clinical symptoms proved that all the three tested bacteria, individually and in

Discussion

combination, reduced DSS-induced intestinal inflammation and might be promising candidates for the treatment of colitis.

Cytokines are connected to the pathogenesis of IBD. Clinical studies have shown that the onset and severity of colon inflammation are often associated with an imbalance between pro and anti-inflammatory cytokines. DSS induces acute colitis by disrupting the intestinal epithelial layer, leading to the activation of mucosal immune cells and subsequent infiltration of inflammatory cells. These infiltrates consist mainly of T and B lymphocytes, macrophages, and neutrophils, which secrete various pro-inflammatory cytokines, including TNF- α , IL-6, IL-13, IL-22, IL-17, and IFN- γ . The upregulation of these cytokines, primarily associated with Th1/Th17-mediated inflammation, is a hallmark of acute DSS-induced colitis (199). In particular, TNF- α as an early inflammatory cytokine promotes T cell differentiation and proliferation, destroys the intestinal barrier, and accelerates intestinal inflammation. In IBD, the source of TNF- α is activated macrophages or monocytes. Studies have shown that blood and colonic tissues from patients with UC exhibit increased TNF- α expression. From this, a therapeutic agent that reduces the levels of TNF- α may effectively ameliorate intestinal inflammation. IL-17A acts in the delayed-type immune reaction, in which it increases chemokine production and the number of monocytes and neutrophils recruited to the inflamed area. IFN- γ , a pro-inflammatory cytokine, has pleiotropic effects such as antiviral activity, increased MHC expression, and stimulation of T and natural killer (NK) cells. IFN- γ appears to play an important role in chronic inflammatory diseases, according to mounting evidence. Ito et al. reported that IFN- γ was increased in the colon of DSS-treated WT mice, but IFN- γ ^{-/-} mice developed less severe colitis following DSS stimulation, as measured by body weight loss, DAI, histological score, and MPO expression. According to this study, IFN- γ is important in the development of DSS colitis, and certain chemokines such as IP-10, MIG, and MCP-1 are produced in an IFN- γ dependent manner.

In the present study, we observed that the protective effect of *F. prausnitzii*, *B. faecis*, *R. intestinalis*, and their combination on DSS-induced colitis in mice is associated with the ability of these bacterial species to regulate the secretion of inflammatory cytokines. The secretion level of IFN- γ , TNF- α , IL-6, IL-4, IL-17A/F, IL-22, and IL-13 was significantly elevated in the colon tissue by DSS treatment and was remarkably suppressed by the administration of the tested commensal bacteria, individual and in combination, at both

Discussion

doses. Increasing evidence demonstrates that IL-13 is responsible for initiating the detrimental inflammatory cascade in colitis. While orchestrating an inflammatory response by immune cells, IL-13 can also directly impact on epithelial cells. In ulcerative colitis, IL-13 has been described as a key effector cytokine acting on epithelial cell function and initiating apoptosis (205).

Interleukin-10 (IL-10) is an immune-regulatory cytokine, and its genetic defect leads to gastrointestinal inflammation in humans and mice. Several studies have shown that IL-10-deficient mice (IL-10^{-/-}) develop colitis spontaneously, and there is an association between a decrease in IL-10 level and the synthesis of pro-inflammatory cytokines such as TNF- α and IL-17. Simon et al. noted that IL-10 deficiency is a primary initiating event in chronic intestinal inflammation in IL-10 deficient mice. Accordingly, in our study we observed that 3.5% DSS treatment profoundly decreased IL-10 levels, however an increase in the expression level of the potent immunoregulatory cytokine IL-10 was noted in DSS-induced colitis mice treated with all three bacterial species and their mixture.

CD4⁺ T cells play a crucial role in the adaptive immune system by releasing different cytokines that can facilitate, suppress, or regulate immune responses. Among the cytokines produced by CD4⁺ T cells, TNF- α and IL-6 are notable examples. The development of IBD is largely attributed to the dysfunction of the adaptive immune system, which may be caused by an excessive number of effector T cells or a shortage of Treg cells. The imbalanced ratio between effector T cells and T regulatory (Treg) cells can result in the overproduction of pro-inflammatory cytokines, which subsequently triggers the onset of IBD (206).

T regulatory (Treg) cells, which are characterized by Foxp3 expression, are important regulators of immunological homeostasis and tolerance. Th1, Th2, and Th17 cells are activated during inflammation, whereas Treg cells are suppressed. Evidence has shown that Treg cell deficiency, dysfunction, or mutation in the Foxp3 gene disrupts the balance of intestinal mucosal immunity and is responsible for fatal, highly aggressive, and systemic autoimmune inflammatory lesions in mice and humans. Many studies have reported that the number of CD4⁺CD25⁺ Treg cells and expression of transcription factor Foxp3 in peripheral blood of patients with inflammatory bowel disease are insufficient (207). Furthermore, mouse models of IBD have demonstrated the protective effects of Treg cells during colitis. Immunodeficient mice that are adoptively transferred with Treg-depleted naïve CD4⁺ T cells develop spontaneous colitis; in contrast, mice transferred

Discussion

naïve CD4⁺ T cells combined with Treg cells do not develop colitis. Consistent with this observation, our results showed that the number of CD4⁺CD25⁺Foxp3⁺ Treg cells in the spleen of mice with untreated colitis was lower than that of the control group. However, the percentage of CD4⁺CD25⁺Foxp3⁺ cells in the spleens of DSS-induced colitis mice was increased following the oral administration of *B. faecis* and *R. intestinalis*. Of note, Treg induction was more pronounced when the mixture of the tested species was administered. This finding indicates that these commensal bacterial species alone and in mixture had protective effects against the development of DSS-induced colitis that were partly mediated by increases in Treg percentages. Our findings are in agreement with other studies investigating the immunomodulatory actions of commensal and probiotic bacteria in murine colitis model (208, 209). A previous study has shown that the anti-inflammatory effects of a probiotic mixture (BIFICO) containing *Bifidobacterium longum*, *Lactobacillus acidophilus*, and *Enterococcus faecalis* were related to the expansion of Tregs in mesenteric lymph nodes of colitis mice and the ratio of Th1 /Th2 might be regulated by Tregs (208).

Zhu et al., demonstrated that *R. intestinalis* can inhibit the secretion of IL-17 and promote the differentiation of Treg in TNBS-induced colitis (210). Similarly, Martin et al have shown that application of *F. prausnitzii* induces Foxp3⁺ and Treg production in the spleen during TNBS-induced colitis (156). These findings suggested that enhancing the activity of Tregs in the gut might aid in the restoration of inflamed colonic tissues, making Tregs a prospective target for treating UC. Even though the exact pathogenesis of IBD is not yet clear, evidence suggests that Th17 and Treg cells have a functional antagonism, in which Tregs act as immunosuppressive cells, and Th17 cells are involved in initiating autoimmune and inflammatory diseases (211). Treg cells, characterized by Foxp3 expression, are essential regulators of immunological homeostasis and tolerance by regulating the release of the inhibitory cytokines IL-10, IL-4, and IL-13 (212). Th17 cells develop by the differentiation of naive T cells, and play a crucial role in the pathogenesis of a number of autoimmune diseases, such as autoimmune encephalitis, allergic asthma, and rheumatoid arthritis (213).

Research has shown that patients with inflammatory bowel disease have reduced levels of CD4⁺CD25⁺ Treg cells in their peripheral blood and elevated levels of IL-17A compared to healthy individuals (214, 215). Notably, the diversity of gut microbiota and its metabolites have a significant impact on modulating the Treg/Th17 balance, which in

Discussion

turn affects the inflammatory responses associated with IBD; the microbiota can induce Th17 cells, leading to aggravated colitis in mouse models while SCFAs, which are microbiota-derived metabolites, promote the differentiation of Treg cells (216).

In our study, we observed that *F. prausnitzii*, *R. intestinalis*, and *B. faecis* efficiently suppressed the secretion of Th1/Th17 cytokines in the colon of DSS-treated mice, as well as Th17 related cytokines including TNF- α , IL-6, IL-17A/F and IL-22. Moreover, this treatment also reduced Th1-related cytokine IFN- γ in the colon. IL-17A/F and TNF- α are Th17 secreted cytokines, whereas IL-6 is an activator of Th17 cell differentiation. Remarkably, the IL-10/IL-17A ratio was significantly higher in the DSS-treated group than in the control and bacterial-treated groups, supporting the hypothesis that Th17 cells induce IL-17A secretion during inflammation. However, the IL-10 secretion was induced by *F. prausnitzii*, *B. faecis*, and *R. intestinalis* intervention, which effectively reversed the IL-10/IL-17A ratio. These decreased cytokines in the colon of DSS-treated mice after treatment with the tested commensals prompted us to the hypothesis that the tested commensal bacteria attenuate DSS-induced colitis which is at least partly mediated by regulating Treg/Th17 cell balance.

IBD is associated with a disturbed intestinal epithelial barrier caused by pathologically altered tight junction proteins (217). Consequently, an uncontrolled translocation of luminal substances throughout the epithelium results in an overactive mucosal immune response. One potential factor leading to the observed changes in barrier function is cytokines secreted from lymphocytes infiltrating the lamina propria. Numerous studies have shown that inflammatory responses influence TJ protein expression. For instance, a higher concentration of pro-inflammatory cytokines (such as IFN- γ , TNF- α , and IL-1 β) reduces the expression of tight junction proteins, thereby increasing epithelial paracellular permeability (66, 65). Moreover, Th2 cytokines such as IL-4 and IL-13 have also been shown to affect tight junction proteins in the intestinal epithelium, by upregulating the expression of Claudin-2 (196, 197). In addition, IL-13 can downregulate the expression of occludin and ZO-1, leading to increase paracellular permeability (197). Furthermore, mice with DSS-induced colitis showed significantly lower expression of TJ proteins and junctional adherence molecules, such as occludin and E-cadherin (218). Gong et al., demonstrated that damaged intestinal epithelial barrier integrity contributes to increased intestinal permeability due to uncontrolled translocation of luminal components across the epithelium (219). Another animal study from Ukena et al., in DSS-induced colitis

Discussion

mice demonstrated that administration of *E. coli Nissle* 1917 to DSS-induced colitis mice prevented increased intestinal permeability while minimizing tight junction protein (ZO-1) down-regulation (220). In our study, oral administration of all three tested commensal bacteria, individually and in combination, significantly affected the expression levels of tight junction proteins, indicating restoration of the epithelial barrier. This positive outcome was confirmed by the barrier function improvement, as seen in the *in vivo* FITC-dextran permeability assay. The diversity and composition of the gut microbiota are crucial for the progression of IBD. Accumulating evidence suggests that alterations in the gut microbial composition lead to metabolite changes affecting the pathogenesis of IBD (221, 222). Therefore, the gut microbiome was studied in all treatment groups at the endpoint of the experiment. At the phylum level, the *R. intestinalis* and *B. faecis* treatments decreased the abundance of *Proteobacteria* to a lower level than that in the control group. Most *Proteobacteria* are LPS-producing, harmful gram-negative bacteria (223), with *Escherichia* and *Shigella* as typical genera. It has been reported that the increased relative abundance of *Proteobacteria* can be used as a microbial biomarker for gut microbiota imbalance (224). Although *Proteobacteria* were found in a higher abundance in the bacterial treatment groups, at the genus and OTU levels, *Escherichia-Shigella* were less abundant in all treatment groups. The depletion of *Lactobacillus* genera has been shown in UC patients (225) and DSS colitis (226, 227), which is consistent with our results from the DSS group. However, bacterial treatment with *F. prausnitzii* and the mixture did not restore the abundance of this genus or *Lactobacillus* OTUs to normal levels.

In this study, we observed several changes in the gut microbiota composition related to the *Muribaculaceae* and *Lachnospiraceae* families. However, the majority of the differences between the groups were found in OTUs with a relative abundance of less than 1%, indicating that the probiotic treatment did not significantly impact the microbiome compared to the DSS group. Although OTU00002 increased in most treatment groups, its significance is difficult to determine due to limited classification at the family level, and further comparison with the NCBI nucleotide collection did not yield any additional insights. The absence of *F. prausnitzii*, *B. faecis*, and *R. intestinalis* demonstrates the transient nature of the probiotic treatment or could be a side effect of the endpoint measurement. Nevertheless, this outcome could indicate the safety of this commensal bacterial treatment approach, as the treatment does not permanently influence

Discussion

the fecal microbiome, which is very important for potential future clinical use of our bacterial cocktail in human.

Mesalazine is widely recognized as a key anti-inflammatory drug primarily prescribed for UC (195). Two pioneering studies, conducted by Kruis et al. in 1997 and 2004, revealed that the probiotic *E. coli* Nissle 1917 exhibits efficacy comparable to mesalazine in sustaining remission among individuals diagnosed with UC (191, 228). Rembacken et al. further supported these results, as they investigated 116 patients with active ulcerative colitis and found that 75% mesalazine treated patients and 68% of *E. coli* Nissle treated patients achieved remission (230). Therefore, *E. coli* Nissle is an alternative treatment option for individuals with ulcerative colitis. Although the exact mechanism of action of mesalazine remains unclear, it is believed to exert immunosuppressive effects by limiting prostaglandins and inhibiting pro-inflammatory cytokines (229). Interestingly, in our experiment, the groups treated with bacteria exhibited an equal or greater inhibitory effect on inflammatory cytokines compared to the group treated with mesalazine. This suggests that the protective effect of these commensal bacteria involves modulating the immune response of the host through the suppression of pro-inflammatory cytokines and/or the induction of anti-inflammatory cytokines. Another mechanism of action proposed for mesalazine is inhibition of IL-2 production in peripheral blood mononuclear cells, which inhibits T-cell proliferation, alters cell adhesion expression patterns, inhibits antibody production and mast cell release, and interferes with macrophage and neutrophil chemotaxis (230, 231). Mesalazine may also reduce IL-1 and TNF- α , cause lymphocyte apoptosis, and regulate NF- κ B (231).

In a study conducted by Huang et al., it was revealed that the *Lactobacillus paracasei* strain R3 possesses comparable efficacy to mesalazine in ameliorating general symptoms of murine colitis. Notably, the strain exhibited the ability to alleviate inflammatory cell infiltration, suppress Th17 response, and promote Treg function in murine DSS-induced colitis (232). In another investigation, the commensal bacterium *Christensenella minuta* was administered to TNBS-induced colitis rats. The results of this microscopic investigation suggest that *C. minuta* may be just as effective at protecting colonic tissue as mesalazine (233). These findings suggest that probiotics exhibit comparable efficacy to mesalazine in managing ulcerative colitis (UC), indicating that probiotics could serve as a potential alternative or supplementary treatment option for individuals with UC in the future. The observed positive effects on symptom alleviation and immune modulation

Discussion

highlight the promise of probiotics as a safe and effective therapeutic approach to maintain remission and improve the overall management of UC.

6 Conclusions

Inflammatory bowel disease which includes ulcerative colitis (UC) and Crohn's disease (CD), is a multifactorial complex disorder characterized by chronic relapsing intestinal inflammation. Recommended treatments such as corticosteroids, amino-salicylates (e.g., mesalazine) and immunosuppressive only relieves symptomatic complications and are accompanied by serious side effects, including loss of immune tolerance and drug resistance. Thus, there are compelling reasons to explore alternative therapeutic strategies, including prebiotics, probiotics, and symbiotics, as complementary or alternative medicines to treat IBD. Alterations in the gut microbiota composition play a crucial role in the pathogenesis of IBD as specific commensal bacterial species are underrepresented in the microbiota of IBD patients. A significantly decreased abundance of members of the Firmicutes phylum in patients with UC was shown in clinical studies. Members of this phylum produce important short-chain fatty acid metabolites such as acetate and butyrate, which are powerful anti-inflammatory. In this work, the therapeutic potential of three commensal bacterial species, *F. prausnitzii*, *B. faecis*, and *R. intestinalis* and their combination in an *in vitro* and *in vivo* model of intestinal inflammation were studied. Results obtained from *in vitro* study demonstrated that all three bacterial species are able to recover the impairment of the epithelial barrier function induced by the inflammatory stimulus, as determined by an amelioration of the TEER and the paracellular permeability of Caco-2 and HT29-MTX cell monolayers. Moreover, the inflammatory stimulus increased claudin-2 expression and decreased occludin expression which improved in the cells treated with commensal bacteria. Furthermore, the commensals were able to counteract the increased release of IL-8 and MCP-1 induced by the inflammatory stimulus. These findings indicated that *F. prausnitzii*, *B. faecis*, and *R. intestinalis* alone and in combination improve the epithelial barrier integrity and limit inflammatory response.

Thus, in part two of this study the effects of the three commensal bacterial species individually and in combination in an *in vivo* mouse model were investigated. To our knowledge, this study is the first to investigate the influence of the commensal bacterial species *F. prausnitzii*, *R. intestinalis* and *B. faecis* as single or mixed formulations on the DSS-induced colitis mouse model.

Conclusion

Acute colitis was induced by using 3.5% DSS through drinking water. The oral administration of *F. prausnitzii*, *B. faecis*, and *R. intestinalis* attenuated the severity of DSS-induced colitis in mice, which was evidenced by increase of body weight, reduction of the DAI, inhibition of colon shortening, amelioration of colonic inflammation and suppression of colonic MPO activity.

IBD is characterized by the imbalance of pro-inflammatory and anti-inflammatory cells in the gastrointestinal tract. Excessive activation of Th1, Th2 and Th17 cells play a key role in the pathogenesis of IBD by instigating the inflammatory cascade. Moreover, it is well known that the dysfunction of the adaptive immune system in the pathogenesis of IBD is associated with excessive activation of effector T cells or impaired function of regulatory T cells. Our result proved that intervention with the tested commensal bacteria, individually and in combination, exhibited significant anti-inflammatory activities on DSS-induced colitis, these positive effects are likely associated with the inhibited production of Th1, Th2 and Th17 cytokines, and increased Foxp3⁺ expression on the CD4⁺ CD25⁺ Treg cells. Moreover, commensal bacterial treatment had no adverse effects on the general gut microbiome structure and was found to be equally effective as the contemporary mesalazine treatment regimen.

7 Limitations

Although this study is a significant step toward understanding the therapeutic potential of these bacterial species, it does have some limitations.

First, although the DSS-induced colitis model is a well-established and widely used model of IBD, it does not fully describe the complex and multifactorial nature of the disease in humans. While this model is useful for studying some aspects of the disease, additional studies using different mouse strains and other animal models are needed to fully understand the effects of these bacterial treatments on IBD.

Second, while the study provides evidence for the anti-inflammatory and immunoregulatory effects of the tested bacteria, the exact mechanisms underlying these effects remain unknown. Future research should focus on identifying the specific mechanisms involved, which could potentially lead to the development of more targeted therapies for IBD. Third, more research is needed to fully understand the microbiome-modulating properties of the bacterial treatments used in this study. Analysis of the abundance of gut microbes at different time points during the experimental protocol could provide valuable insights into the potential long-term effects of the treatments on the gut microbiome.

Finally, the study focuses on the effects of the bacterial treatments on an episode of DSS-induced colitis. However, in patients with UC, the disease is characterized by chronic relapsing episodes of disbalance. Therefore, an additional study using the bacterial treatment cocktail to study protection against multiple episodes of DSS-induced disbalances would be beneficial.

8 References

1. Sensoy I. A review on the food digestion in the digestive tract and the used in vitro models. *Current research in food science* 2021; 4:308–19.
2. DeSesso JM, Jacobson CF. Anatomical and physiological parameters affecting gastrointestinal absorption in humans and rats. *Food and chemical toxicology* 2001; 39(3):209–28.
3. Mowat AM, Agace WW. Regional specialization within the intestinal immune system. *Nature Reviews Immunology* 2014; 14(10):667–85.
4. Chaudhry SR, Liman MNP, Peterson DC. Anatomy, Abdomen and Pelvis, Stomach. In: *StatPearls*. Treasure Island (FL); 2022.
5. Dumont F, Da Re C, Goéré D, Honoré C, Elias D. Options and outcome for reconstruction after extended left hemicolectomy. *Colorectal Dis* 2013; 15(6):747–54.
6. Suzuki T. Regulation of intestinal epithelial permeability by tight junctions. *Cellular and Molecular Life Sciences* 2013; 70(4):631–59.
7. Kiela PR, Ghishan FK. Ion transport in the intestine. *Current opinion in gastroenterology* 2009; 25(2):87.
8. Keita AV, Söderholm JD. The intestinal barrier and its regulation by neuroimmune factors. *Neurogastroenterol Motil* 2010; 22(7):718–33.
9. Ferraris RP, Diamond J. Regulation of intestinal sugar transport. *Physiological reviews* 1997; 77(1):257–302.
10. Baum B, Georgiou M. Dynamics of adherens junctions in epithelial establishment, maintenance, and remodeling. *Journal of Cell Biology* 2011; 192(6):907–17.
11. Rodriguez-Boulan E, Macara IG. Organization and execution of the epithelial polarity programme. *Nature reviews Molecular cell biology* 2014; 15(4):225–42.
12. Brandtzaeg P, Kiyono H, Pabst R, Russell MW. Terminology: nomenclature of mucosa-associated lymphoid tissue. *Mucosal Immunology* 2008; 1(1):31–7.
13. Mowat AM. Anatomical basis of tolerance and immunity to intestinal antigens. *Nature Reviews Immunology* 2003; 3(4):331–41.

References

14. Mason KL, Huffnagle GB, Noverr MC, Kao JY. Overview of gut immunology. *GI microbiota and regulation of the immune system* 2008:1–14.
15. Scaldaferri F, Pizzoferrato M, Gerardi V, Lopetuso L, Gasbarrini A. The gut barrier: new acquisitions and therapeutic approaches. *J Clin Gastroenterol* 2012; 46:S12-S17.
16. Bergstrom KSB, Kisson-Singh V, Gibson DL, Ma C, Montero M, Sham HP et al. Muc2 protects against lethal infectious colitis by disassociating pathogenic and commensal bacteria from the colonic mucosa. *PLoS pathogens* 2010; 6(5):e1000902.
17. Bevins CL, Salzman NH. Paneth cells, antimicrobial peptides and maintenance of intestinal homeostasis. *Nat Rev Microbiol* 2011; 9(5):356–68.
18. Takiishi T, Fenero CIM, Câmara NOS. Intestinal barrier and gut microbiota: Shaping our immune responses throughout life. *Tissue Barriers* 2017; 5(4):e1373208.
19. Gieryńska M, Szulc-Dąbrowska L, Struzik J, Mielcarska MB, Gregorczyk-Zboroch KP. Integrity of the intestinal barrier: The involvement of epithelial cells and microbiota-A mutual relationship. *Animals (Basel)* 2022; 12(2).
20. Segain JP, La Blétière DR de, Bourreille A, Leray V, Gervois N, Rosales C et al. Butyrate inhibits inflammatory responses through NFκB inhibition: implications for Crohn's disease. *Gut* 2000; 47(3):397–403.
21. Resta SC. Effects of probiotics and commensals on intestinal epithelial physiology: implications for nutrient handling. *The Journal of physiology* 2009; 587(17):4169–74.
22. Russell WR, Hoyles L, Flint HJ, Dumas M-E. Colonic bacterial metabolites and human health. *Current opinion in microbiology* 2013; 16(3):246–54.
23. Denker BM, Nigam SK. Molecular structure and assembly of the tight junction. *American Journal of Physiology-Renal Physiology* 1998; 274(1):F1-F9.
24. Farquhar MG, Palade GE. Junctional complexes in various epithelia. *Journal of Cell Biology* 1963; 17(2):375–412.
25. Ulluwishewa D, Anderson RC, Young W, McNabb WC, van Baarlen P, Moughan PJ et al. Live *F aecalibacterium prausnitzii* in an apical anaerobic model of the intestinal epithelial barrier. *Cellular microbiology* 2015; 17(2):226–40.

References

26. Furuse M, Hirase T, Itoh M, Nagafuchi A, Yonemura S, Tsukita S et al. Occludin: a novel integral membrane protein localizing at tight junctions. *J Cell Biol* 1993; 123(6):1777–88.
27. Ikenouchi J, Furuse M, Furuse K, Sasaki H, Tsukita S, Tsukita S. Tricellulin constitutes a novel barrier at tricellular contacts of epithelial cells. *Journal of Cell Biology* 2005; 171(6):939–45.
28. Stuart RO, Nigam SK. Regulated assembly of tight junctions by protein kinase C. *Proceedings of the national academy of sciences* 1995; 92(13):6072–6.
29. Cunningham KE, Turner JR. Myosin light chain kinase: pulling the strings of epithelial tight junction function. *Ann N Y Acad Sci* 2012; 1258(1):34–42.
30. Vetrano S, Ploplis V, Sala E, Sandoval-Cooper M, Donahue D, Correale C et al. Unexpected role of anticoagulant protein C in controlling epithelial barrier integrity and intestinal inflammation. *Proc Natl Acad Sci U S A* 2011; 108(49):19830–5.
31. Thompson MR, Kaminski JJ, Kurt-Jones EA, Fitzgerald KA. Pattern recognition receptors and the innate immune response to viral infection. *Viruses* 2011; 3(6):920–40.
32. Garg AD, Nowis D, Golab J, Vandenabeele P, Krysko DV, Agostinis P. Immunogenic cell death, DAMPs and anticancer therapeutics: an emerging amalgamation. *Biochimica et Biophysica Acta (BBA)-Reviews on Cancer* 2010; 1805(1):53–71.
33. Matzinger P. The danger model: a renewed sense of self. *Science* 2002; 296(5566):301–5.
34. Martin SJ, Henry CM, Cullen SP. A perspective on mammalian caspases as positive and negative regulators of inflammation. *Molecular cell* 2012; 46(4):387–97.
35. Neutra MR, Pringault E, Kraehenbuhl JP. Antigen sampling across epithelial barriers and induction of mucosal immune responses. *Annu Rev Immunol* 1996; 14:275–300.
36. Reis e Sousa C. Toll-like receptors and dendritic cells: for whom the bug tolls. *Semin Immunol* 2004; 16(1):27–34.
37. Simmons DP, Wearsch PA, Canaday DH, Meyerson HJ, Liu YC, Wang Y et al. Type I IFN drives a distinctive dendritic cell maturation phenotype that allows continued class II MHC synthesis and antigen processing. *Journal of immunology (Baltimore, Md.: 1950)* 2012; 188(7):3116–26.
38. Lutz MB, Schuler G. Immature, semi-mature and fully mature dendritic cells: which signals induce tolerance or immunity? *Trends in immunology* 2002; 23(9):445–9.

References

39. Rescigno M, Rotta G, Valzasina B, Ricciardi-Castagnoli P. Dendritic cells shuttle microbes across gut epithelial monolayers. *Immunobiology* 2001; 204(5):572–81.
40. Robles-Vera I, La Visitación N de, Sánchez M, Gómez-Guzmán M, Jiménez R, Moleón J et al. Mycophenolate improves brain-gut axis inducing remodeling of gut microbiota in DOCA-Salt hypertensive rats. *Antioxidants (Basel)* 2020; 9(12).
41. Rescigno M. Intestinal dendritic cells. *Adv Immunol* 2010; 107:109–38.
42. Zhu X, Zhu J. CD4 T helper cell subsets and related human immunological disorders. *Int J Mol Sci* 2020; 21(21).
43. Dudek AM, Martin S, Garg AD, Agostinis P. Immature, Semi-Mature, and Fully Mature Dendritic Cells: Toward a DC-Cancer Cells Interface That Augments Anticancer Immunity. *Front Immunol* 2013; 4:438.
44. Steinman RM, Mellman I. Immunotherapy: bewitched, bothered, and bewildered no more. *Science* 2004; 305(5681):197–200.
45. Okeke EB, Uzonna JE. The pivotal role of regulatory t cells in the regulation of innate immune cells. *Front Immunol* 2019; 10:680.
46. Rocamora-Reverte L, Melzer FL, Würzner R, Weinberger B. The complex role of regulatory T cells in immunity and aging. *Front Immunol* 2020; 11:616949.
47. Afzali B, Lombardi G, Lechler RI, Lord GM. The role of T helper 17 (Th17) and regulatory T cells (Treg) in human organ transplantation and autoimmune disease. *Clin Exp Immunol* 2007; 148(1):32–46.
48. Lozupone C, Stombaugh J, González A, Ackermann G, Doug W, Vázquez-Baeza Y et al. Meta-analyses of studies of the human microbiota. *Genome research* 2013; 23.
49. Lozupone CA, Stombaugh JI, Gordon JI, Jansson JK, Knight R. Diversity, stability and resilience of the human gut microbiota. *Nature* 2012; 489(7415):220–30.
50. Ley RE, Peterson DA, Gordon JI. Ecological and evolutionary forces shaping microbial diversity in the human intestine. *Cell* 2006; 124(4):837–48.
51. Artis D. Epithelial-cell recognition of commensal bacteria and maintenance of immune homeostasis in the gut. *Nat Rev Immunol* 2008; 8(6):411–20.
52. Velasquez-Manoff M. Gut microbiome: the peacekeepers. *Nature* 2015; 518(7540):S3-11.

References

53. Eckburg PB, Bik EM, Bernstein CN, Purdom E, Dethlefsen L, Sargent M et al. Diversity of the human intestinal microbial flora. *Science* 2005; 308(5728):1635–8.
54. Hattori M, Taylor TD. The human intestinal microbiome: a new frontier of human biology. *DNA Res* 2009; 16(1):1–12.
55. Arumugam M, Raes J, Pelletier E, Paslier D, Le Yamada T, Mende DR et al. Enterotypes of the human gut microbiome. *Nature* 2011; 473(7346):174–80.
56. Walker AW, Sanderson JD, Churcher C, Parkes GC, Hudspith BN, Rayment N et al. High-throughput clone library analysis of the mucosa-associated microbiota reveals dysbiosis and differences between inflamed and non-inflamed regions of the intestine in inflammatory bowel disease. *BMC Microbiol* 2011; 11:7.
57. Flint HJ, Scott KP, Louis P, Duncan SH. The role of the gut microbiota in nutrition and health. *Nature reviews Gastroenterology & hepatology* 2012; 9(10):577–89.
58. Ramirez-Farias C, Slezak K, Fuller Z, Duncan A, Holtrop G, Louis P. Effect of inulin on the human gut microbiota: stimulation of *Bifidobacterium adolescentis* and *Faecalibacterium prausnitzii*. *British Journal of Nutrition* 2008; 101(4):541–50.
59. Sartor RB. Microbial influences in inflammatory bowel diseases. *Gastroenterology* 2008; 134(2):577–94.
60. Prakash S, Rodes L, Coussa-Charley M, Tomaro-Duchesneau C. Gut microbiota: next frontier in understanding human health and development of biotherapeutics. *Biologics: targets and therapy* 2011:71–86.
61. Hammami R, Fernandez B, Lacroix C, Fliss I. Anti-infective properties of bacteriocins: an update. *Cellular and Molecular Life Sciences* 2013; 70:2947–67.
62. Carding S, Verbeke K, Vipond DT, Corfe BM, Owen LJ. Dysbiosis of the gut microbiota in disease. *Microb Ecol Health Dis* 2015; 26:26191.
63. Alam MT, Amos GCA, Murphy ARJ, Murch S, Wellington EMH, Arasaradnam RP. Microbial imbalance in inflammatory bowel disease patients at different taxonomic levels. *Gut Pathog* 2020; 12:1.
64. Shanahan F. The colonic microbiota in health and disease. *Current opinion in gastroenterology* 2013; 29(1):49–54.

References

65. Lavelle A, Sokol H. Gut microbiota-derived metabolites as key actors in inflammatory bowel disease. *Nat Rev Gastroenterol Hepatol* 2020; 17(4):223–37.
66. Arpaia N, Campbell C, Fan X, Dikiy S, van der Veecken J, deRoos P et al. Metabolites produced by commensal bacteria promote peripheral regulatory T-cell generation. *Nature* 2013; 504(7480):451–5.
67. Pascale A, Marchesi N, Marelli C, Coppola A, Luzi L, Govoni S et al. Microbiota and metabolic diseases. *Endocrine* 2018; 61:357–71.
68. Hijova E, Chmelarova A. Short chain fatty acids and colonic health. *Bratisl Lek Listy* 2007; 108(8):354–8.
69. Hamer HM, Jonkers D, Venema K, Vanhoutvin S, Troost FJ, Brummer R-J. Review article: the role of butyrate on colonic function. *Aliment Pharmacol Ther* 2008; 27(2):104–19.
70. Gibson GR, Roberfroid MB. Dietary modulation of the human colonic microbiota: introducing the concept of prebiotics. *J Nutr* 1995; 125(6):1401–12.
71. Rimoldi M, Chieppa M, Salucci V, Avogadri F, Sonzogni A, Sampietro GM et al. Intestinal immune homeostasis is regulated by the crosstalk between epithelial cells and dendritic cells. *Nat Immunol* 2005; 6(5):507–14.
72. Zeuthen LH, Fink LN, Frokiaer H. Epithelial cells prime the immune response to an array of gut-derived commensals towards a tolerogenic phenotype through distinct actions of thymic stromal lymphopoietin and transforming growth factor-beta. *Immunology* 2008; 123(2):197–208.
73. Peterson LW, Artis D. Intestinal epithelial cells: regulators of barrier function and immune homeostasis. *Nature Reviews Immunology* 2014; 14(3):141–53.
74. Sanz Y, Santacruz A, Gauffin P. Gut microbiota in obesity and metabolic disorders. *Proc Nutr Soc* 2010; 69(3):434–41.
75. Rijkers GT, Bengmark S, Enck P, Haller D, Herz U, Kalliomaki M et al. Guidance for substantiating the evidence for beneficial effects of probiotics: current status and recommendations for future research. *J Nutr* 2010; 140(3):671S–6S.
76. Molodecky NA, Soon IS, Rabi DM, Ghali WA, Ferris M, Chernoff G et al. Increasing incidence and prevalence of the inflammatory bowel diseases with time, based on systematic review. *Gastroenterology* 2012; 142(1):46–54.e42; quiz e30.

References

77. Olsson R, Danielsson Å, Järnerot G, Lindström E, Lööf L, Rolny P et al. Prevalence of primary sclerosing cholangitis in patients with ulcerative colitis. *Gastroenterology* 1991; 100(5, Part 1):1319–23.
78. Braegger CP, Ballabeni P, Rogler D, Vavricka SR, Friedt M, Pittet V et al. Epidemiology of inflammatory bowel disease: is there a shift towards onset at a younger age? *Journal of pediatric gastroenterology and nutrition* 2011; 53(2):141–4.
79. MacDonald TT, Monteleone G. Immunity, inflammation, and allergy in the gut. *Science* 2005; 307(5717):1920–5.
80. Kumar V, Abbas AK, Fausto N, Aster JC. Robbins and Cotran pathologic basis of disease, professional edition e-book. Elsevier health sciences; 2014.
81. Jostins L, Ripke S, Weersma RK, Duerr RH, McGovern DP, Hui KY et al. Host–microbe interactions have shaped the genetic architecture of inflammatory bowel disease. *Nature* 2012; 491(7422):119–24.
82. Ek WE, D’Amato M, Halfvarson J. The history of genetics in inflammatory bowel disease. *Annals of gastroenterology: quarterly publication of the Hellenic Society of Gastroenterology* 2014; 27(4):294.
83. Hugot J-P, Chamaillard M, Zouali H, Lesage S, Cézard J-P, Belaiche J et al. Association of NOD2 leucine-rich repeat variants with susceptibility to Crohn's disease. *Nature* 2001; 411(6837):599–603.
84. Ogura Y, Bonen DK, Inohara N, Nicolae DL, Chen FF, Ramos R et al. A frameshift mutation in NOD2 associated with susceptibility to Crohn's disease. *Nature* 2001; 411(6837):603–6.
85. Ferguson LR, Shelling AN, Browning BL, Huebner C, Petermann I. Genes, diet and inflammatory bowel disease. *Mutation Research/Fundamental and Molecular Mechanisms of Mutagenesis* 2007; 622(1-2):70–83.
86. Sarlos P, Kovesdi E, Magyari L, Banfai Z, Szabo A, Javorhazy A et al. Genetic update on inflammatory factors in ulcerative colitis: Review of the current literature. *World journal of gastrointestinal pathophysiology* 2014; 5(3):304.
87. Shih DQ, Targan SR, McGovern D. Recent advances in IBD pathogenesis: genetics and immunobiology. *Current gastroenterology reports* 2008; 10(6):568–75.

References

88. M'koma AE. Inflammatory bowel disease: an expanding global health problem. *Clinical Medicine Insights: Gastroenterology* 2013; 6:CGast-S12731.
89. Selvaratnam S, Gullino S, Shim L, Lee E, Lee A, Paramsothy S et al. Epidemiology of inflammatory bowel disease in South America: A systematic review. *World J Gastroenterol* 2019; 25(47):6866–75.
90. Lakatos PL, Lakatos L. Risk for colorectal cancer in ulcerative colitis: changes, causes and management strategies. *World journal of gastroenterology: WJG* 2008; 14(25):3937.
91. Sokol H, Pigneur B, Watterlot L, Lakhdari O, Bermúdez-Humarán LG, Gratadoux J-J et al. *Faecalibacterium prausnitzii* is an anti-inflammatory commensal bacterium identified by gut microbiota analysis of Crohn disease patients. *Proceedings of the national academy of sciences* 2008; 105(43):16731–6.
92. Wu N, Mah C, Koentgen S, Zhang L, Grimm MC, El-Omar E et al. Inflammatory bowel disease and the gut microbiota. *Proc Nutr Soc* 2021; 80(4):424–34.
93. Burger D, Travis S. Conventional medical management of inflammatory bowel disease. *Gastroenterology* 2011; 140(6):1827–37.
94. Carter MJ, Lobo AJ, Travis SPL. Guidelines for the management of inflammatory bowel disease in adults. *Gut* 2004; 53 Suppl 5(Suppl 5):V1-16.
95. Mowat C, Cole A, Windsor A, Ahmad T, Arnott I, Driscoll R et al. Guidelines for the management of inflammatory bowel disease in adults. *Gut* 2011; 60(5):571–607.
96. Khan I, Ullah N, Zha L, Bai Y, Khan A, Zhao T et al. Alteration of gut microbiota in inflammatory bowel disease (IBD): cause or consequence? IBD treatment targeting the gut microbiome. *Pathogens* 2019; 8(3):126.
97. Triantafyllidis JK, Merikas E, Georgopoulos F. Current and emerging drugs for the treatment of inflammatory bowel disease. *Drug design, development and therapy* 2011:185–210.
98. Iacucci M, Silva S de, Ghosh S. Mesalazine in inflammatory bowel disease: a trendy topic once again? *Can J Gastroenterol* 2010; 24(2):127–33.
99. Buchman AL. Side effects of corticosteroid therapy. *J Clin Gastroenterol* 2001; 33(4):289–94.
100. Wang B, Ren S, Feng W, Zhong Z, Qin C. Kui jie qing in the treatment of chronic non-specific ulcerative colitis. *J Tradit Chin Med* 1997; 17(1):10–3.

References

101. Langmead L, Feakins RM, Goldthorpe S, Holt H, Tsironi E, Silva A de et al. Randomized, double-blind, placebo-controlled trial of oral aloe vera gel for active ulcerative colitis. *Aliment Pharmacol Ther* 2004; 19(7):739–47.
102. Ben-Arye E, Goldin E, Wengrower D, Stamper A, Kohn R, Berry E. Wheat grass juice in the treatment of active distal ulcerative colitis: a randomized double-blind placebo-controlled trial. *Scandinavian journal of gastroenterology* 2002; 37(4):444–9.
103. Hilsden RJ, Verhoef MJ, Best A, Pocobelli G. Complementary and alternative medicine use by Canadian patients with inflammatory bowel disease: results from a national survey. *Am J Gastroenterol* 2003; 98(7):1563–8.
104. Angell M, Kassirer JP. Alternative medicine--the risks of untested and unregulated remedies. *N Engl J Med* 1998; 339(12):839–41.
105. Borriello SP, Hammes WP, Holzapfel W, Marteau P, Schrezenmeir J, Vaara M et al. Safety of probiotics that contain lactobacilli or bifidobacteria. *Clinical infectious diseases* 2003; 36(6):775–80.
106. Gomes AMP, Malcata FX. Bifidobacterium spp. and Lactobacillus acidophilus: biological, biochemical, technological and therapeutical properties relevant for use as probiotics. *Trends in Food Science & Technology* 1999; 10(4-5):139–57.
107. Fedorak RN, Feagan BG, Hotte N, Des Leddin, Dieleman LA, Petrunia DM et al. The probiotic VSL# 3 has anti-inflammatory effects and could reduce endoscopic recurrence after surgery for Crohn's disease. *Clinical Gastroenterology and Hepatology* 2015; 13(5):928–35.
108. Loguercio C, Federico A, Tuccillo C, Terracciano F, D'Auria MV, Simone C de et al. Beneficial effects of a probiotic VSL# 3 on parameters of liver dysfunction in chronic liver diseases. *J Clin Gastroenterol* 2005; 39(6):540–3.
109. Cheng F-S, Pan D, Chang B, Jiang M, Sang L-X. Probiotic mixture VSL# 3: An overview of basic and clinical studies in chronic diseases. *World Journal of Clinical Cases* 2020; 8(8):1361.
110. Lopez-Siles M, Enrich-Capó N, Aldeguer X, Sabat-Mir M, Duncan SH, Garcia-Gil LJ et al. Alterations in the abundance and co-occurrence of Akkermansia muciniphila and Faecalibacterium prausnitzii in the colonic mucosa of inflammatory bowel disease subjects. *Frontiers in cellular and infection microbiology* 2018; 8:281.

References

111. Blumberg RS, Saubermann LJ, Strober W. Animal models of mucosal inflammation and their relation to human inflammatory bowel disease. *Curr Opin Immunol* 1999; 11(6):648–56.
112. Bouma G, Strober W. The immunological and genetic basis of inflammatory bowel disease. *Nat Rev Immunol* 2003; 3(7):521–33.
113. Brandwein SL, McCabe RP, Cong Y, Waites KB, Ridwan BU, Dean PA et al. Spontaneously colitic C3H/HeJBir mice demonstrate selective antibody reactivity to antigens of the enteric bacterial flora. *Journal of immunology (Baltimore, Md.: 1950)* 1997; 159(1):44–52.
114. Strober W, Fuss IJ, Blumberg RS. The immunology of mucosal models of inflammation. *Annu Rev Immunol* 2002; 20:495–549.
115. Hoshi N, Schenten D, Nish SA, Walther Z, Gagliani N, Flavell RA et al. MyD88 signalling in colonic mononuclear phagocytes drives colitis in IL-10-deficient mice. *Nat Commun* 2012; 3:1120.
116. Nell S, Suerbaum S, Josenhans C. The impact of the microbiota on the pathogenesis of IBD: lessons from mouse infection models. *Nat Rev Microbiol* 2010; 8(8):564–77.
117. Lee I-A, Bae E-A, Hyun Y-J, Kim D-H. Dextran sulfate sodium and 2,4,6-trinitrobenzene sulfonic acid induce lipid peroxidation by the proliferation of intestinal gram-negative bacteria in mice. *J Inflamm (Lond)* 2010; 7:7.
118. Nieto N, Torres MI, Fernandez MI, Giron MD, Rios A, Suarez MD et al. Experimental ulcerative colitis impairs antioxidant defense system in rat intestine. *Digestive diseases and sciences* 2000; 45:1820–7.
119. Ohkusa T. Production of experimental ulcerative colitis in hamsters by dextran sulfate sodium and changes in intestinal microflora. *Nihon Shokakibyō Gakkai Zasshi* 1985; 82(5):1327–36.
120. Whittam CG, Williams AD, Williams CS. Murine Colitis modeling using Dextran Sulfate Sodium (DSS). *J Vis Exp* 2010; (35).
121. Perše M, Cerar A. Dextran sodium sulphate colitis mouse model: traps and tricks. *J Biomed Biotechnol* 2012; 2012:718617.
122. Melgar S, Karlsson A, Michaëlsson E. Acute colitis induced by dextran sulfate sodium progresses to chronicity in C57BL/6 but not in BALB/c mice: correlation between symptoms and inflammation. *Am J Physiol Gastrointest Liver Physiol* 2005; 288(6):G1328–38.

References

123. Yan Y, Kolachala V, Dalmasso G, Nguyen H, Laroui H, Sitaraman SV et al. Temporal and spatial analysis of clinical and molecular parameters in dextran sodium sulfate induced colitis. *PLOS one* 2009; 4(6):e6073.
124. Rogler G, Andus T. Cytokines in inflammatory bowel disease. *World J Surg* 1998; 22(4):382–9.
125. Tsukita S, Furuse M, Itoh M. Multifunctional strands in tight junctions. *Nature reviews Molecular cell biology* 2001; 2(4):285–93.
126. Hudcovic T, Stěpánková R, Cebra J, Tlaskalová-Hogenová H. The role of microflora in the development of intestinal inflammation: acute and chronic colitis induced by dextran sulfate in germ-free and conventionally reared immunocompetent and immunodeficient mice. *Folia Microbiol (Praha)* 2001; 46(6):565–72.
127. Nyström T. Stationary-phase physiology. *Annu Rev Microbiol* 2004; 58:161–81.
128. Cooper HS, Murthy SN, Shah RS, Sedergran DJ. Clinicopathologic study of dextran sulfate sodium experimental murine colitis. *Lab Invest* 1993; 69(2):238–49.
129. Martin M. Cutadapt removes adapter sequences from high-throughput sequencing reads. *EMBnet j.* 2011; 17(1):10.
130. Kozich JJ, Westcott SL, Baxter NT, Highlander SK, Schloss PD. Development of a dual-index sequencing strategy and curation pipeline for analyzing amplicon sequence data on the MiSeq Illumina sequencing platform. *Applied and Environmental Microbiology* 2013; 79(17):5112–20.
131. Quast C, Pruesse E, Yilmaz P, Gerken J, Schweer T, Yarza P et al. The SILVA ribosomal RNA gene database project: improved data processing and web-based tools. *Nucleic Acids Res* 2013; 41(Database issue):D590–6.
132. Jacobse J, Li J, Rings EHHM, Samsom JN, Goettel JA. Intestinal regulatory T cells as specialized tissue-restricted immune cells in intestinal immune homeostasis and disease. *Front Immunol* 2021; 12:716499.
133. Anderson RC, Young W, Clerens S, Cookson AL, McCann MJ, Armstrong KM et al. Human oral isolate *Lactobacillus fermentum* AGR1487 reduces intestinal barrier integrity by increasing the turnover of microtubules in Caco-2 cells. *PLOS one* 2013; 8(11):e78774.

References

134. Yu Q, Yuan L, Deng J, Yang Q. Lactobacillus protects the integrity of intestinal epithelial barrier damaged by pathogenic bacteria. *Frontiers in cellular and infection microbiology* 2015; 5:26.
135. Duncan SH, Hold GL, Harmsen HJM, Stewart CS, Flint HJ. Growth requirements and fermentation products of *Fusobacterium prausnitzii*, and a proposal to reclassify it as *Faecalibacterium prausnitzii* gen. nov., comb. nov. *International journal of systematic and evolutionary microbiology* 2002; 52(6):2141–6.
136. Wilkins TD, Chalgren S. Medium for use in antibiotic susceptibility testing of anaerobic bacteria. *Antimicrobial agents and chemotherapy* 1976; 10(6):926–8.
137. Chen S, Einspanier R, Schoen J. Transepithelial electrical resistance (TEER): a functional parameter to monitor the quality of oviduct epithelial cells cultured on filter supports. *Histochem Cell Biol* 2015; 144(5):509–15.
138. Ouwehand AC, Tuomola EM, Tölkö S, Salminen S. Assessment of adhesion properties of novel probiotic strains to human intestinal mucus. *International Journal of Food Microbiology* 2001; 64(1-2):119–26.
139. Morita H, He F, Fuse T, Ouwehand AC, Hashimoto H, Hosoda M et al. Adhesion of lactic acid bacteria to caco-2 cells and their effect on cytokine secretion. *Microbiol Immunol* 2002; 46(4):293–7.
140. Tuomola EM, Salminen SJ. Adhesion of some probiotic and dairy Lactobacillus strains to Caco-2 cell cultures. *International Journal of Food Microbiology* 1998; 41(1):45–51.
141. Del Re B, Sgorbati B, Miglioli M, Palenzona D. Adhesion, autoaggregation and hydrophobicity of 13 strains of *Bifidobacterium longum*. *Letters in applied microbiology* 2000; 31(6):438–42.
142. Vallance BA, Finlay BB. Exploitation of host cells by enteropathogenic *Escherichia coli*. *Proc Natl Acad Sci U S A* 2000; 97(16):8799–806.
143. Moroni O, Kheadr E, Boutin Y, Lacroix C, Fliss I. Inactivation of adhesion and invasion of food-borne *Listeria monocytogenes* by bacteriocin-producing *Bifidobacterium* strains of human origin. *Applied and Environmental Microbiology* 2006; 72(11):6894–901.
144. Weinstein DL, O'Neill BL, Hone DM, Metcalf ES. Differential early interactions between *Salmonella enterica* serovar Typhi and two other pathogenic *Salmonella* serovars with intestinal epithelial cells. *Infect Immun* 1998; 66(5):2310–8.

References

145. Frick JS, Fink K, Kahl F, Niemiec MJ, Quitadamo M, Schenk K et al. Identification of commensal bacterial strains that modulate *Yersinia enterocolitica* and dextran sodium sulfate-induced inflammatory responses: implications for the development of probiotics. *Infect Immun* 2007; 75(7):3490–7.
146. Anderson RC, Cookson AL, McNabb WC, Kelly WJ, Roy NC. *Lactobacillus plantarum* DSM 2648 is a potential probiotic that enhances intestinal barrier function. *FEMS Microbiology Letters* 2010; 309(2):184–92.
147. Coconnier MH, Klaenhammer TR, Kerneis S, Bernet MF, Servin A. Protein-mediated adhesion of *Lactobacillus acidophilus* BG2FO4 on human enterocyte and mucus-secreting cell lines in culture. *Applied and Environmental Microbiology* 1992; 58(6):2034–9.
148. Laparra JM, Sanz Y. Comparison of in vitro models to study bacterial adhesion to the intestinal epithelium. *Letters in applied microbiology* 2009; 49(6):695–701.
149. Bernet M-F, Brassart D, Neeser J-R, Servin AL. Adhesion of human bifidobacterial strains to cultured human intestinal epithelial cells and inhibition of enteropathogen-cell interactions. *Applied and Environmental Microbiology* 1993; 59(12):4121–8.
150. Monteagudo-Mera A, Rastall RA, Gibson GR, Charalampopoulos D, Chatzifragkou A. Adhesion mechanisms mediated by probiotics and prebiotics and their potential impact on human health. *Applied microbiology and biotechnology* 2019; 103:6463–72.
151. Garcia-Gonzalez N, Prete R, Battista N, Corsetti A. Adhesion properties of food-associated *Lactobacillus plantarum* strains on human intestinal epithelial cells and modulation of IL-8 release. *Frontiers in Microbiology* 2018; 9:2392.
152. Moussavi M, Adams MC. An in vitro study on bacterial growth interactions and intestinal epithelial cell adhesion characteristics of probiotic combinations. *Current microbiology* 2010; 60:327–35.
153. Collado MC, Meriluoto J, Salminen S. In vitro analysis of probiotic strain combinations to inhibit pathogen adhesion to human intestinal mucus. *Food Research International* 2007; 40(5):629–36.
154. Ulrich Schillinger, Claudia Guigas, Wilhelm Heinrich Holzapfel. In vitro adherence and other properties of lactobacilli used in probiotic yoghurt-like products. *International Dairy Journal* 2005; 15(12):1289–97.

References

155. Pramod K Gopal, Jaya Prasad, John Smart, Harsharanjit S Gill. In vitro adherence properties of *Lactobacillus rhamnosus* DR20 and *Bifidobacterium lactis* DR10 strains and their antagonistic activity against an enterotoxigenic *Escherichia coli*. *International Journal of Food Microbiology* 2001; 67(3):207–16.
156. Martín R, Miquel S, Benevides L, Bridonneau C, Robert V, Hudault S et al. Functional characterization of novel *Faecalibacterium prausnitzii* strains isolated from healthy volunteers: A step forward in the use of *F. prausnitzii* as a next-generation probiotic. *Frontiers in Microbiology* 2017; 8.
157. Linden SK, Sutton P, Karlsson NG, Korolik V, McGuckin MA. Mucins in the mucosal barrier to infection. *Mucosal Immunology* 2008; 1(3):183–97.
158. Katsikogianni M, Missirlis YF. Concise review of mechanisms of bacterial adhesion to biomaterials and of techniques used in estimating bacteria-material interactions. *Eur Cell Mater* 2004; 8(3):37–57.
159. Guglielmetti S, Tamagnini I, Minuzzo M, Arioli S, Parini C, Comelli E et al. Study of the adhesion of *Bifidobacterium bifidum* MIMBb75 to human intestinal cell lines. *Current microbiology* 2009; 59(2):167–72.
160. Suzuki T. Regulation of intestinal epithelial permeability by tight junctions. *Cell Mol Life Sci* 2013; 70(4):631–59.
161. Baum B, Georgiou M. Dynamics of adherens junctions in epithelial establishment, maintenance, and remodeling. *J Cell Biol* 2011; 192(6):907–17.
162. Denker BM, Nigam SK. Molecular structure and assembly of the tight junction. *Am J Physiol* 1998; 274(1):F1-9.
163. Van Itallie C., Anderson J. Claudins and epithelial paracellular transport. *Annu Rev Physiol* 2006; 68:403–29.
164. Alvarez C-S, Badia J, Bosch M, Giménez R, Baldomà L. Outer membrane vesicles and soluble factors released by probiotic *Escherichia coli* Nissle 1917 and commensal ECOR63 enhance barrier function by regulating expression of tight junction proteins in intestinal epithelial cells. *Frontiers in Microbiology* 2016; 7:1981.
165. Balda MS, Whitney JA, Flores C, González S, Cerejido M, Matter K. Functional dissociation of paracellular permeability and transepithelial electrical resistance and disruption of the apical-

References

basolateral intramembrane diffusion barrier by expression of a mutant tight junction membrane protein. *J Cell Biol* 1996; 134(4):1031–49.

166. Karczewski J, Troost FJ, Konings I, Dekker J, Kleerebezem M, Brummer R-JM et al. Regulation of human epithelial tight junction proteins by *Lactobacillus plantarum* in vivo and protective effects on the epithelial barrier. *Am J Physiol Gastrointest Liver Physiol* 2010; 298(6):G851-G859.

167. Klingberg TD, Pedersen MH, Cencic A, Budde BB. Application of measurements of transepithelial electrical resistance of intestinal epithelial cell monolayers to evaluate probiotic activity. *Applied and Environmental Microbiology* 2005; 71(11):7528–30.

168. Orlando A, Linsalata M, Notarnicola M, Tutino V, Russo F. *Lactobacillus GG* restoration of the gliadin induced epithelial barrier disruption: the role of cellular polyamines. *BMC Microbiol* 2014; 14:19.

169. Shimada Y, Kinoshita M, Harada K, Mizutani M, Masahata K, Kayama H et al. Commensal bacteria-dependent indole production enhances epithelial barrier function in the colon. *PLOS one* 2013; 8(11):e80604.

170. Singh R, Chandrashekarappa S, Bodduluri SR, Baby BV, Hegde B, Kotla NG et al. Enhancement of the gut barrier integrity by a microbial metabolite through the Nrf2 pathway. *Nat Commun* 2019; 10(1):89.

171. Luettig J, Rosenthal R, Barmeyer C, Schulzke JD. Claudin-2 as a mediator of leaky gut barrier during intestinal inflammation. *Tissue Barriers* 2015; 3(1-2):e977176.

172. Dai C, Zhao D-H, Jiang M. VSL#3 probiotics regulate the intestinal epithelial barrier in vivo and in vitro via the p38 and ERK signaling pathways. *Int J Mol Med* 2012; 29(2):202–8.

173. Otte J-M, Podolsky DK. Functional modulation of enterocytes by gram-positive and gram-negative microorganisms. *Am J Physiol Gastrointest Liver Physiol* 2004; 286(4):G613-26.

174. Seth A, Yan F, Polk DB, Rao RK. Probiotics ameliorate the hydrogen peroxide-induced epithelial barrier disruption by a PKC- and MAP kinase-dependent mechanism. *Am J Physiol Gastrointest Liver Physiol* 2008; 294(4):G1060-9.

175. Wang B, Li J, Chen J, Huang Q, Li N, Li J. Effect of live *Lactobacillus plantarum* L2 on TNF- α -induced MCP-1 production in Caco-2 cells. *International Journal of Food Microbiology* 2010; 142(1-2):237–41.

References

176. La Pine TR, Hill HR. Host Defense Mechanisms Against Bacteria. In: *Fetal and Neonatal Physiology*. Elsevier; 2011. p. 1553–66.
177. Deshmane SL, Kremlev S, Amini S, Sawaya BE. Monocyte chemoattractant protein-1 (MCP-1): an overview. *J Interferon Cytokine Res* 2009; 29(6):313–26.
178. Ren D-Y, Li C, Qin Y-Q, Yin R-L, Du S-W, Ye F et al. Lactobacilli reduce chemokine IL-8 production in response to TNF- α and Salmonella challenge of Caco-2 cells. *Journal of Biomedicine and Biotechnology* 2013; 2013:925219.
179. Zhang L, Li N, Caicedo R, Neu J. Alive and dead *Lactobacillus rhamnosus* GG decrease tumor necrosis factor-alpha-induced interleukin-8 production in Caco-2 cells. *J Nutr* 2005; 135(7):1752–6.
180. Zimmermann C, Schild M, Kunz C, Zimmermann K, Kuntz S. Effects of Live and Heat-Inactivated *E. coli* Strains and Their Supernatants on Immune Regulation in HT-29 Cells. *Eur J Microbiol Immunol (Bp)* 2018; 8(2):41–6.
181. Miquel S, Leclerc M, Martin R, Chain F, Lenoir M, Raguideau S et al. Identification of metabolic signatures linked to anti-inflammatory effects of *Faecalibacterium prausnitzii*. *mBio* 2015; 6(2).
182. Shen Z-H, Zhu C-X, Quan Y-S, Yang Z-Y, Wu S, Luo W-W et al. Relationship between intestinal microbiota and ulcerative colitis: Mechanisms and clinical application of probiotics and fecal microbiota transplantation. *World J Gastroenterol* 2018; 24(1):5–14.
183. Wang H, Jatmiko YD, Bastian SEP, Mashtoub S, Howarth GS. Effects of Supernatants from *Escherichia coli* Nissle 1917 and *Faecalibacterium prausnitzii* on Intestinal Epithelial Cells and a Rat Model of 5-Fluorouracil-Induced Mucositis. *Nutr Cancer* 2017; 69(2):307–18.
184. Tan B, Luo W, Shen Z, Xiao M, Wu S, Meng X et al. *Roseburia intestinalis* inhibits oncostatin M and maintains tight junction integrity in a murine model of acute experimental colitis. *Scandinavian journal of gastroenterology* 2019; 54(4):432–40.
185. Ghosh S, May MJ, Kopp EB. NF-kappa B and Rel proteins: evolutionarily conserved mediators of immune responses. *Annu Rev Immunol* 1998; 16:225–60.
186. Maeda S, Hsu L-C, Liu H, Bankston LA, Iimura M, Kagnoff MF et al. Nod2 mutation in Crohn's disease potentiates NF-kappaB activity and IL-1beta processing. *Science* 2005; 307(5710):734–8.

References

187. Ma TY, Iwamoto GK, Hoa NT, Akotia V, Pedram A, Boivin MA et al. TNF-alpha-induced increase in intestinal epithelial tight junction permeability requires NF-kappa B activation. *Am J Physiol Gastrointest Liver Physiol* 2004; 286(3):G367-76.
188. He F, Peng J, Deng X, Yang L, Camara AD, Omran A et al. Mechanisms of tumor necrosis factor-alpha-induced leaks in intestine epithelial barrier. *Cytokine* 2012; 59(2):264-72.
189. Kelly D, Campbell JI, King TP, Grant G, Jansson EA, Coutts AGP et al. Commensal anaerobic gut bacteria attenuate inflammation by regulating nuclear-cytoplasmic shuttling of PPAR-gamma and RelA. *Nat Immunol* 2004; 5(1):104-12.
190. Neish AS, Gewirtz AT, Zeng H, Young AN, Hobert ME, Karmali V et al. Prokaryotic regulation of epithelial responses by inhibition of IkappaB-alpha ubiquitination. *Science* 2000; 289(5484):1560-3.
191. Kruis W, Fric P, Pokrotnieks J, Lukás M, Fixa B, Kascák M et al. Maintaining remission of ulcerative colitis with the probiotic *Escherichia coli* Nissle 1917 is as effective as with standard mesalazine. *Gut* 2004; 53(11):1617-23.
192. Vrese M de, Schrezenmeir J. Probiotics, prebiotics, and synbiotics. *Adv Biochem Eng Biotechnol* 2008; 111:1-66.
193. Foligne B, Nutten S, Grangette C, Dennin V, Goudercourt D, Poiret S et al. Correlation between in vitro and in vivo immunomodulatory properties of lactic acid bacteria. *World J Gastroenterol* 2007; 13(2):236-43.
194. Bermudez-Brito M, Plaza-Díaz J, Muñoz-Quezada S, Gómez-Llorente C, Gil A. Probiotic mechanisms of action. *Ann Nutr Metab* 2012; 61(2):160-74.
195. Sehgal P, Colombel J-F, Aboubakr A, Narula N. Systematic review: safety of mesalazine in ulcerative colitis. *Aliment Pharmacol Ther* 2018; 47(12):1597-609.
196. Jiminez JA, Uwiera TC, Douglas Inglis G, Uwiera RRE. Animal models to study acute and chronic intestinal inflammation in mammals. *Gut Pathog* 2015; 7:29.
197. Elson CO, Sartor RB, Tennyson GS, Riddell RH. Experimental models of inflammatory bowel disease. *Gastroenterology* 1995; 109(4):1344-67.

References

198. Dieleman LA, Arends A, Tonkonogy SL, Goerres MS, Craft DW, Grenther W et al. *Helicobacter hepaticus* does not induce or potentiate colitis in interleukin-10-deficient mice. *Infect Immun* 2000; 68(9):5107–13.
199. Alex P, Zachos NC, Nguyen T, Gonzales L, Chen T-E, Conklin LS et al. Distinct cytokine patterns identified from multiplex profiles of murine DSS and TNBS-induced colitis. *Inflamm Bowel Dis* 2009; 15(3):341–52.
200. Moodley K, Mackraj I, Naidoo Y. Cardiovascular effects of *Tulbaghia violacea* Harv. (Alliaceae) root methanolic extract in Dahl salt-sensitive (DSS) rats. *J Ethnopharmacol* 2013; 146(1):225–31.
201. Geboes K, Riddell R, Ost A, Jensfelt B, Persson T, Löfberg R. A reproducible grading scale for histological assessment of inflammation in ulcerative colitis. *Gut* 2000; 47(3):404–9.
202. Azad S, Sood N, Sood A. Biological and histological parameters as predictors of relapse in ulcerative colitis: a prospective study. *Saudi J Gastroenterol* 2011; 17(3):194–8.
203. Saiki T. Myeloperoxidase concentrations in the stool as a new parameter of inflammatory bowel disease. *Kurume Med J* 1998; 45(1):69–73.
204. Han J, Ma D, Zhang M, Yang X, Tan D. Natural antioxidant betanin protects rats from paraquat-induced acute lung injury interstitial pneumonia. *Biomed Res Int* 2015; 2015:608174.
205. Heller F, Florian P, Bojarski C, Richter J, Christ M, Hillenbrand B et al. Interleukin-13 is the key effector Th2 cytokine in ulcerative colitis that affects epithelial tight junctions, apoptosis, and cell restitution. *Gastroenterology* 2005; 129(2):550–64.
206. Wallace KL, Zheng L-B, Kanazawa Y, Shih DQ. Immunopathology of inflammatory bowel disease. *World J Gastroenterol* 2014; 20(1):6–21.
207. Geng X, Xue J. Expression of Treg/Th17 cells as well as related cytokines in patients with inflammatory bowel disease. *Pak J Med Sci* 2016; 32(5):1164–8.
208. Zhang Y, Zhao X, Zhu Y, Ma J, Ma H, Zhang H. Probiotic mixture protects dextran sulfate sodium-induced colitis by altering tight junction protein expressions and increasing. *Mediators Inflamm* 2018; 2018:9416391.

References

209. O'Mahony C, Scully P, O'Mahony D, Murphy S, O'Brien F, Lyons A et al. Commensal-induced regulatory T cells mediate protection against pathogen-stimulated NF-kappaB activation. *PLoS pathogens* 2008; 4(8):e1000112.
210. Zhu C, Song K, Shen Z, Quan Y, Tan B, Luo W et al. Roseburia intestinalis inhibits interleukin-17 excretion and promotes regulatory T cells differentiation in colitis. *Mol Med Rep* 2018; 17(6):7567–74.
211. Noack M, Miossec P. Th17 and regulatory T cell balance in autoimmune and inflammatory diseases. *Autoimmun Rev* 2014; 13(6):668–77.
212. Fan L, Qi Y, Qu S, Chen X, Li A, Hendi M et al. *B. adolescentis* ameliorates chronic colitis by regulating Treg/Th2 response and gut microbiota remodeling. *Gut Microbes* 2021; 13(1):1–17.
213. Shale M, Schiering C, Powrie F. CD 4+ T-cell subsets in intestinal inflammation. *Immunological reviews* 2013; 252(1):164–82.
214. Geng X, Xue J. Expression of Treg/Th17 cells as well as related cytokines in patients with inflammatory bowel disease. *Pak J Med Sci* 2016; 32(5):1164.
215. McGeachy MJ, Cua DJ, Gaffen SL. The IL-17 Family of Cytokines in Health and Disease. *Immunity* 2019; 50(4):892–906.
216. Smith PM, Howitt MR, Panikov N, Michaud M, Gallini CA, Bohlooly-Y M et al. The microbial metabolites, short-chain fatty acids, regulate colonic Treg cell homeostasis. *Science* 2013; 341(6145):569–73.
217. Vetrano S, Ploplis VA, Sala E, Sandoval-Cooper M, Donahue DL, Correale C et al. Unexpected role of anticoagulant protein C in controlling epithelial barrier integrity and intestinal inflammation. *Proceedings of the national academy of sciences* 2011; 108(49):19830–5.
218. Gong Y, Liu L, He X, Zhao H, Yang J, Li L et al. The th17/treg immune balance in ulcerative colitis patients with two different chinese syndromes: dampness-heat in large intestine and spleen and kidney yang deficiency syndrome. *Evid Based Complement Alternat Med* 2015; 2015:264317.
219. Gong Y, Liu L, He X, Zhao H, Yang J, Li L et al. The th17/treg immune balance in ulcerative colitis patients with two different chinese syndromes: dampness-heat in large intestine and spleen and kidney yang deficiency syndrome. *Evidence-Based Complementary and Alternative Medicine* 2015; 2015.

References

220. Ukena SN, Singh A, Dringenberg U, Engelhardt R, Seidler U, Hansen W et al. Probiotic *Escherichia coli* Nissle 1917 inhibits leaky gut by enhancing mucosal integrity. *PLOS one* 2007; 2(12):e1308.
221. Park J-S, Choi JW, Jhun J, Kwon JY, Lee B-I, Yang CW et al. *Lactobacillus acidophilus* improves intestinal inflammation in an acute colitis mouse model by regulation of Th17 and Treg cell balance and fibrosis development. *Journal of medicinal food* 2018; 21(3):215–24.
222. Kim W-K, Jang YJ, Han DH, Seo B, Park S, Lee CH et al. Administration of *Lactobacillus fermentum* KBL375 causes taxonomic and functional changes in gut microbiota leading to improvement of atopic dermatitis. *Front Mol Biosci* 2019; 6:92.
223. Ohkusa T, Koido S. Intestinal microbiota and ulcerative colitis. *J Infect Chemother* 2015; 21(11):761–8.
224. Shin N-R, Whon TW, Bae J-W. Proteobacteria: microbial signature of dysbiosis in gut microbiota. *Trends Biotechnol* 2015; 33(9):496–503.
225. Yu P, Ke C, Guo J, Zhang X, Li B. *Lactobacillus plantarum* L15 alleviates colitis by inhibiting lps-mediated NF- κ B activation and ameliorates dss-induced gut microbiota dysbiosis. *Front Immunol* 2020; 11:575173.
226. Niu MM, Guo HX, Cai JW, Meng XC. *Bifidobacterium breve* alleviates DSS-induced Colitis in mice by maintaining the mucosal and epithelial barriers and modulating gut microbes. *Nutrients* 2022; 14(18).
227. Ott SJ, Musfeldt M, Wenderoth DF, Hampe J, Brant O, Fölsch UR, Timmis KN, Schreiber S. Reduction in diversity of the colonic mucosa associated bacterial microflora in patients with active inflammatory bowel disease. *Gut* 2004; 53(5):685–93.
228. Kruis W, Schütz E, Fric P, Fixa B, Judmaier G, Stolte M. Double-blind comparison of an oral *Escherichia coli* preparation and mesalazine in maintaining remission of ulcerative colitis. *Aliment Pharmacol Ther* 1997; 11(5):853–8.
229. Nakashima J, Preuss CV. Mesalamine (USAN). In: StatPearls. Treasure Island (FL); 2023.
230. Fujiwara M, Mitsui K, Yamamoto I. Inhibition of proliferative responses and interleukin 2 productions by salazosulfapyridine and its metabolites. *The Japanese Journal of Pharmacology* 1990; 54(2):121–31.

References

231. Doering J, Begue B, Lentze MJ, Rieux-Laucat F, Goulet O, Schmitz J et al. Induction of T lymphocyte apoptosis by sulphasalazine in patients with Crohn's disease. *Gut* 2004; 53(11):1632–8.
232. Huang J, Yang Z, Li Y, Chai X, Liang Y, Lin B et al. *Lactobacillus paracasei* R3 protects against dextran sulfate sodium (DSS)-induced colitis in mice via regulating Th17/Treg cell balance. *Journal of Translational Medicine* 2021; 19(1):356.
233. Kropp C, Le Corf K, Relizani K, Tambosco K, Martinez C, Chain F et al. The Keystone commensal bacterium *Christensenella minuta* DSM 22607 displays anti-inflammatory properties both in vitro and in vivo. *Scientific Reports* 2021; 11(1):11494.

9 Acknowledgment

At this point, I would like to take the opportunity to express my gratitude to all the people who have supported me and accompanied me through my doctoral journey.

First and foremost, I extend my heartfelt appreciation to my supervisor, Prof. Dr. Bernd Kreikemeyer, for giving me the opportunity to work on such an interesting and challenging topic in his research group. Dear Bernd, it was a great pleasure to be your student. Thank you for all your guidance, unwavering support, and invaluable insights that were instrumental throughout this journey. Thanks for always having an open door for me, no matter how busy you were. I am deeply thankful to my mentor, Dr. Anne Breitrück. Your generous investment of time, effort, and the wealth of advice and discussions we shared were instrumental in keeping my spirits high and my research on track. I must also express my gratitude to the entire IMIKRO research group, including fellow researchers and technical assistants. Working with all of you in such a harmonious atmosphere has been a delightful experience. I want to extend special thanks to Dr. Tomas Fiedler, whose assistance extended beyond proofreading the discussion section of my thesis. His insightful comments were invaluable. I also appreciate his support with the administrative tasks along the road to completing this thesis. I'm also grateful to Dr. Nadja Patenge for always being approachable and responsive to my sudden questions.

Lastly, but by no means least, I wish to convey my deep and sincere gratitude to my family. To my beloved parents, Zohreh Joon and Majid Joon, words will always fall short in expressing my gratitude. Your unwavering support and unconditional love have been the cornerstone of my journey. I am forever indebted to you for providing the opportunities and conditions that have shaped me into who I am today. To my brother, Arash, I extend my heartfelt thanks for your unfailing support and your ability to inject humor into the toughest of times.

And to Amin, my love and life partner, I want to express my heartfelt gratitude for always being there to accompany me to the lab at mid night and early morning to prepare bacterial overnight cultures. Your love and unwavering belief in me, despite the challenges I faced, have been a constant source of strength throughout this journey. Thank you for standing by my side.

To all, thank you !!

Declaration of Independence

I hereby declare that I have written this thesis independently and without external help. For this purpose I have not used any aids or sources other than those indicated by me. Passages taken verbatim and in terms of content from the works are marked accordingly. Parts of the present work have already been published in :

Moheballi N, Ekati K, Kreikemeyer B, Breitrück A. Barrier Protection and Recovery Effects of Gut Commensal Bacteria on Differentiated Intestinal Epithelial Cells In Vitro. *Nutrients*. 2020 Jul 28;12(8):2251. doi: 10.3390/nu12082251. PMID: 32731411; PMCID: PMC7468801.

Moheballi N, Weigel M, Hain T, Sütel M, Bull J, Kreikemeyer B, Breitrück A. Faecalibacterium prausnitzii, Bacteroides faecis and Roseburia intestinalis attenuate clinical symptoms of experimental colitis by regulating Treg/Th17 cell balance and intestinal barrier integrity. *Biomed Pharmacother*. 2023 Nov;167:115568. doi: 10.1016/j.biopha.2023.115568. Epub 2023 Oct 2. PMID: 37793274.

Nooshin Moheballi,
Rostock, 2023

Selbstständigkeitserklärung

Ich versichere hiermit, dass ich die vorliegende Arbeit selbstständig verfasst und keine anderen Hilfsmittel und Quellen als die angegebenen verwendet habe. Die Stellen, die anderen Werken dem Wortlaut oder dem Sinn nach entnommen sind, habe ich in jedem einzelnen Fall durch Angabe der Quelle kenntlich gemacht.

Teile der vorliegenden Arbeit wurden bereits in geteilter Erstautorenschaft veröffentlicht in:

Moheballi N, Ekati K, Kreikemeyer B, Breitrück A. Barrier Protection and Recovery Effects of Gut Commensal Bacteria on Differentiated Intestinal Epithelial Cells In Vitro. *Nutrients*. 2020 Jul 28;12(8):2251. doi: 10.3390/nu12082251. PMID: 32731411; PMCID: PMC7468801.

Moheballi N, Weigel M, Hain T, Sütel M, Bull J, Kreikemeyer B, Breitrück A. Faecalibacterium prausnitzii, Bacteroides faecis and Roseburia intestinalis attenuate clinical symptoms of experimental colitis by regulating Treg/Th17 cell balance and intestinal barrier integrity. *Biomed*

Pharmacother. 2023 Nov;167:115568. doi: 10.1016/j.biopha.2023.115568. Epub 2023 Oct 2.
PMID: 37793274.

Nooshin Mohebali,
Rostock, 2023

Curriculum Vitae

Personal information

Name Nooshin Mohebali
Date of birth 08.08.1986
Nationality Iranian
E-Mail Nooshin.mohebali@med.uni-rostock.de

Education

2004 - 2009 Bachelor of Biology , Azad University, Tehran, Iran.
2010-2014 Master of Biotechnology, University Malaya, Kuala Lumpur, Malaysia.
Thesis Title: Production and recovery of lignin peroxidase derived from *Pleurotus pulmonarius* (Fr) Quel by Aqueous two-phase system.
2018 - 2021 PhD Candidate and Research Scientist, at Institute of Medical Microbiology, Virology and Hygiene, University Medicine Rostock, Germany.
2021-Present Research Scientist at Department of Gastroenterology and Endocrinology at the University Medicine Rostock, Germany.

Publication

1. Ashok Kumar Pandurangan, **Nooshin Mohebali** ,Mohadeseh Hasanpourghadi, Norhaizan Mohd Esa. Caffeic acid phenethyl ester attenuates dextran sulfate sodium-induced ulcerative colitis through modulation of NF-KB and cell adhesion molecules. Applied Biochemistry and Biotechnology (2022). <https://doi.org/10.1007/s12010-021-03788-2>
2. Anne Breitrück, Markus Weigel, Jacqueline Hofrichter, Kai Sempert, Claus Kerkhoff, **Nooshin Mohebali**, Steffen Mitzner, Torsten Hain and Bernd Kreikemeyer. Smectite as a Preventive Oral Treatment to Reduce Clinical Symptoms of DSS Induced Colitis in Balb/c Mice. International journal of molecular sciences (2021). 10.3390/ijms22168699
3. **Nooshin Mohebali**, Katharina Ekat, Bernd Kreikemeyer and Anne Breitrück. Barrier protection and recovery effects of gut commensal

bacteria on differentiated intestinal epithelial cells in vitro. *Nutrients* (2020). doi.org/10.3390/nu12082251

4. **Nooshin Mohebali**, Ashok Kumar Panduranga, Mohd Rais Mustafa, Suresh Kumar Anandasadagopan and Tamilselvi Alagumuthu. Vernodalin induces apoptosis through the activation of ROS/JNK pathway in human colon cancer cells. *Journal of biochemical molecular toxicology* (2020). doi.org/10.1002/jbt.22587
5. Arshia Hematpoor, Mohammadjavad Paydar , Sook Yee Liew, Yasodha Sivasothy, **Nooshin Mohebali**, Chung Yeng Looi, Won Fen Wong, Mohd Sofian Azirun and Khalijah Awang. Phenylpropanoids isolated from *Piper sarmentosum* Roxb. induce apoptosis in breast cancer cells through reactive oxygen species and mitochondrial-dependent pathways. *Chemico-Biological Interactions* (2018). doi.org/10.1016/j.cbi.2017.11.014
6. Ashok Kumar Pandurangan, **Nooshin Mohebali**, Mohadeseh Hasanpourghadi, Chung Yeng Looi, Mohd Rais Mustafa and Norhaizan Mohd. Esa.,. Boldine suppresses dextran sulfate sodium -induced mouse ulcerative colitis: NF- κ B and IL- 6/STAT3 as potential targets. *BioFactors*. (2016). doi: 10.1002/biof.1267
7. Arezoo Dadrasnia , Mohammed Maikudi Usman, Kelvin Swee Chuan Wei, Rita Devi Velappan, Hossein Jamali, **Nooshin Mohebali**, Salmah Ismaila. Native soil bacterial isolate in Malaysia exhibit promising supplements on degrading organic pollutants. *Process Safety and Environmental Protection* (2016). doi:org/10.1016/j.psep.2016.02.00
8. Atiqah Aziz, Hairin Taha, **Nooshin Mohebali**, Chung Yeng Looi, Nor Hadiani Ismail, Muhammad Zubair Abu Bakar And Farida Zuraina Mohd Yusof. Anti-cancer potential of *pseuduvaria macrophylla* in human cancer cell lines. *Journal of Advanced Research in Applied Sciences and Engineering Technology* (2016)
9. Suresh Kumar Ananda Sadagopan*, **Nooshin Mohebali***, Chung Yeng Looi, Mohadeseh Hasanpourghadi, Aditya Arya, Hamed Karimian , Mohd Rais Mustafa. Forkhead Box Transcription Factor (FOXO3a Mediates the Cytotoxic Effect of Vernodalin In vitro and Inhibits the Breast Tumor Growth In vivo. *journal of experimental and clinical cancer research*. (*Equal contributors). (2015). doi :10.1186/s13046- 015-0266-y
10. Ashok Kumar Pandurangan, **Nooshin Mohebali**, Norhaizan Mohd. Esa, Chung Yeng Looi. Gallic acid attenuates dextran sodium sulfate (DSS)-induced experimental acute ulcerative colitis in BALB/c mice. *Drug Design, Development and Therapy* (2015). doi:10.2147/DDDT.S86345.
11. Ashok Kumar Pandurangan, **Nooshin Mohebali**, Norhaizan Mohd. Esa, Chung Yeng Looi , Salmiah Ismail , Zeinab Saadatdoust. Gallic acid suppresses inflammation in dextran sodium sulfate-induced colitis in mice:

Possible mechanisms. International Immunopharmacology (2015).
doi:10.1016/j.intimp.2015.08.019

Conference

1. **Nooshin Mohebali**, Bernd Kreikemeyer and Anne Breitrück. Barrier Recovery Effects Of Gut Commensal Bacteria On Intestinal Epithelial Cells. 6th Joint Conference of the DGHM & VAAM , Leipzig, Germany, **March 2020.**